NRC Research Press

ARTICLE

A new simplified method and its verification for calculation of consolidation settlement of a clayey soil with creep

Jian-Hua Yin and Wei-Qiang Feng

Abstract: The calculation of the consolidation settlement of clayey soils with creep behaviour has been a challenging issue with a long history. After a brief review the assumptions made in the two methods based on Hypothesis A and Hypothesis B, the authors present a new simplified hypothesis B method for calculation of consolidation settlement of a clayey soil with creep. Equations of this method are derived based on the "equivalent time" concept for different stress–strain states. This simplified Hypothesis B method is then used to calculate the consolidation settlement of a number of typical consolidation problems. The approximation and verification of this simplified method are examined by comparing the calculated settlements with settlements computed using two fully coupled finite element (FE) consolidation analysis programs using elastic viscoplastic (EVP) constitutive models (Hypothesis B) and the Hypothesis A method. It is found that the curves calculated using the new Hypothesis B simplified method with a factor $\alpha = 0.8$ are close to curves from two FE model simulations with relative errors in the range 0.37%~8.42% only for three layers of Hong Kong marine clay (HKMC). In overall, the settlements calculated using Hypothesis A method are smaller than those from the two FE simulations with relative error in the range 6.52%~46.17% for the three layers of HKMC. In addition, this new simplified Hypothesis B method is used to calculate the average strain of consolidation tests done by Berre and Iversen in 1972. The calculated results are compared with the test data, and values from a fully coupled finite difference (FD) consolidation analysis using Yin and Graham's EVP constitutive model (Hypothesis B), and Hypothesis A method. It is found that, again, the results from the new simplified Hypothesis B method are very close to the measured data. In conclusion, the new simplified Hypothesis B method is a suitable simple method, by spread-sheet calculation of the consolidation settlement of a single layer of a clayey soil with creep.

Key words: clay, settlement, consolidation, time-dependent, creep, viscoplastic.

Résumé : Le calcul du tassement de consolidation des sols argileux avec un comportement de fluage a été un enjeu difficile avec une longue histoire. Après un bref examen des hypothèses formulées dans les deux méthodes basées sur l'Hypothèse A et l'Hypothèse B, les auteurs présentent une nouvelle méthode d'Hypothèse B simplifiée pour le calcul du tassement de la consolidation d'un sol argileux avec fluage. Les équations de cette méthode sont dérivées basées sur le concept de « temps equivalent » pour différents états de contrainte–déformation. Cette méthode d'Hypothèse B simplifiée est ensuite utilisée pour calculer le tassement de la consolidation d'un certain nombre de problèmes typiques de consolidation. Le rapprochement et la vérification de cette méthode simplifiée sont examinés en comparant les tassements calculées avec les tassements calculées en utilisant deux programmes d'analyse de consolidation par éléments finis (EF) entièrement couplés en utilisant des modèles élastiques viscoplastiques constitutifs des méthodes (Hypothèse B) et l'Hypothèse A. On constate que les courbes calculées en utilisant la nouvelle méthode simplifiée d'Hypothèse B avec un facteur $\alpha = 0.8$ sont proches de courbes à partir de deux simulations de modèles à EF avec des erreurs relatives dans la gamme de 0,37~8,42 % seulement pour trois couches d'argile marine de Hong Kong (« Hong Kong marine clay (HKMC) »). Dans l'ensemble, les tassements calculées en utilisant une méthode d'Hypothèse A sont plus petits que ceux des deux simulations d'EF avec erreur relative dans la gamme de 6,52~46,17 % pour les trois couches de HKMC. En outre, cette nouvelle méthode d'Hypothèse B simplifiée est utilisée pour calculer la déformation moyenne des essais de consolidation réalisés par Berre et Iversen en 1972. Les résultats calculés sont comparés avec les données d'essai, et les valeurs d'une analyse de consolidation de la différence finie entièrement couplée en utilisant le modèle constitutif viscoplastique élastique de Yin et Graham (Hypothèse B), et l'Hypothèse A. On constate que, encore une fois, les résultats de la nouvelle méthode d'Hypothèse B simplifiée sont très proches des données mesurées. En conclusion, la nouvelle méthode d'Hypothèse B simplifiée est une méthode simple appropriée, par le calcul du tassement de consolidation d'une couche unique d'une terre argileuse avec fluage. [Traduit par la Rédaction]

Mots-clés : argile, tassement, consolidation, en fonction du temps, fluage, viscoplastique.

Introduction

It is well known that the stress–strain behaviour of clayey soils is time-dependent due to the viscous nature of the skeleton of the soils (Bjerrum 1967; Graham et al. 1983; Leroueil et al. 1985; Olson 1998). The physical phenomena, such as creep, relaxation, strain rate effects, "apparent pre-consolidation pressure", etc., are all part of the time-dependent stress–strain behaviour. Under loading, the clayey soils in a saturated condition are subjected to a consolidation process, in which the excess pore-water pressure dissipates with time, resulting in compression of the soils or set-

Received 17 June 2015. Accepted 23 August 2016.

J.-H. Yin and W.-Q. Feng. Department of Civil and Environmental Engineering, The Hong Kong Polytechnic University, Hung Hom, Kowloon, Hong Kong, China.

Corresponding author: Jian-Hua Yin (email: cejhyin@polyu.edu.hk).

Fig. 1. Curve of void ratio versus log (time) and "secondary" compression coefficient. [Colour online.]

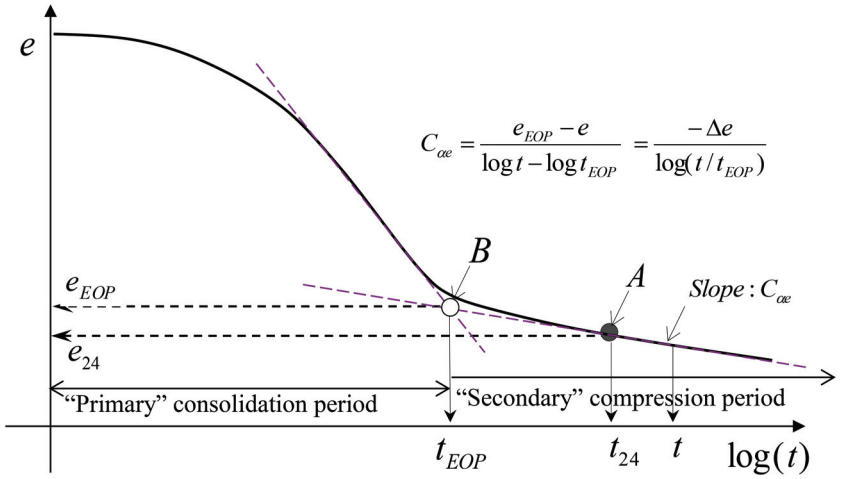

tlement. For the design of structures, such as reclamation or foundation on the clayey soils, we need to calculate the consolidation settlement of the soils with certain accuracy.

Terzaghi (1943) first presented a theory and equations for analysis of the consolidation of soil in one-dimensional (1-D) straining (oedometer condition). His 1-D consolidation theory was based on eight assumptions (Terzaghi 1943; Craig 2004). The most questionable assumption is that "there is a unique relationship, independent of time, between void ratio and effective stress" (Craig 2004). In fact, the relationship between void ratio and effective stress is time-dependent and strain-rate dependent. Therefore, in reality, Terzaghi's 1-D consolidation theory cannot be applied to consolidation settlement calculation of clayey soils with creep. Many researchers have taken efforts to propose improved methods for calculation of consolidation settlement of clayey soils by considering creep. These improved methods can be divided in two types: one is based on hypothesis A (Ladd et al. 1977; Mesri and Godlewski 1977) and the other one is based on Hypothesis B (Gibson and Lo 1961; Barden 1965, 1969; Bjerrum 1967; Garlanger 1972; Leroueil et al. 1985; Hinchberger and Rowe 2005; Kelln et al. 2008). The assumptions used in the two methods are examined more closely in the following paragraphs.

It shall be pointed out that the calculation of consolidation settlement in this paper is confined to the case of 1-D straining condition and one single soil layer with constant soil properties. The assumptions used in the method based on Hypothesis A for the calculation of consolidation settlement are

1. There exists a so-called "end-of-primary" (EOP) point between "primary consolidation" period and "secondary compression" without excess pore-water pressure ($u_e = 0$) with the corresponding time t_{EOP} (see Fig. 1).
2. There is no creep compression during the primary consolidation period; but the creep compression occurs only in the secondary compression starting at t_{EOP} (see Fig. 1).
3. The creep compression occurs in the secondary compression period can be described by the "secondary consolidation coefficient" $C_{\alpha e}$, which is $C_{\alpha e} = -\Delta e/\Delta \log t$, where e is void ratio and t is the duration time of the present loading (see Fig. 1).

Based on the above assumptions, a mathematical equation of the method based on Hypothesis. A for the calculation of the total consolidation settlement S_{totalA} in the field is

$$(1)\quad S_{totalA} = S_{primary} + S_{secondary} = \begin{cases} U_v S_f & \text{for } t < t_{EOP,field} \\ U_v S_f + \dfrac{C_{\alpha e}}{1 + e_o} \log\left(\dfrac{t}{t_{EOP,field}}\right) H & \text{for } t > t_{EOP,field} \end{cases}$$

where $S_{primary}$ is the primary consolidation settlement at time t and is equal to $U_v S_f$ in which U_v is the average degree of consolidation and S_f is the final primary consolidation settlement. In eq. (1), e_o is the initial void ratio and H is the total thickness of the soil layer. The "secondary" compression settlement is $S_{secondary} = \dfrac{C_{\alpha e}}{1+e_o} \log\left(\dfrac{t}{t_{EOP,field}}\right) H$ and is calculated as of $t > t_{EOP,field}$, which is the time at EOP in the field condition. The $t_{EOP,field}$ is dependent on the thickness of the soil layer and hydraulic permeability of the soil. The two main problems in eq. (1) are as follows:

1. The separation of the primary consolidation period and secondary consolidation period is subjective and not accurate. According to the Tergazhi's 1-D consolidation theory, the time corresponding to excess pore-water pressure $u_e = 0$, that is, $U_v = 100\%$, is infinite, that is, $t_{EOP,field}$ shall be infinite. To get around this problem, it is often assumed that the time corresponding to $U_v \geq 98\%$ is the time $t_{EOP,field}$ at "EOP".
2. There is no creep when time $t < t_{EOP,field}$ as shown in eq. (1), that is, no creep in the primary consolidation; however, creep occurs right after $t_{EOP,field}$ as secondary compression.

In fact, under the action of the effective stress, the skeleton of a clayey soil exhibits viscous deformation, or ongoing settlement in 1-D straining case. Even in the primary consolidation period, there are effective stresses, which may vary significantly with time. The rate of creep compression depends on the state of consolidation, such as normal consolidation (NC) or overconsolidation (OC). Therefore, due to the exclusion of creep compression in the primary consolidation period, the method based on Hypothesis A normally underestimates the total consolidation settlement.

In a different approach, the method based on Hypothesis B does not need these assumptions in Hypothesis A. The method based on Hypothesis B is a coupled consolidation analysis using a proper constitutive relationship for the time-dependent stress–strain behaviour of clayey soils. The time-dependent compression of the clay skeleton, for example, creep in the primary consolidation, is naturally included in the coupled consolidation analysis. The equations of the method based Hypothesis B can be expressed as follows.

From the mass continuity condition, we can derive

$$(2)\qquad \frac{k_v}{\gamma_w}\frac{\partial^2 u_e}{\partial z^2} = -\frac{\partial \varepsilon_z}{\partial t}$$

where k_v is the vertical hydraulic conductivity (assumed to be constant here for simplicity); u_e is the excess pore-water pressure; ε_z is the vertical strain (compression strain is positive here); γ_w is the unit weight of water; z is the vertical co-ordinate axis. There are two unknowns in eq. (2), that is, u_e and ε_z. A constitutive model equation is needed.

Yin and Graham (1989, 1994) developed, validated, and applied a 1-D elastic viscoplastic (1D EVP) constitutive model for the time-dependent stress–strain behaviour of clayey soils. The 1D EVP constitutive model equation is

$$(3)\qquad \dot{\varepsilon}_z = \frac{\kappa}{V}\frac{\dot{\sigma}'_z}{\sigma'_z} + \frac{\psi}{Vt_o}\exp\left[-\left(\varepsilon_z - \varepsilon_{zo}^{ep}\right)\frac{V}{\psi}\right]\left(\frac{\dot{\sigma}'_z}{\sigma'_{zo}}\right)^{\lambda/\psi}$$

where $\dot{\varepsilon}_z$ and ε_z are the vertical strain rate and strain; κ/V together is considered to be one parameter related to the elastic compression of the soil; $\dot{\sigma}'_z$ and σ'_z are the vertical effective stress rate and effective stress, respectively; ψ is the creep parameter that describes the linear relationship between vertical strain and ln(time); V is equal to $(1 + e_o)$, called specific volume; λ is defined as $\Delta e/\ln(\sigma'_z/\sigma'_{z0})$ for elastic–plastic compression, and the slope of the normal compression line of the soil is λ/V; the three parameters λ/V, ε_{zo}^{ep}, σ'_{zo} define a "reference time line" (Yin and Graham 1989, 1994); and the two parameters ψ/V and t_o are related to the creep compression of the soil. The 1D EVP model in eq. (3) is an extension of the Maxwell's linear elastic viscoplastic (EVP) model in which a linear elastic spring is connected to a linear viscous dash pot (Yin 2015).

For a soil layer in 1-D straining, the total stress σ_z and original or static pore-water pressure u_s in the soil layer are normally known. Therefore, according to the effective stress principle and noting the total pore-water pressure $u = u_s + u_e$ we have $\sigma'_z = \sigma_z - u = \sigma_z - u_s - u_e$. Substituting $\sigma'_z = \sigma_z - u = \sigma_z - u_s - u_e$ into eq. (3), we have

$$(4)\qquad \frac{\partial \varepsilon_z}{\partial t} = \frac{\kappa}{V}\frac{1}{(\sigma_z - u_s - u_e)}\frac{\partial(\sigma_z - u_s - u_e)}{\partial t} + \frac{\psi}{Vt_o}\exp\left[-(\varepsilon_z - \varepsilon_{zo}^{ep})\frac{V}{\psi}\right]\left(\frac{\sigma_z - u_s - u_e}{\sigma'_{zo}}\right)^{\lambda/\psi}$$

By solving eq. (2) together with eq. (4), we can obtain the excess pore-water pressure, u_e, from which we can obtain the effective stress, σ'_z; the vertical strain, ε_z; and the total settlement, $S_{totalB} = \int_o^H \varepsilon_z\, dz$.

Yin and Graham (1996) used a finite difference (FD) method to solve eqs. (2) and (4) from Hypothesis B and obtained curves of the settlement, strains, and excess pore-water pressure with time. They used this approach to calculate the settlement and excess pore-water pressure of a clay in laboratory physical model tests done by Berre and Iversen (1972). The calculated data were compared with the measured data by Berre and Iversen (1972) and were found to be in good agreement. They also found that the method based on Hypothesis A underestimated the total settlement.

Nash and Ryde (2000, 2001) used the method based on Hypothesis B with the constitutive equation in eq. (3) to analyze the 1-D consolidation settlement of an embankment on soft ground with vertical drains. They used a FD method (Yin and Graham 1996) to solve the coupled consolidation equations. Their computed settlement values were in good agreement with the observed values.

One limitation of the above rigorous Hypothesis B method is that a numerical method is needed to solve a set of nonlinear partial different equations and a computer program for this method is needed. Such computer program is still not readily available to engineers or difficult for them to use. How to develop a simple method, which is a good approximation of the solutions from the above rigorous method and, at the same time, is easy to use by engineers, has been a very challenging task in past decades. The main objective of this paper is to propose a new simplified method based on Hypothesis B for easy spread-sheet calculation of consolidation settlements of clayey soils with creep and the verification of this simplified method.

Main equation of a new simplified method based on Hypothesis B for settlement calculation of a soil layer with creep

The key point in the new simplified method based on Hypothesis B (called a new simplified Hypothesis B method) is that creep occurs in the whole consolidation period, both within and after the primary consolidation, as shown in Fig. 1. The main equation of the new simplified Hypothesis B method for the calculation of the total consolidation settlement, S_{totalB}, can be expressed as

$$(5)\qquad S_{totalB} = S_{primary} + S_{creep} = U_v S_f + [\alpha S_{creep,f} + (1 - \alpha)S_{secondary}] \quad \text{for all } t \geq 1 \text{ day } (t \geq t_{EOP,field} \text{ for } S_{secondary})$$

where α is the parameter to reasonably consider the creep compression coupled with consolidation; $S_{creep,f}$ is the creep settlement under the final effective vertical stress without excess pore-water pressure coupling; $S_{secondary}$ is the same as that in eq. (1); and $t_{EOP,field}$ is the time at $U_v = 98\%$.

In eq. (5), a parameter α is introduced and shall be in the range from 0 to 1, that is, $0 \leq \alpha \leq 1$. If $\alpha = 1$, eq. (5) becomes the old Yin's simplified Hypothesis B method (Yin 2011). If $\alpha = 0$, eq. (5) becomes Hypothesis A method in eq. (1). The most suitable value α will be determined by comparing the calculated settlement using eq. (5) with settlements from coupled consolidation analysis further in this paper. Comparing eq. (5) to eq. (1), it is seen that the creep settlement S_{creep} is included for the loading time $t \geq 0$, that is, creep compression occurs from the beginning.

It is noted that $S_{creep} = [\alpha_{Screep,f} + (1 - \alpha)S_{secondary}]$ in eq. (5), and that Yin (2011) proposed a simplified method by using $S_{creep} = S_{creep,f}$; that is, the case $\alpha = 1$ in eq. (5). It is found that the total consolidation settlement using $S_{creep} = S_{creep,f}$ is overestimated. For example, as shown in Fig. 2, if the initial effective stress–strain state is at point 1 and the final effective stress–strain state is at point 4, $S_{creep,f}$ is calculated to be the creep under the final effective stress σ'_{z4}. This path from point 1 to point 3 to point 4 is assumed to be an instant loading path without excess pore-water pressure coupling. This path may be correct for the soil at the drainage boundary. However, the effective stress–strain paths inside the clay away from the drainage boundary will be delayed as shown in Fig. 2. This is why the use of $S_{creep} = S_{creep,f}$ with $\alpha = 1$ in eq. (5) will overestimate the creep settlement. It is also noted that when $\alpha = 0$, $S_{creep} = S_{secondary}$, which is calculated for $t \geq t_{EOP,field}$. This approach is based on Hypothesis A, which underestimates the settlement as explained before because of ignoring creep in the primary consolidation period. The new simplified Hypothesis B method in eq. (5) with a suitable value of α takes a more accurate approach to calculating the creep settlement during and after primary consolidation. It is found later in this paper that if $\alpha = 0.8$, the settlements calculated using this new simplified hypothesis B method are closer to the settlements from the fully coupled consolidation modelling.

Fig. 2. Relationship of void ratio (or strain) and log(effective stress) with different consolidation states. [Colour online.]

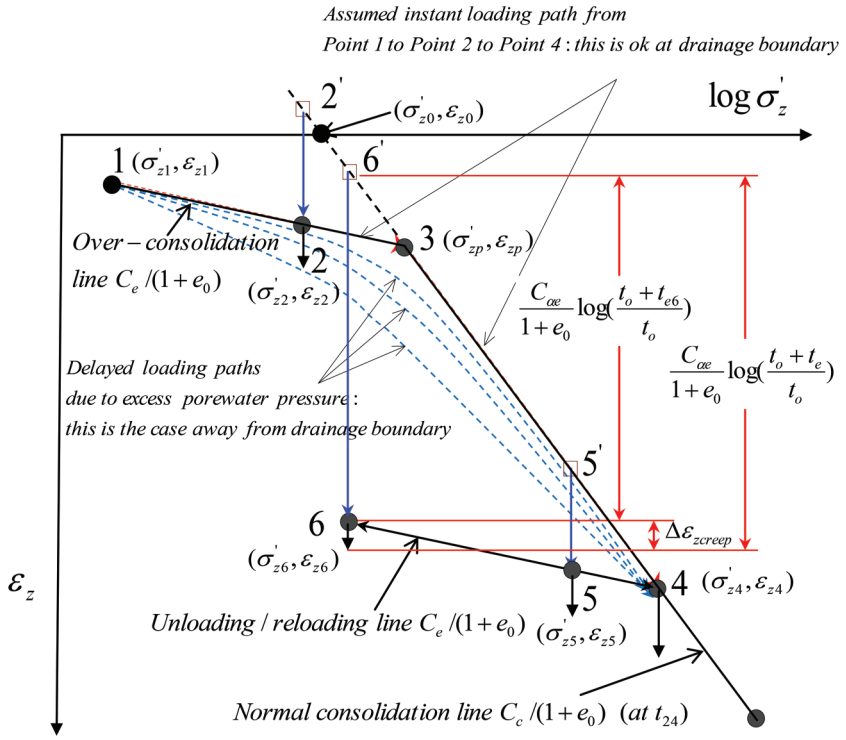

The S_f in eq. (5) is normally calculated using the "swelling" index, C_e; that is, unloading–reloading (or the OC compression) slope and compression index, C_c, using the compression data from oedometer tests. It shall be noted that the compression of a clayey soil is time-dependent. The selection of the compression data at different times will result in different compression curves. For example, referring to Fig. 1 under a certain vertical stress, the compression can be selected as the value at the EOP consolidation in the laboratory ($t_{EOP,lab}$) ($t_{EOP,lab}$ is normally a few minutes) or the time at 24 h (t_{24}). If we plot the compressions and corresponding stresses for the two durations of $t_{EOP,lab}$ and t_{24}, we have the two curves as shown in Fig. 3. It is noted that the curve using data at $t_{EOP,lab}$ is normally above the curve using data at t_{24}. The two slopes in the NC section given by the compression index C_c at $t_{EOP,lab}$ and C_c at t_{24} are about the same. In the OC range, the slope is given by C_e, which is considered to be the same for the two durations ($t_{EOP,lab}$ and t_{24}). It is also noted that the curve in unloading or reloading is normally a loop, but, is normally simplified as a straight line with the same slope as C_e as in the OC range. The only difference of the two curves in Fig. 3 is the points of the pre-consolidation stress and strain; that is, the point (σ'_{zp}, ε_{zp}) at $t_{EOP,lab}$ shall be higher than (σ'_{zp}, ε_{zp}) at t_{24}.

An oedometer test is normally done on the same specimen in oedometer in multi-stages. According to British standard 1377 (BSI 1990), the duration for each load shall normally last for 24 h. In this paper, we consider the indexes C_e, C_c, and (σ'_{zp}, ε_{zp}) are all determined from the standard oedometer test with duration of 24 h (1 day) for each load. The idealized relationship between the vertical strain and the log(effective stress) is shown in Fig. 2 with loading, unloading, and reloading states. Based on Fig. 2, the final settlements S_f in eq. (5) for two cases are calculated as follows:

Point 1 to point 2:

$$S_f = \Delta\varepsilon_{z,1\text{–}2}H = \frac{C_e}{1+e_o}\log\left(\frac{\sigma'_{z2}}{\sigma'_{z1}}\right)H \tag{6a}$$

The $\Delta\varepsilon_{z,1\text{–}2}$ is the vertical strain increase due to stress increases from σ'_{z1} to σ'_{z2}. Similar strain increase symbols are used in the following equations.

Point 1 to point 4:

$$S_f = \Delta\varepsilon_{z,1\text{–}4}H = \left[\frac{C_e}{1+e_o}\log\left(\frac{\sigma'_{zp}}{\sigma'_{z1}}\right) + \frac{C_c}{1+e_o}\log\left(\frac{\sigma'_{z4}}{\sigma'_{zp}}\right)\right]H \tag{6b}$$

where σ'_{zp} is the pre-consolidation stress.

The key part in eq. (5) is how to calculate the creep settlement $S_{creep,f}$ at the final effective stress state. Other researchers such as Mesri and Godlewski (1977) and Mesri and Choi (1984) used the ratio of $C_{\alpha e}/C_c$ to obtain the secondary compression coefficient first and used it to calculate the secondary consolidation settlement. It is noted that the ratio of $C_{\alpha e}/C_c$ varies with OC ratio (OCR). Therefore, it is difficult to use this ratio to obtain the $C_{\alpha e}$ for various stress–strain state. They only started calculating creep strains after primary consolidation at EOP.

In this paper, the authors use only two parameters for creep compression in the NC condition, for the calculation of the creep settlement $S_{creep,f}$ under any loading condition, including OC, unloading, and reloading conditions. The theoretical base of this method relies on the "equivalent time" concept (Bjerrum 1967; Yin and Graham 1989, 1994).

Figure 4 illustrates curved "time lines" in the coordinates of vertical effective stress and void ratio from 1-D straining oedometer tests (Bjerrum 1967). These parallel "time limes" also represent lines of constant plastic strain rate. Others, for example Kelln et al. (2008) have developed an EVP model that emphasizes strain rates and otherwise is very compatible with the model by Yin and Graham (1989) and Yin (2015). Yin and Graham (1989, 1994) and Yin (2015) explained that these time lines can be interoperated as equivalent time lines. The word of "equivalent" here means that the creep strain rate at a certain stress–strain state, which is reached under any loading path, is equal to the creep strain rate at

Fig. 3. Relationship of void ratio and log(effective stress) from compressions at $t_{EOP,lab}$ and t_{24}. [Colour online.]

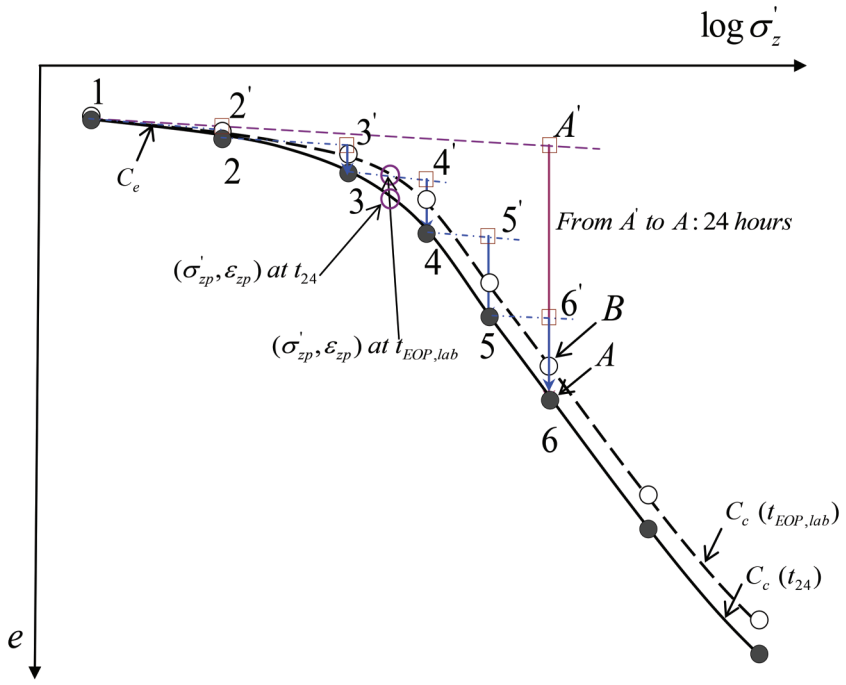

Fig. 4. Relationship of void ratio and vertical effective stress in log-scale, time lines, loading paths, and creep rate. [Colour online.]

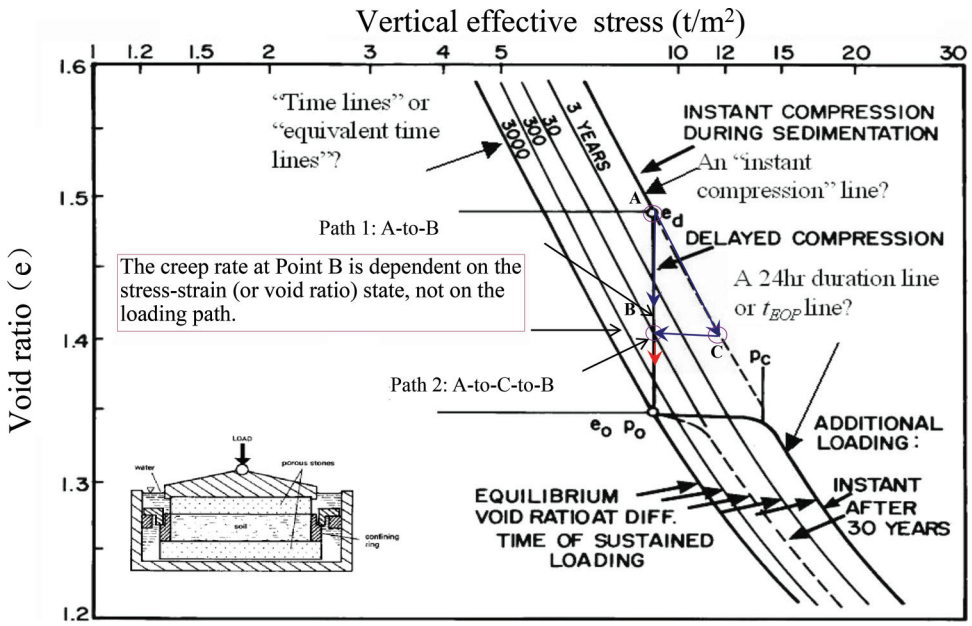

the same point, which is reached from a normal 1-D creep test loading path with the creep duration time t from a reference time line. The time t here is considered to be the equivalent time t_e with $t = t_e$. Referring to Fig. 4, we can run a normal 1-D creep test under a constant vertical stress from point A to point B (path 1: A–B). It is well known that the creep strain rate decreases with time in this case. At point B, there is still creep strain rate, say, $\dot{\varepsilon}_{zB(Path1)}$. In another approach as shown in Fig. 4, we can increase the vertical stress from point A to point C, and unload to point B and then run creep test (path 2: point A–C–B). Under this loading path, we have creep strain rate $\dot{\varepsilon}_{zB(Path2)}$. We have $\dot{\varepsilon}_{zB(Path1)} = \dot{\varepsilon}_{zB(Path2)}$. This means that the creep rate at point B is dependent on the stress–strain (or void ratio) state, not on the loading path (Yin 2015).

For the creep compression in Fig. 1, the authors suggest using the following function to fit:

$$e = e_0 - C_{\alpha e}\log\frac{t_o + t_e}{t_o} \quad (7)$$

where the parameter $C_{\alpha e}$ is newly defined in eq. (7), called creep coefficient, and t_o is another independent creep parameter with unit of time. It is noted that eq. (7) has a definition when time $t_e = 0$. The $C_{\alpha e}$ in eq. (7) is similar to the secondary consolidation coefficient $C_{\alpha e}$ as shown in Fig. 1 and in eq. (1). Why the authors use the same symbol $C_{\alpha e}$ as that in eq. (1) is not to introduce a new symbol to make the new method diffi-

cult to be used by practicing engineers. In fact, the value of the newly defined $C_{\alpha e}$ is nearly equal to the value of the old $C_{\alpha e}$.

If C_c and C_e are determined from the compression with time 24 h of duration, the authors propose t_o = 24 h = 1 day. If C_c and C_e are determined from the compression at the end of primary consolidation in the laboratory with time $t_{EOP,lab}$, then, the authors propose $t_o = t_{EOP,lab}$. The choice of time t_o and value of $C_{\alpha e}$ here does not make a significant difference to calculated creep strains.

The variable t_e in eq. (7) is the equivalent time as explained before. Equation (7) is valid when time $t_e = 0$, which is needed to consider creep occurring from the beginning of the loading. However, in the old definition of $C_{\alpha e}$ in Fig. 1, eq. (1) is not valid when the time is or near to zero.

According to the equivalent time concept (Yin and Graham 1989, 1994), the total strain ε_z at any stress–strain state in Fig. 4 can be calculated by the following equation:

$$\varepsilon_z = \varepsilon_{zp} + \frac{C_c}{V}\log\frac{\sigma'_z}{\sigma'_{zp}} + \frac{C_{\alpha e}}{V}\log\frac{t_o + t_e}{t_o} \tag{8}$$

where $\varepsilon_{zp} + \frac{C_c}{V}\log\frac{\sigma'_z}{\sigma'_{zp}}$ is the strain on the NC line (NCL) under stress σ'_z and $\frac{C_{\alpha e}}{V}\log\frac{t_o+t_e}{t_o}$ is the creep strain occurring from the NCL under the same stress σ'_z. The above equation is valid for any 1-D loading path.

Derivation of specific equations of the simplified method based on Hypothesis B for different stress–strain states

With eqs. (5), (6), (7), and (8) and the equivalent time concept, the authors derive the following specific equations for the calculation of the creep settlement $S_{creep,f}$ and the total consolidation settlement S_{totalB} for different 1-D stress–strain states.

Final stress–strain point in a NC state

Referring to Fig. 2, we assume the vertical stress is increased from the initial point 1 to point 4, which is on the NCL. The total consolidation settlement S_{totalB} is calculated by

$$S_{totalB} = S_{primary} + S_{creep} = U_v S_f + [\alpha S_{creep,f} + (1-\alpha)S_{secondary}] \quad \text{for all } t \geq 1 \text{ day } (t \geq t_{EOP,field} \text{ for } S_{secondary}) \tag{9a}$$

where

$$S_{creep,f} = \frac{C_{\alpha e}}{1+e_o}\log\left(\frac{t_o + t_e}{t_o}\right)H \tag{9b}$$

where H is the thickness of the soil layer. In this case, the equivalent time $t_e = t - t_o$, where t is duration time of the current total vertical stress. Why $t_e = t - t_o$ is explained as follows.

Assume there is no pore-water pressure coupling, this means U_v = 1. From eqs. (9) and (6*b*), we have

$$S_{totalB} = S_{primary} + S_{creep} = \frac{C_e}{1+e_o}\log\frac{\sigma'_{zp}}{\sigma'_{z1}}H + \frac{C_c}{1+e_o}\log\frac{\sigma'_{z4}}{\sigma'_{zp}}H + S_{creep} \tag{10a}$$

It is noted that $S_{creep} = \alpha\frac{C_{\alpha e}}{1+e_0}\log\left(\frac{t_o+t_e}{t_o}\right)H + (1-\alpha)\frac{C_{\alpha e}}{1+e_0}\log\left(\frac{t}{t_{EOP,field}}\right)H$. Noting t_o = 1 day (24 h), and $t_e = t - t_o = t - 1$ (day), $t_{EOP,field}$ = 1 (day) because the compression index in Fig. 2 is determined at 1 day. Therefore, at time t = 1 (day), the creep settlement is

$$S_{creep} = \alpha\frac{C_{\alpha e}}{1+e_0}\log\left(\frac{1}{1}\right)H + (1-\alpha)\frac{C_{\alpha e}}{1+e_0}\log\left(\frac{1}{1}\right)H = 0$$

If t = 1 day, eq. (10*a*) becomes

$$S_{totalB} = \frac{C_e}{1+e_o}\log\frac{\sigma'_{zp}}{\sigma'_{z1}}H + \frac{C_c}{1+e_o}\log\frac{\sigma'_{z4}}{\sigma'_{zp}}H = \Delta\varepsilon_{z,1\text{–}4}H \tag{10b}$$

It is seen from eq. (10*b*) that when time t = 1 day, the stress–strain state point is at point 4 on NCL. As explained before, the line NCL has duration of 1 day (or 24 h) from a standard oedometer test.

It should be pointed out that in eq. (9), the settlement due to dissipation of excess pore-water pressure represented by U_v is decoupled from the creep compression of the soil skeleton. This is why the present method is called a simplified one, compared to the fully coupled method in the section titled "Verification of the new simplified Hypothesis B method by comparing calculated values with test data and results from a fully coupled consolidation analysis".

Final stress–strain point in an OC state

In this section, equations are derived for calculation of the total consolidation settlement S_{totalB} when the final loading stress–strain point is in an OC state after an additional vertical stress is applied. For example, point 2, point 5, and point 6 in Fig. 2 are all in an OC state. Firstly, we derive an equation for calculating the creep strain (or settlement) for a stress–strain point in an OC state. We use point 6 as an example for this purpose.

According to the definition of equivalent time (Yin and Graham 1989, 1994), the creep strain rate at the present point 2, no matter how this point is reached in a real situation, can be considered to reach point 2 from point 2′ on the extension of the NCL by creep with an equivalent time value t_{e2}. According to eq. (8), the strain at point 2 ε_{z2} can be calculated as

$$\varepsilon_{z2} = \varepsilon_{zp} + \frac{C_c}{V}\log\frac{\sigma'_{z2}}{\sigma'_{zp}} + \frac{C_{\alpha e}}{V}\log\frac{t_o + t_{e2}}{t_o} \tag{11a}$$

From the above, we have

$$\log\frac{t_o + t_{e2}}{t_o} = (\varepsilon_{z2} - \varepsilon_{zp})\frac{V}{C_{\alpha e}} - \frac{C_c}{C_{\alpha e}}\log\frac{\sigma'_{z2}}{\sigma'_{zp}}$$

$$\therefore \frac{t_o + t_{e2}}{t_o} = 10^{(\varepsilon_{z2}-\varepsilon_{zp})(V/C_{\alpha e}) + \log(\sigma'_{z2}/\sigma'_{zp})^{C_c/C_{\alpha e}}} = 10^{(\varepsilon_{z2}-\varepsilon_{zp})(V/C_{\alpha e})}\left(\frac{\sigma'_{z2}}{\sigma'_{zp}}\right)^{-\frac{C_c}{C_{\alpha e}}}$$

From which we obtain

$$t_{e2} = t_o 10^{(\varepsilon_{z2}-\varepsilon_{zp})(V/C_{\alpha e})}\left(\frac{\sigma'_{z2}}{\sigma'_{zp}}\right)^{-\frac{C_c}{C_{\alpha e}}} - t_o \tag{11b}$$

It is seen from eq. (11*b*) that the equivalent time t_{e2} at point 2 is uniquely related to the stress–strain point (σ'_{z2}, ε_{z2}).

If we assume reloading from point 1 to point 2, the corresponding consolidation settlement can be calculated as

$$(12)\quad S_{totalB} = S_{primary} + S_{creep} = U_v S_f + [\alpha S_{creep,f} + (1-\alpha)S_{secondary}] = U_v S_f + \alpha\frac{C_{\alpha e}}{1+e_0}\log\left(\frac{t_o + t_e}{t_o + t_{e2}}\right)H + (1-\alpha)S_{secondary} \quad \text{for all } t \geq 1 \text{ day } (t \geq t_{EOP,field} \text{ for } S_{secondary})$$

in which S_f can be calculated using eq. (6*a*). t_e in eq. (12) is the total equivalent time value for creeping from point 2′ to point 2 and further downward.

The final creep settlement in eq. (12) is

$$(13)\quad S_{creep,f} = \frac{C_{\alpha e}}{1+e_0}\log\left(\frac{t_o + t_e}{t_o + t_{e2}}\right)H$$

that can be written

$$(14a)\quad S_{creep,f} = \left[\frac{C_{\alpha e}}{1+e_0}\log\left(\frac{t_o + t_e}{t_o}\right) - \frac{C_{\alpha e}}{1+e_0}\log\left(\frac{t_o + t_{e2}}{t_o}\right)\right]H = \Delta\varepsilon_{zcreep}H$$

$$(14b)\quad \Delta\varepsilon_{zcreep} = \frac{C_{\alpha e}}{1+e_0}\log\left(\frac{t_o + t_e}{t_o}\right) - \frac{C_{\alpha e}}{1+e_0}\log\left(\frac{t_o + t_{e2}}{t_o}\right)$$

Referring to Fig. 2, it is seen that $\frac{C_{\alpha e}}{1+e_0}\log\left(\frac{t_o + t_{e2}}{t_o}\right)$ is the strain from point 2′ to point 2; while $\frac{C_{\alpha e}}{1+e_0}\log\left(\frac{t_o + t_e}{t_o}\right)$ is the strain from point 2′ to point 2 and further downward. The increased strain for further creep done from point 2 is $\Delta\varepsilon_{zcreep}$, which is what we want to use to calculate creep settlement under loading at point 2. It is noted that the relationship between t_e and the creep duration time t under the stress σ'_{z2} is

$$(15)\quad t_e = t_{e2} + t - t_o$$

Substituting eq. (15) into eq. (13), we have

$$(16)\quad S_{creep,f} = \frac{C_{\alpha e}}{1+e_0}\log\left(\frac{t + t_e}{t_o + t_{e2}}\right)H$$

Therefore, the final total consolidation settlement is

$$(17)\quad S_{totalB} = S_{primary} + S_{creep} = U_v S_f + \left[\alpha\frac{C_{\alpha e}}{1+e_0}\log\left(\frac{t + t_{e2}}{t_o + t_{e2}}\right)H + (1-\alpha)S_{secondary}\right] \quad \text{for all } t \geq 1 \text{ day } (t \geq t_{EOP,field} \text{ for } S_{secondary})$$

Why is t_e calculated using eq. (14)? The explanation is similar to that in eq. (10).

If we consider the unloading from point 4 to point 6 in Fig. 2, using the same approach as for the loading from point 1 to point 2, we can derive the following equations:

$$(18)\quad t_{e6} = t_o 10^{(\varepsilon_{z6}-\varepsilon_{zp})(V/C_{\alpha e})}\left(\frac{\sigma'_{z6}}{\sigma'_{zp}}\right)^{-\frac{C_c}{C_{\alpha e}}} - t_o$$

The total consolidation settlement for unloading from point 4 to point 6 is

Fig. 5. Three layers (free drainage in the top and impermeable in the bottom) of Hong Kong marine clay (HKMC) for consolidation analyses with thicknesses of (*a*, *d*) 2 m, (*b*, *e*) 4 m, and (*c*, *f*) 8 m: (*a*–*c*) models used for Consol analysis and (*d*–*f*) models used for Plaxis analysis. [Colour online.]

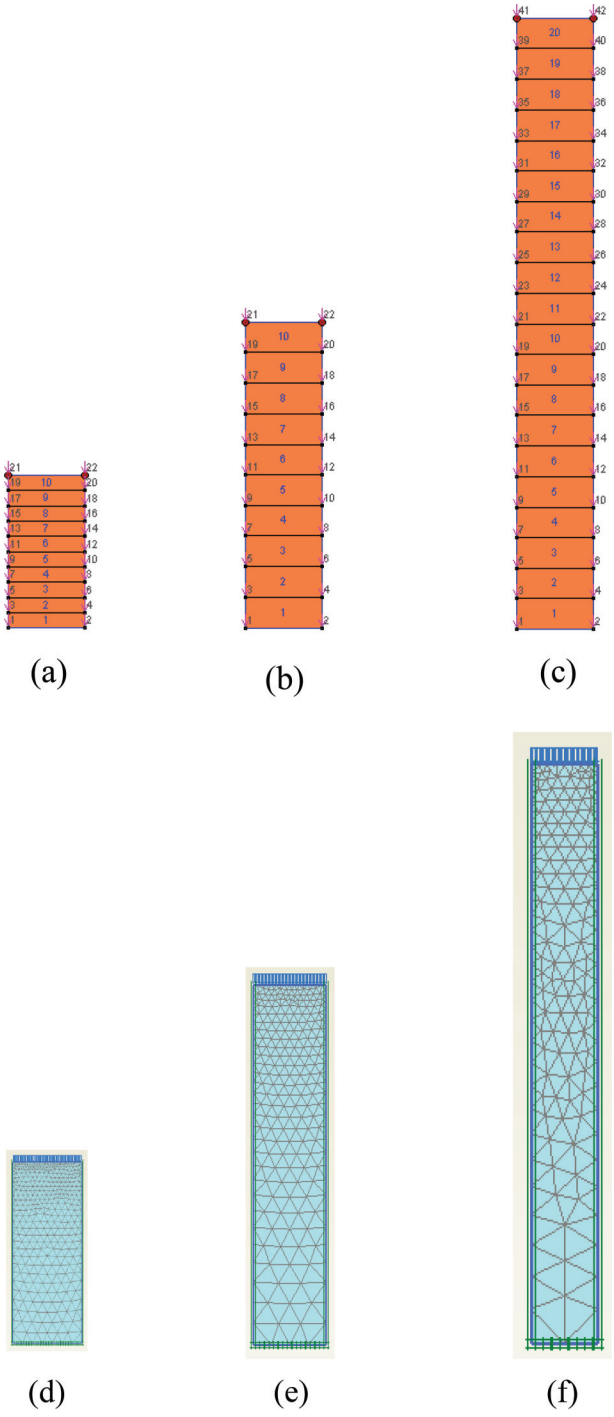

$$(19)\quad S_{totalB} = S_{primary} + S_{creep} = U_v S_f + \left[\alpha\frac{C_{\alpha e}}{1+e_0}\log\left(\frac{t + t_{e6}}{t_o + t_{e6}}\right)H + (1-\alpha)S_{secondary}\right] \quad \text{for all } t \geq 1 \text{ day } (t \geq t_{EOP,field} \text{ for } S_{secondary})$$

The following sections present the application and verification of the above equations of the new simplified Hypothesis B method.

Table 1. Values of parameters for upper marine clay of Hong Kong.

(*a*) Values of basic property							
$V = 1 + e_o$		γ_{clay} (kN/m³)	OCR		w_i (%)		
3.65		15	1, 1.5, 2		100		
(*b*) Values of parameters used in Consol software							
κ/V	λ/V	ψ/V	t_o (day)	k_v (m/day)	σ'_{z0} (kPa)		
0.01086	0.174	0.0076	1	1.90×10^{-4}	1		
(*c*) Values of parameters used in PLAXIS							
κ^*	λ^*	μ^*	t_o (day)	k_v (m/day)	OCR	c' (kPa)	ϕ' (°)
0.02172	0.174	0.0076	1	1.90×10^{-4}	1, 1.5, 2	0.1	30
(*d*) Values of parameters used in the new simplified Hypothesis B method							
C_e (= κ/ln(10))	C_c (= λ/ln(10))	$C_{\alpha e}$ (= ψ/ln(10))	V	t_o (day)	k_v (m/day)		
0.0913	1.4624	0.0639	3.65	1	1.90×10^{-4}		

Note: $\sigma'_{z0,i}$, value of effective vertical stress when vertical strain of treference time line is zero ($\varepsilon_{z0} = 0$) (further details can be found in Zhu and Yin (2000)); κ^*, modified swelling index ($\approx 2C_e/[2.3(1 + e_0)]$); λ^*, modified compression index ($= C_c/[2.3(1 + e_0)]$); μ^*, modified creep index ($= C_{\alpha e}/[2.3(1 + e_0)]$); c', effective cohesion; ϕ', effective friction angle.

Application and verification of the simplified method for consolidation settlement calculation of three Hong Kong marine clay (HKMC) layers with different overconsolidation ratio (OCR) values

Hong Kong marine clays (HKMCs) in the seabed of Hong Kong waters are problematic soils for construction of infrastructures and houses on reclamations on HKMCs in Hong Kong. For the existing two runways of Hong Kong International Airport (HKIA) on Lantau Island, all marine clays in the seabed under the runways were dredged, moved, and dumped at another seabed location. HKIA is planning to construct a third runway. For environment and political concerns, all marine deposits, including HKMC, cannot be removed and must be kept or improved in situ. In this case, the settlement, especially the post-construction settlement will be a bigger concern to safe operation of the third runway. In fact, the current construction of artificial islands on the seabed of Hong Kong as part of Hong Kong–Zhuhai–Macau Link project (29.6 km in length) will also face the problem of possible large settlements in the future.

In this section, authors select three idealized layers of HKMC (Fig. 5) to apply the new simplified method with constant values of soil parameters to calculate the consolidation settlement up to 50 years for two layers with 1 and 4 m thickness and 100 years for an 8 m layer. At the same time, two finite element (FE) programs using EVP models are also used to analyze the same layers and results are used to evaluate the accuracy of the simplified method.

Koutsoftas et al. (1987) reported findings from site investigation at an offshore field test site in Hong Kong related to construction of the existing two runways of HKIA. They found that, at this site, there were an "upper marine clay" layer in the top of the seabed (thickness from 2 to 8 m), underlain by an "upper alluvium" layer (thickness from 3 to 8 m), followed by a "lower marine clay" layer (thickness from 5 to 10 m), and a "lower alluvium" layer (thickness from 6 to 8 m) in the seabed. Handfelt et al. (1987) reported the monitoring data of a test fill at this site. Zhu et al. (2001) developed and used a FE program with Yin and Graham's 1D EVP model (Yin and Graham 1989, 1994) to analyze the consolidation settlement and excess pore-water dissipation of the soils underneath the test fill.

In this section, authors select the upper marine clay layer (called HKMC herein) for consolidation analysis with values of soil parameters from papers by Koutsoftas et al. (1987) and Zhu et al. (2001). To better interpolate the creep settlement, different OCR values (OCR = 1, 1.5, 2) are adopted in the calculation and simulation. Two FE programs are used for fully coupled consolidation analysis of the HKMC layers: one is Consol software developed by Zhu and Yin (1999, 2000), and the other one is Plaxis software (2D 2015 version). In the analysis, the 1D EVP model (Yin and Graham 1989, 1994) implemented in software Consol and a soft soil creep model in Plaxis software (2D 2015 version) are adopted in the FE simulations. The 1D EVP model was applied by Zhu and Yin (1999, 2000, 2001) for consolidation analysis. For a description of the soft soil creep model irefer to Vermeer and Neher (1999) and Plaxis user's manual (2015 version). This soft soil model has been widely used in consolidation simulations by Degago et al. (2011) and Nash and Brown (2015).

Table 2. Summary of main values used in the simplified Hypothesis B method.

Thickness (m)	t (year)	OCR	ε_{zp}	s_f (m)	m_v (kPa⁻¹)	c_v (m²/day)
2	50	1	0	0.625	0.0156	0.00124
		1.5	0.0044	0.493	0.0123	0.00157
		2	0.0075	0.399	0.0100	0.00194
4	50	1	0	0.918	0.0115	0.00169
		1.5	0.0044	0.653	0.0082	0.00237
		2	0.0075	0.465	0.0058	0.00333
8	100	1	0	1.271	0.0079	0.00244
		1.5	0.0044	0.742*	0.0046	0.00418
		2	0.0075	0.487*	0.0030	0.00636

*Final stress states of some divided sublayers are in the overconsolidation state.

The three layers of HKMC for calculation and simulation are shown in Fig. 5. In Fig. 5, the top three FE models (Figs. 5*a*–5*c*) are used for Consol analysis and the bottom three FE models (Figs. 5*d*–5*f*) for Plaxis analysis. The bottom of all layers is considered impermeable and the top of all layers is free to drain. The initial OCR value in the FE simulation is input easily in a menu in Plaxis; while this OCR value is calculated by giving the pre-consolidation pressure with depth in Consol software (Zhu et al. 2001). Values of all parameters used in FE consolidation simulation are listed in Table 1. In all FE simulations, a vertical stress of 20 kPa is assumed to be instantly applied on the top surface and kept constant for a period of 18 250 days (50 years) for two layers of 2 and 4 m thickness and 36 500 days (100 years) for the 8 m layer. The material properties reflect HKMC, but the thicknesses and boundary conditions do not.

Table 3. Values of "equivalent time" t_{e2} for all sublayers of 8 m layer with OCR = 2.

No.	Depth at middle of each sublayer (m)	$\sigma'_{z0,i}$ (kPa)	$\sigma'_{zp,i}$ (kPa)	$\sigma'_{zf,i}$ (kPa)	ε_{zp}	$\varepsilon_{zf,i}$	t_{e2}
1–8	0.25~3.75	1.3~19.46	2.6~38.93	21.3~39.5	0.0075	—	0
9	4.25	22.06	44.12	42.06	0.0075	0.00701	1.79
10	4.75	24.65	49.31	44.65	0.0075	0.00645	7.39
11	5.25	27.25	54.50	47.25	0.0075	0.00598	20.40
12	5.75	29.84	59.69	49.84	0.0075	0.00557	46.87
13	6.25	32.44	64.88	52.44	0.0075	0.00522	95.43
14	6.75	35.03	70.07	55.03	0.0075	0.00491	177.39
15	7.25	37.63	75.26	57.62	0.0075	0.00463	306.61
16	7.75	40.22	80.45	60.22	0.0075	0.00438	499.17

Approach used in the simplified method for consolidation settlement calculation of a 2 m thick layer

For the simplified method calculation, referring to Fig. 2, the initial and final stress–strain states in this 2 m thick layer must be correctly determined. Assuming the initial strain is zero under the initial stress state, while the initial effective stress state and pre-consolidation stress are different at different depths and different OCR values. If the thickness of a soil layer is less than 1 m, we can assume the initial effective stress and pre-consolidation stress to be constant with negligible error. However for a thick layer, it is necessary to consider such variations. The total layer thickness in this case is 2 m. We divide this layer into four soil sublayers with 0.5 m thickness for calculation of consolidation settlement to obtain sufficiently accurate results.

Firstly, the initial effective stress state is determined from the saturated unit weight of the HKMC at the mid-depth of each sublayer, considering the water unit weight as 9.81 kN/m^3. Based on the initial effective stress state, the pre-consolidation stress and final effective stress state at the center of each part can be calculated from eq. (20)

$$\begin{aligned} \sigma'_{z0,i} &= (\gamma_{clay} - \gamma_w)z_i \\ \sigma'_{zf,i} &= \sigma'_{z0,i} + \Delta\sigma'_z \\ \sigma'_{zf,i} &= \mathrm{OCR}\sigma'_{z0,i} \end{aligned} \tag{20}$$

where γ_{clay} is unit weight of clay, z_i is the mid-depth location of each sublayer i, $\Delta\sigma'_z$ is the stress increment, taken as 20 kPa in this calculation, $\sigma'_{z0,i}$, $\sigma'_{zf,i}$, and $\sigma'_{zp,i}$ are the initial effective stress states, final effective stress states, and pre-consolidation stresses for different depths soil sublayers, respectively. Referring to Fig. 2, the initial effective stress state is schematically at point 1 for OCR = 1.5 or 2; while the initial effective stress state is at point 3 for OCR = 1 (a NC case).

Secondly, in this case, after the stress increase of 20 kPa, final effective is always larger than pre-consolidation stress for each sublayer, which indicates that the final stress–strain state is in a NC state, that is, at point 4 (σ'_{z4}, ε_{z4}) as shown in Fig. 2. As a result, eq. (6*b*) is adopted to determine the primary consolidation final settlement $S_{f,i}$ for each sublayer i of 0.5 m thickness for OCR = 1.5 or 2, and eq. (6*b*) is used in the case of OCR = 1. By summing "primary consolidation" final settlements of all sublayers, the average values of "coefficient of volume compressibility", m_v, and the "coefficient of consolidation", c_v, can be obtained from eq. (21)

$$\begin{aligned} S_f &= \sum_{i=1}^{n} S_{f,i} \\ m_v &= \frac{1}{H}\frac{S_f}{\Delta\sigma'_z} \\ c_v &= \frac{k_v}{m_v\gamma_w} \end{aligned} \tag{21}$$

where H is the thickness of the whole soil layer. Average values of S_f, m_v, and c_v for different OCR values of the whole soil layer are listed in Table 2. It is noted that coefficient of volume compressibility, m_{vi}, and the coefficient of consolidation, c_{vi}, are different for different sublayers. Thirdly, the time factor, T_v, and the average degree of consolidation, U_v, can be calculated by substituting the value of c_v into following equations:

$$\begin{aligned} U_v &= \sqrt{\frac{4T_v}{\pi}} \quad \text{for } U_v \le 0.6 \\ U_v &= 1 - 10^{-[(T_v+0.085)/0.933]} \quad \text{for } U_v > 0.6 \end{aligned} \tag{22}$$

where $T_v = c_v t/d^2$ and d is the length of the longest drainage path. When top of the soil layer is drainage and the bottom is impermeable, $d = H$, while both top and bottom of the soil layer are drainage, $d = H/2$. In this case, $d = 2$ m is adopted for the boundary condition mentioned above. Lastly, the creep compression is calculated by adopting eqs. (9*a*) and (9*b*) as the final effective stress–strain state is in a NC state for all three OCR values.

To compare all methods for the creep settlement calculations, hypothesis A method is also used to calculate the curve of settlement and log(time) in both primary consolidation and the secondary consolidation period using eq. (1).

Approach used in the simplified method for consolidation settlement calculation of a 4 m thick layer

All the procedures and steps used in the 2 m thick layer case are adopted for consolidation settlement calculation of a 4 m thick layer case here. The final effective stress–strain state in all sublayers of the 4 m thick later is in a NC state for all three OCR values. Values of the final settlement of "primary consolidation" S_f, the average values of "coefficient of volume compressibility", m_v, and "coefficient of consolidation", c_v, of the whole layer are obtained and listed in Table 2.

Approach used in the simplified method for consolidation settlement calculation of an 8 m thick layer

Following the same procedures used in the 2 m layer case, the initial effective stress state, final effective stress state, and pre-consolidation stress for each sublayer (0.5 m) of an 8 m thick layer are determined. It is found that all the final effective stress states are in the NC state for OCR = 1, which means all calculations are similar to 4 m thick layer. However, it is found that some sublayers of the soil are still in an OC state for OCR = 1.5 or 2 after the stress increment of 20 kPa. As a result, the total consolidation settlement for the final stress–strain state in the OC state should be considered in this section.

Take OCR = 2 as an example, the final stress–strain state after the 20 kPa is in the NC state for each part of the top 4 m while OC state for the bottom 4 m, corresponding to point 2 (σ'_{z2}, ε_{z2}) in Fig. 2. The primary consolidation final settlement $S_{f,i}$ of each part is calculated from eq. (6*b*) for each sublayer of the soil in a NC state; eq. (6*a*) for each sublayer of the soil in an OC state. Values of

Fig. 6. Comparison of settlement–log(time) curves from the old simplified Hypothesis B method, Hypothesis A method, two finite element (FE) models, and the new simplified Hypothesis B method for 2 m thick layer: (*a*) OCR = 1, (*b*) OCR = 1.5, and (*c*) OCR = 2. [Colour online.]

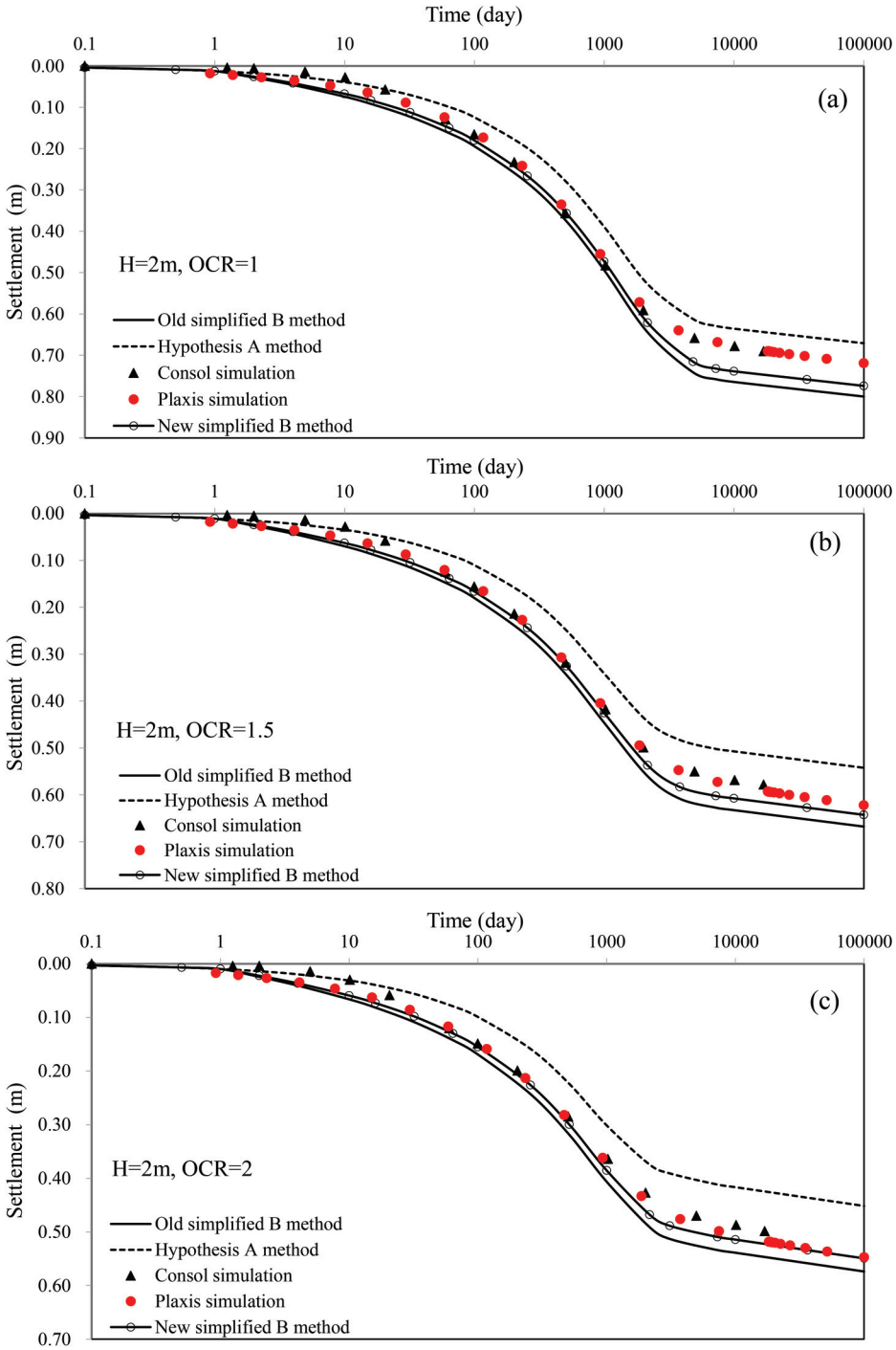

S_f, m_v, and c_v, of the whole layer can be calculated from eq. (21) and listed in Table 2. Then, values of T_v and U_v are calculated using eq. (22). To obtain the creep compression with eq. (13) for the final effective stress state in an OC state, the equivalent time t_{e2} should be correctly calculated for each sublayer using eq. (11*b*). All values of equivalent time t_{e2} use eq. (11*b*) and are listed in Table 3.

Comparison and discussion of results from the old and new simplified Hypothesis B methods, Hypothesis A method, and FE simulations

Settlements calculated using the old simplified Hypothesis B method, $S_{totalB\text{-}old}$ (Yin 2011); Hypothesis A method, S_{totalA}; two FE simulations (Consol and Plaxis); and the new simplified Hypothesis B method, $S_{totalB\text{-}new}$, for all three soil layers (2, 4, and 8 m) mentioned above are examined in this section. It is noted that for each soil layer, we consider three OCRs of 1, 1.5, and 2. Figure 6 shows comparison of settlement–log(time) curves from the old simplified hypothesis B method (α = 1), Hypothesis A method (α = 0), two FE models (Consol simulation and Plaxis simulation), and the new simplified Hypothesis B method (α = 0.8) for OCR = 1, 1.5, and 2. It is found that the Plaxis simulation results with the soft soil creep model are in good consistence and agreement with results from Consol analysis using the 1D EVP model (Yin and Graham 1989, 1994). The

Fig. 7. Comparison of settlement–log(time) curves from the old simplified Hypothesis B method, Hypothesis A method, two FE models, and the new simplified Hypothesis B method for 4 m thick layer: (*a*) OCR = 1, (*b*) OCR = 1.5, and (*c*) OCR = 2. [Colour online.]

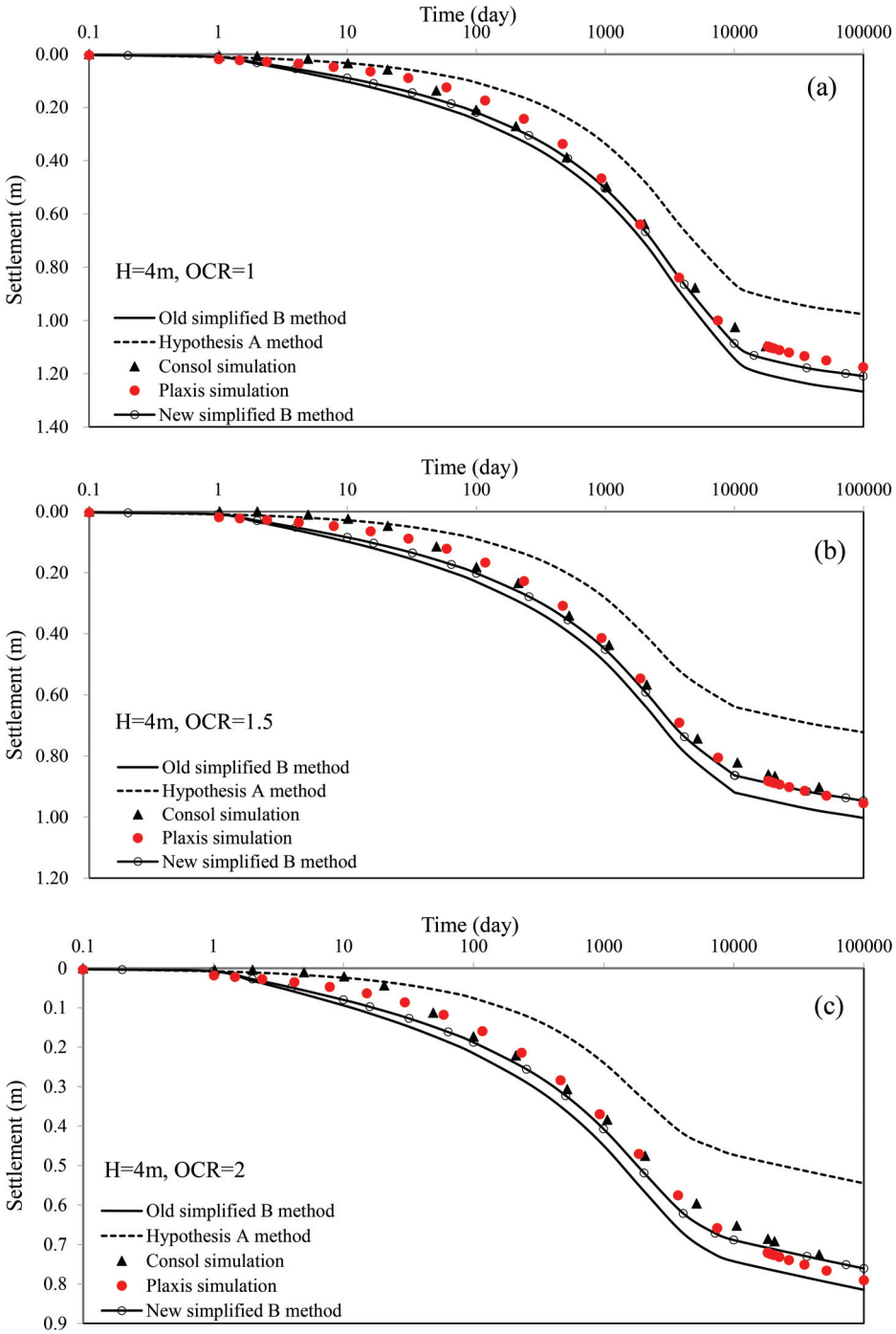

FE models are for fully coupled consolidation analysis of soils with creep and shall be credible as the rigorous Hypothesis B method.

Comparing with the FE results in Fig. 6, Hypothesis A method ($\alpha = 0$) underestimates the total settlement; while the old simplified Hypothesis B method ($\alpha = 1$) (Yin 2011) overestimates the total settlement. In overall, the settlement curves calculated using the new simplified Hypothesis B method ($\alpha = 0.8$) is much closer to curves computed using Plaxis (2015 version) and Consol (Zhu and Yin 1999, 2000) when compared to other two methods.

Based on the comparison of curves in Fig. 6 for three OCR values, it is observed that the curves from the old simplified method ($\alpha = 1$) are always below the curves from Plaxis and Consol simulations. The reason for the overestimation of the settlement is that the creep part in eq. (9*b*) in the old simplified Hypothesis B method is directly calculated based on the final effective stress–strain state, ignoring the time needed to arrive at this final effective stress state during consolidation (see Fig. 2). The old simplified Hypothesis B method may be valid for a very thin soil layer, say less than 0.1 m; while thicker soil layers need more time to arrive at the final effective stress–strain state, especially when hydraulic conductivity is low. The soil layer thickness in Fig. 6 is 2 m with bottom impermeable and the time t_{EOP} at 98% of consolidation is 4840 days for OCR equal to 1. This is why the old simplified Hypothesis B method overpredicts the creep compression. To overcome this limita-

Fig. 8. Comparison of settlement–log(time) curves from the old simplified Hypothesis B method, Hypothesis A method, two FE models, and the new simplified Hypothesis B method for 8 m thick layer: (*a*) OCR = 1, (*b*) OCR = 1.5, and (*c*) OCR = 2. [Colour online.]

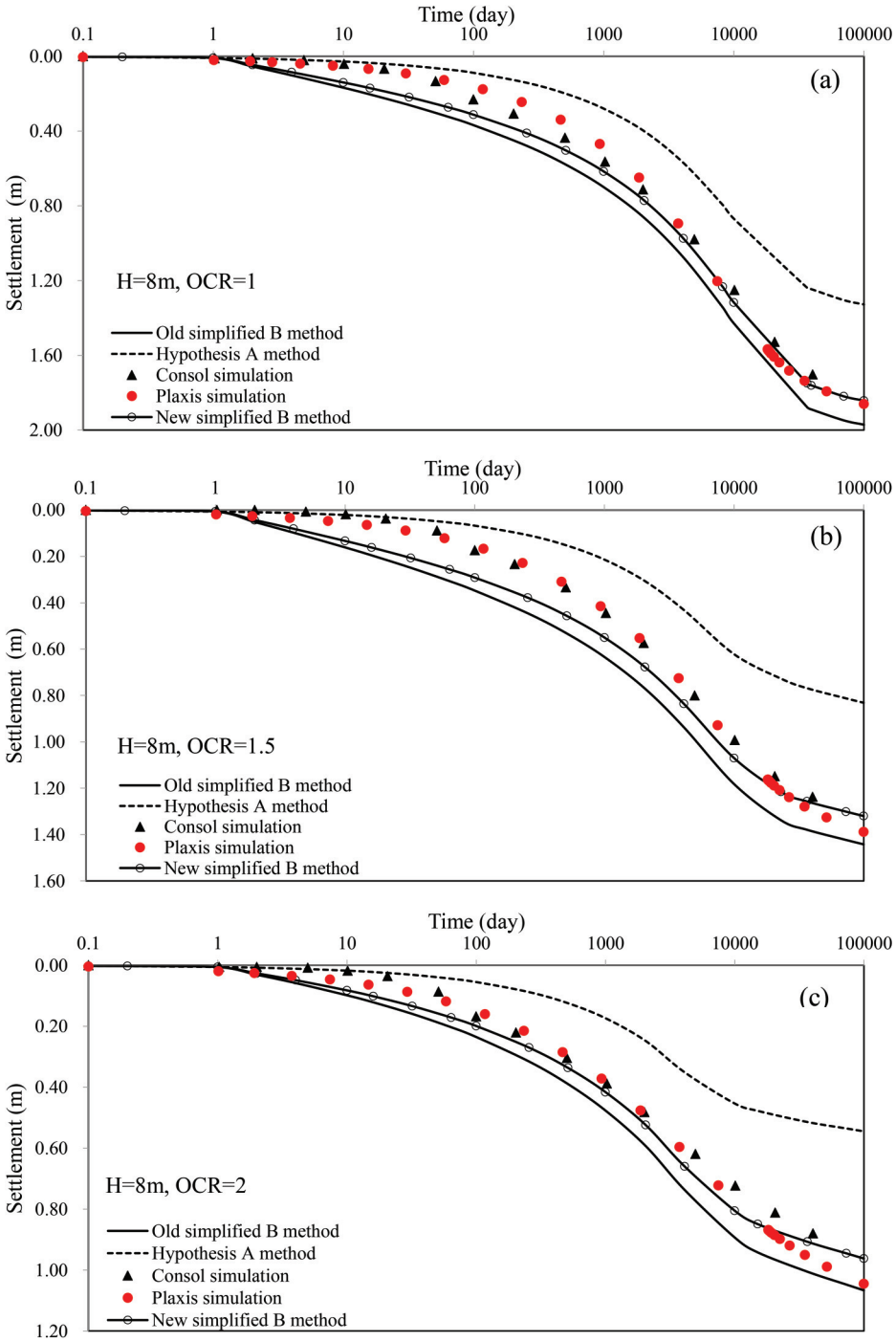

tion, the authors have tried different values of α in eq. (5) or (9). It is found that the value of 0.8 for α results in calculated curves that are in the best overall agreement with curves from Plaxis and Consol, not only for the layer thickness of 2 m, but also for 4 and 8 m cases (see Figs. 6, 7, and 8).

The authors have calculated relative errors of the old simplified Hypothesis B method, the new simplified Hypothesis B method, and Hypothesis A method for the final settlements at 50 years for 2 and 4 m layers by comparing with the settlements from Plaxis simulation. For example, the relative error for the new simplified hypothesis B method is defined as

$$\text{Relative error} = \left| \frac{S_{\text{totalB,-new}} - S_{\text{FE,Plaxis}}}{S_{\text{FE,Plaxis}}} \right| \quad (\%)$$

where $S_{\text{totalB–new}}$ is the total settlement calculated using the new simplified hypothesis B at 50 years for 2 and 4 m thick layers (or 100 years for 8 m thick layer) of HKMC; $S_{\text{FE,Plaxis}}$ is the settlement from Plaxis at the same time for the same layer.

All values of the relative errors are listed in Table 4. It is found that the relative errors of Hypothesis A method are in the range 6.52%~17.86% with underestimation of the settlements. The rela-

Table 4. Settlements and relative error values for Hypothesis A method, the old and new simplified Hypothesis B methods for three Hong Kong marine clay (HKMC) layers.

Case: layer thickness; duration	OCR	S_{FE} Plaxis FE result (m)	S_{totalA} (m)	$S_{totalB-old}$ (m)	$S_{totalB-new}$ (m)	S_{totalA} error (%)	$S_{totalB-old}$ error (%)	$S_{totalB-new}$ error (%)
2 m; 50 years	1	0.690	0.645	0.774	0.748	6.52	12.16	8.42
	1.5	0.593	0.516	0.642	0.616	12.91	8.22	4.00
	2	0.518	0.426	0.548	0.523	17.86	5.71	0.99
4 m; 50 years	1	1.098	0.919	1.209	1.151	16.34	10.13	4.83
	1.5	0.882	0.670	0.951	0.894	24.01	7.78	1.42
	2	0.721	0.493	0.763	0.709	31.60	5.83	1.65
8 m; 100 years	1	1.742	1.238	1.877	1.748	28.95	7.70	0.37
	1.5	1.286	0.768	1.379	1.257	40.24	7.24	2.26
	2	0.955	0.514	1.005	0.907	46.17	5.26	5.02

tive errors of the old simplified Hypothesis B method are in the range 5.71%~12.16% with overestimation of the settlements. The relative errors of the new simplified Hypothesis B method are generally in the range 0.99%~8.42% with settlements closer to those from the two FE simulations.

Figure 7 presents the comparisons of curves calculated using the old simplified Hypothesis B method, Hypothesis A method, two FE models, and the new simplified Hypothesis B method for a soil layer with 4 m thick. Again, Hypothesis A method underestimates the total settlement during the whole stage. The curves from the new simplified Hypothesis B method are much closer to the curves from two FE simulations. Values of the relative errors are also listed in Table 4.

Figure 8 shows the comparisons of calculated curves using the old simplified Hypothesis B method, Hypothesis A method, two FE models, and the new simplified Hypothesis B method for an 8 m thick soil layer. Again, the curves from the new simplified Hypothesis B method are much closer to the curves from two FE simulations compared with other two methods. Values of the relative error are also listed in Table 4.

This paper has been built on the idea of equivalent times proposed originally in Yin and Graham (1989, 1994). It assumes that viscous behaviour is a fundamental property of clays. More recently, Kelln et al. (2008) have expressed very similar ideas in terms of strain rates.

Verification of the new simplified Hypothesis B method by comparing calculated values with test data and results from a fully coupled consolidation analysis

Berre and Iversen (1972) presented a laboratory physical modeling study on the consolidation behaviour of a natural post-glacial marine clay from Drammen exhibiting creep. Yin and Graham (1996) applied the 1D EVP model in eq. (3) in the fully coupled consolidation analysis in eq. (2) of all consolidation tests by Berre and Iversen (1972). The consolidation problem was solved using a FD method. The calculated results were compared with the measured data and were found in good agreement (Yin and Graham 1996). In this section, we use the old simplified Hypothesis B method and the new simplified hypothesis B method to calculate the curves of average strain ($\Delta S/H_0$) versus log(time) with a comparison with the test data and curves from the fully coupled consolidation analysis computed by Yin and Graham (1996) using a FD method (denoted as FD EVP model), and where ΔS is the settlement increment under increment 5 and H_0 is the initial thickness of the soil layers in test 6 and test H4 in the original paper. Basic parameters used in the simplified methods are listed in Table 5. Values of initial stress, initial strain, and time duration for two tests at increment 5 are listed in Table 6.

As the tests consisted of multi-staged loading with various time durations, the stress–strain state should be correctly determined before the simplified method is used. In addition, it is important

Table 5. Values of parameters used in the simplified Hypothesis B method based on data from Berre and Iversen (1972).

C_e (= κ/ln(10))	C_c (= λ/ln(10))	$C_{\alpha e}$ (= ψ/ln(10))	V	t_0 (min)	σ'_{z0} (kPa)	k_v (m/min)
0.0236	0.9313	0.0413	2.56	40	79.2	3.0×10^{-6}

to determine the pre-consolidation pressure σ'_{zp}. As both point (σ'_{z0}, ε_{z0}) and point 3 (σ'_{zp}, ε_{zp}) are on the reference time line, as shown in Fig. 2, we shall have

$$\varepsilon_{zp} = \varepsilon_{z0} + \frac{C_c}{V}\log\left(\frac{\sigma'_{zp}}{\sigma'_{z0}}\right) \quad (23)$$

Referring to Fig. 2, if we assume the known initial effective stress–strain state is point 1 (σ'_{z1}, ε_{z1}) on the OC line, there should be a relationship with the pre-consolidation pressure, point 3 (σ'_{zp}, ε_{zp}), as follows:

$$\varepsilon_{zp} = \varepsilon_{z1} + \frac{C_e}{V}\log\left(\frac{\sigma'_{zp}}{\sigma'_{z1}}\right) \quad (24)$$

Combining eqs. (23) and (24)

$$\log\sigma'_{zp} = \left[(\varepsilon_{z1} - \varepsilon_{z0}) + \left(\frac{C_c}{V}\log\sigma'_{z0} - \frac{C_e}{V}\log\sigma'_{z1}\right)\right]\frac{V}{C_c - C_e}$$

$$\sigma'_{zp} = 10^{\left\{(\varepsilon_{z1}-\varepsilon_{z0})+\left[(C_c/V)\log\sigma'_{z0}-(C_e/V)\log\sigma'_{z1}\right]\right\}[V/(C_c-C_e)]} \quad (25)$$

With eq. (25), the pre-consolidation pressure, σ'_{zp}, can be calculated; values of σ'_{zp} are listed in Table 6. After the increment stress, the final effective stresses in two tests are corresponding to point 4. The calculation steps are similar to those in the previous sections. Values of the corresponding incremental final strain for primary consolidation, the average values of m_v, and c_v, of the whole layer are also determined and listed in Table 6. Figure 9 shows a comparison of curves from tests, an FD EVP model, the old simplified Hypothesis B method, Hypothesis A method, the new simplified Hypothesis B method for test 6 and test H4 at increment 5.

Similar to those comparisons with curves from two FE simulations in Figs. 6, 7, and 8, it is found that the Hypothesis A method largely underestimates the average strain ($\Delta S/H_0$), for test 6 and test H4. And curves from the old simplified Hypothesis B method agree well with the measured data for test 6; while quite below the test data for H4. It is noted that the soil specimen of test H4 had thickness of 0.45 m; while the specimen thickness of test 6 was only 0.0757 m.

When the correction factor α of 0.8 is applied, as shown in Fig. 9, the curves from the new simplified Hypothesis B method

Table 6. Summary of main values calculated and used in the simplified Hypothesis B method at increment 5 from Berre and Iversen (1972).

Test No.	t (min)	ε_{z1} (%)	σ'_{z1} (kPa)	σ'_{zp} (kPa)	$\sigma'_{z,f}$ (kPa)	$\Delta\varepsilon_f$ (%)	m_v (KPa^{-1})	c_v (×10^{-6} m^2/min)
6	5694	5.51	90.3	112.88	140.5	3.55	0.0744	4.11
H4	61 450	5.25	89.2	111.05	134.7	3.14	0.0690	4.43

Fig. 9. Comparison settlement/thickness ($\Delta S/H_0$) – log(time) curves from two tests, an FD EVP model, the old simplified Hypothesis B method, Hypothesis A method, and the new simplified Hypothesis B method for (*a*) test 6 and (*b*) test H4 at increment 5. [Colour online.]

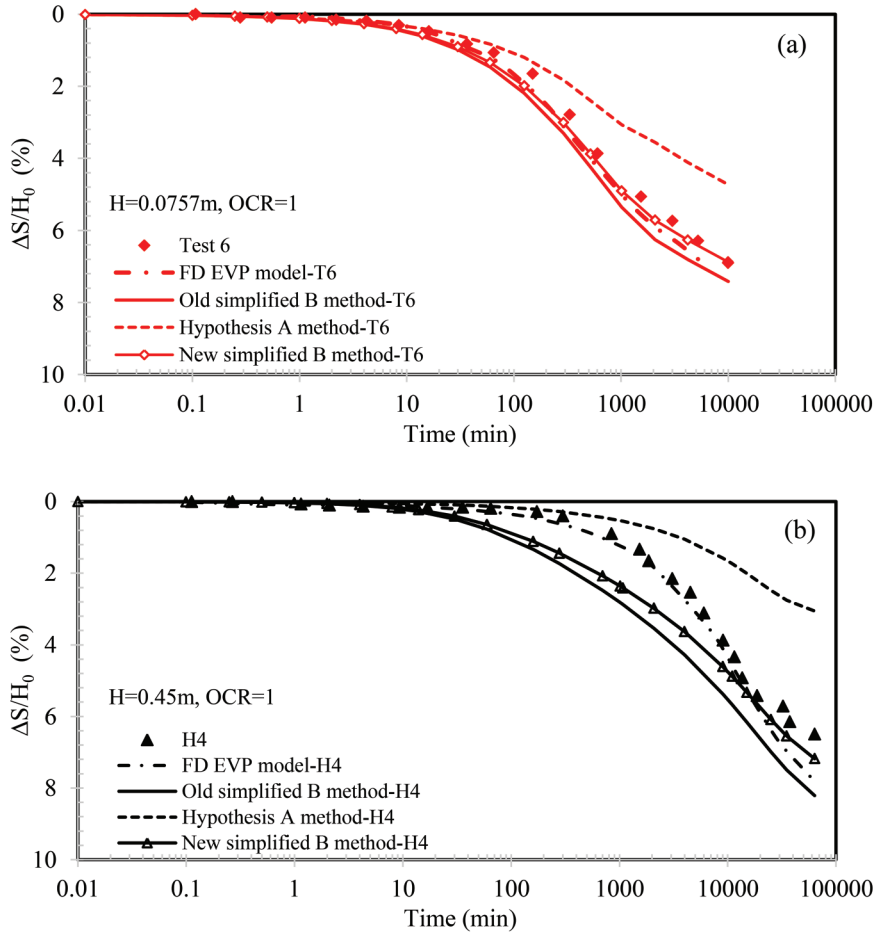

Table 7. Relative error values for Hypothesis A method, the old simplified hypothesis B method, and the new simplified Hypothesis B method for three tests at increment 5 from Berre and Iversen (1972).

Test No.	Test data ($\Delta S/H$) (%)	S_{totalA} ($\Delta S/H$) (%)	$S_{totalB-old}$ ($\Delta S/H$) (%)	$S_{totalB-new}$ ($\Delta S/H$) (%)	S_{totalA} error (%)	$S_{totalB-old}$ error (%)	$S_{totalB-new}$ error (%)
6	6.905	4.64	7.415	6.86	32.79	7.38	0.65
H4	6.497	3.055	8.21	7.18	52.98	26.42	10.52

are much closer to the test data. Values of the relative errors are listed in Table 7. The relative error here is defined as the absolute difference between the calculated value and the measured data at the end of the test over the measured data. Again, the relative errors of the new simplified Hypothesis B method are the lowest among all three simple methods.

With the verification of the new simplified Hypothesis B method by using test data from Berre and Iversen (1972), it is confirmed that the new simplified Hypothesis B method is more accurate than Hypothesis A method and the old simplified Hypothesis B method, and can be applied in reality to predict the 1-D consolidation settlement of a single layer of soil with creep with good accuracy.

Conclusions

Based on the equivalent time concept, a new simplified Hypothesis B method has been proposed to calculate the consolidation settlement of a single layer of a clayey soil with creep for different stress–strain states. To verify the accuracy of the new simplified Hypothesis B method, the values from two fully coupled FE consolidation analysis programs and previous laboratory measured

data have been compared with curves obtained using the old simplified Hypothesis B method, the new simplified Hypothesis B method, and Hypothesis A method. Based on the results and discussion in the previous sections, main conclusions are drawn as follows:

1. The proposed new simplified Hypothesis B method is a suitable simple method by spread-sheet calculation of the 1-D consolidation settlement of a single layer of a clayey soil with creep.
2. For cases of three layers of HKMC with OCR of 1, 1.5, and 2, it is found that hypothesis A method generally underestimates the consolidation settlement compared to the FE simulations. The relative errors for the three HKMC layers are in the range of 6.52%~46.17%, which is too large to be acceptable for any design.
3. The old simplified Hypothesis B method (Yin 2011) overestimates the final consolidation settlement with errors in the range of 5.26%~12.16% for all the cases of the three HKMC layers. The reason of the overestimation is that the creep part is calculated based on the final effective stress–strain state, ignoring the consolidation time (or the excess pore-water pressure coupling) to arrive at this final stress state. To overcome this limitation, a correction factor $\alpha = 0.8$ is used in the creep parts of the new simplified Hypothesis B method in eq. (5). By comparison, it is found that results from the new simplified Hypothesis B method are much closer to curves from the FE simulations and data from tests. The relative errors of the new simplified Hypothesis B method are in the range of 0.37% to 8.42%, the smallest among all three simplified methods.
4. It is found that the curves from the new simplified Hypothesis B method are in good consistency and agreement with test data from Berre and Iversen (1972). This comparison verifies the accuracy and applicability of the new simplified Hypothesis B method.

Based on the comparison, discussion, and findings above, the authors recommend that the new simplified Hypothesis B method with $\alpha = 0.8$ can be used for calculation of consolidation settlement of a single layer of a soil with creep for designs. The authors also recognise that more comparisons with fully coupled consolidation simulations and physical model tests are necessary to further examine the validation of this new simplified Hypothesis B method.

Acknowledgements

The work in this paper is supported by a research grant (project No. 51278442) from the National Natural Science Foundation of China (NSFC), a general research fund (GRF) (project No. PolyU 152196/14E) from Research Grants Council (RGC) of Hong Kong Special Administrative Region Government of China, and grants (4-BCAW, G-YM28, G-YN97, B-Q43L) from The Hong Kong Polytechnic University, China.

References

Barden, L. 1965. Consolidation of clay with non-linear viscosity. Géotechnique, **15**(4): 345–362. doi:10.1680/geot.1965.15.4.345.

Barden, L. 1969. Time-dependent deformation of normally consolidated clays and peats. Journal of the Soil Mechanics and Foundation Division, ASCE, **95**(SM1): 1–31.

Berre, T., and Iversen, K. 1972. Oedometer tests with different specimen heights on a clay exhibiting large secondary compression. Géotechnique, **22**(1): 53–70. doi:10.1680/geot.1972.22.1.53.

Bjerrum, L. 1967. Engineering geology of Norwegian normally-consolidated marine clays as related to the settlements of buildings. Géotechnique, **17**(2): 83–118. doi:10.1680/geot.1967.17.2.83.

BSI. 1990. Methods of test for soils for civil engineering purposes (Part 5). British standard 1377-5. British Standards Institution, London.

Craig, R.F. 2004. Soil mechanics. 7th ed. Spon Press, New York.

Degago, S.A., Grimstad, G., Jostad, H.P., Nordal, S., and Olsson, M. 2011. Use and misuse of the isotache concept with respect to creep hypotheses A and B. Géotechnique, **61**(10): 897–908. doi:10.1680/geot.9.P.112.

Garlanger, J.E. 1972. The consolidation of soils exhibiting creep under constant effective stress. Géotechnique, **22**(1): 71–78. doi:10.1680/geot.1972.22.1.71.

Gibson, R.E., and Lo, K.-Y. 1961. A theory of consolidation for soils exhibiting secondary compression. Publication 41, pp. 1–16. Norwegian Geotechnical Institute, Oslo.

Graham, J., Crooks, J.H.A., and Bell, A.L. 1983. Time effects on the stress-strain behaviour of natural soft clays. Géotechnique, **33**: 327–340. doi:10.1680/geot.1983.33.3.327.

Handfelt, L.D., Koutsoftas, D.C., and Foott, R. 1987. Instrumentation for test fill in Hong Kong. Journal of Geotechnical Engineering, **113**(GT2): 127–146. doi:10.1061/(ASCE)0733-9410(1987)113:2(127).

Hinchberger, S.D., and Rowe, R.K. 2005. Evaluation of the predictive ability of two elastic-viscoplastic constitutive equations. Canadian Geotechnical Journal, **42**(6): 1675–1694. doi:10.1139/t05-082.

Kelln, C., Sharma, J., Hughes, D., and Graham, J. 2008. An improved elastic-viscoplastic soil model. Canadian Geotechnical Journal, **45**(10): 1356–1376. doi:10.1139/T08-057.

Koutsoftas, D.C., Foott, R., and Handfelt, L.D. 1987. Geotechnical investigations offshore Hong Kong. Journal of Geotechnical Engineering, **113**(2): 87–105. doi:10.1061/(ASCE)0733-9410(1987)113:2(87).

Ladd, C.C., Foott, R., Ishihara, K., Schlosser, F., and Poulos, H.J. 1977. Stress-deformation and strength characteristics. *In* Proceedings, 9th International Conference on Soil Mechanics and Foundation Engineering, Tokyo, 4210494. Estimating settlements of structures supported on cohesive soils. Special summer program.

Leroueil, S., Kabbaj, M., Tavenas, F., and Bouchard, R. 1985. Stress-strain-time rate relation for the compressibility of sensitive natural clays. Géotechnique, **35**(2): 159–180. doi:10.1680/geot.1985.35.2.159.

Mesri, G., and Choi, Y.K. 1984. Time effect on the stress-strain behaviour of natural soft clays [Discussion]. Géotechnique, **34**(3): 439–442.

Mesri, G., and Godlewski, P.M. 1977. Time- and stress-compressibility interrelationship. Journal of Geotechnical Engineering, **103**(GT5): 417–430.

Nash, D., and Brown, M. 2015. Influence of destructuration of soft clay on time-dependent settlements: comparison of some elastic viscoplastic models. International Journal of Geomechanics, **15**: A4014004. doi:10.1061/(ASCE)GM.1943-5622.0000281.

Nash, D.F.T., and Ryde, S.J. 2000. Modelling the effects of surcharge to reduce long term settlement of reclamations over soft clays. *In* Proceedings of the Soft Soil Engineering Conference, Japan, 2000.

Nash, D.F.T., and Ryde, S.J. 2001. Modelling consolidation accelerated by vertical drains in soils subject to creep. Géotechnique, **51**(3): 257–273. doi:10.1680/geot.2001.51.3.257.

Olson, R.E. 1998. Settlement of embankments on soft clays (The Thirty-First Terzaghi Lecture). Journal of Geotechnical and Environmental Engineering, **124**(4): 278–288. doi:10.1061/(ASCE)1090-0241(1998)124:4(278).

Terzaghi, K. 1943. Theoretical soil mechanics. Wiley, New York.

Vermeer, P.A., and Neher, H.P. 1999. A soft soil model that accounts for creep. *In* Proceedings of Beyond 2000 in Computational Geotechnics10 Years of Plaxis International, Balkema, pp. 249–261.

Yin, J.H. 2011. From constitutive modeling to development of laboratory testing and optical fiber sensor monitoring technologies. Chinese Journal of Geotechnical Engineering, **33**(1): 1–15. [14th "Huang Wen-Xi Lecture" in China.]

Yin, J.H. 2015. Fundamental issues of constitutive modelling of the time-dependent stress-strain behavior of geomaterials. International Journal of Geomechanics, **15**(5): A4015002, 1~9. doi:10.1061/(ASCE)GM.1943-5622.0000485.

Yin, J.-H., and Graham, J. 1989. Viscous-elastic-plastic modelling of one-dimensional time-dependent behaviour of clays. Canadian Geotechnical Journal, **26**(2): 199–209. doi:10.1139/t89-029.

Yin, J.-H., and Graham, J. 1994. Equivalent times and one-dimensional elastic viscoplastic modelling of time-dependent stress–strain behaviour of clays. Canadian Geotechnical Journal, **31**(1): 42–52. doi:10.1139/t94-005.

Yin, J.-H., and Graham, J. 1996. Elastic visco-plastic modelling of one-dimensional consolidation. Geotechnique, **46**(3): 515–527. doi:10.1680/geot.1996.46.3.515.

Zhu, G.F., and Yin, J.-H. 1999. Finite element analysis of consolidation of layered clay soils using an elastic visco-plastic model. International Journal for Numerical and Analytical Methods in Geomechanics, **23**: 355–374. doi:10.1002/(SICI)1096-9853(19990410)23:4<355::AID-NAG975>3.0.CO;2-D.

Zhu, G.F., and Yin, J.-H. 2000. Elastic visco-plastic finite element consolidation modeling of Berthierville test embankment. International Journal of Numeric and Analytical Methods in Geomechanics, **24**: 491–508. doi:10.1002/(SICI)1096-9853(20000425)24:5<491::AID-NAG78>3.0.CO;2-V.

Zhu, G.F., Yin, J.H., and Graham, J. 2001. Consolidation modelling of soils under the Test Embankment at Chek Lap Kok International Airport in Hong Kong using a simplified finite element method. Canadian Geotechnical Journal, **38**(2): 349–363. doi:10.1139/t00-103.

INTERNATIONAL JOURNAL FOR NUMERICAL AND ANALYTICAL METHODS IN GEOMECHANICS
Int. J. Numer. Anal. Meth. Geomech. 2017; **41**:899–917
Published online 16 November 2016 in Wiley Online Library (wileyonlinelibrary.com). DOI: 10.1002/nag.2635

A new simplified Hypothesis B method for calculating consolidation settlements of double soil layers exhibiting creep

W.-Q. Feng[1,2] and J.-H. Yin[1,2,*,†]

[1]*PolyU Shenzhen Research Institute, Shenzhen, China*
[2]*Department of Civil and Environmental Engineering, The Hong Kong Polytechnic University, Hung Hom, Kowloon, Hong Kong*

SUMMARY

This paper presents a new simplified method, based on Hypothesis B, for calculating the consolidation settlements of double soil layers exhibiting creep. In the new simplified Hypothesis B method, different stress–strain states including over-consolidation and normal consolidation states can be considered with the help of the 'equivalent time' concept. Zhu and Yin method and US Navy method are adopted to calculate the average degree of consolidation for a double soil layer profile. This new simplified Hypothesis B method is then used to calculate the consolidation settlements of double soil layers, which have two different total thicknesses of soil layer (4 m and 8 m) and three different OCR values (Over-Consolidation Ratio, $OCR = 1$, 1.5 and 2). The accuracy and verification of this new simplified method are examined by comparing the calculated results with simulation results from a fully coupled finite element (FE) program using a soft soil creep model. Four cases of double layer soil profiles are analyzed. Hypothesis A method with US Navy method for the average degree of consolidation has also been used to for calculating consolidation settlements of the same cases. For *Case I*(4*m*) and *Case III*(8*m*), it is found that curves of the new simplified Hypothesis B method using both Zhu and Yin method and US Navy method are very close to the results from FE simulations with the *relative errors* within 8.5%. For *Case II*(4*m*) and *Case IV*(8*m*), it is found that curves of the new simplified Hypothesis B method using Zhu and Yin method agree better with results from FE simulations with the *relative errors* within 11.7% than curves of the new simplified Hypothesis B method adopting US Navy method with the *relative error* up to 36.1%. Curves of Hypothesis A method adopting US Navy method have the *relative error* up to 55.0% among all four cases. In overall, the new simplified Hypothesis B method is suitable for calculation of consolidation settlements of double soil layers exhibiting creep, in which, Zhu and Yin method is recommended to obtain the average degree of consolidation. Copyright © 2016 John Wiley & Sons, Ltd.

Received 2 February 2016; Revised 26 September 2016; Accepted 4 October 2016

KEY WORDS: double soil layers; consolidation settlement; creep; visco-plastic

1. INTRODUCTION

The time-dependent phenomenon of soils can be attributed to hydrodynamic lags (consolidation) and viscous deformation of the soil skeleton [1]. The consolidation of a clayey soil is caused by the dissipation of the excess pore water pressure while viscous deformation is because of the viscosity of the soil skeleton, including the creep, stress relaxation, and strain rate dependency. The design of geotechnical projects, such as the reclamation, needs to consider the consolidation settlement of the soil exhibiting creep [2, 3].

*Correspondence to: Jian-Hua Yin, Department of Civil and Environmental Engineering, The Hong Kong Polytechnic University, Hung Hom, Kowloon, Hong Kong.
†E-mail: 11901182r@connect.polyu.hk

Ladd *et al.* [4] questioned whether the creep occurs during 'primary' consolidation, which led to two extreme methods in terms of Hypotheses A and B: Hypothesis A assumes that creep contribution can be included independently after 'primary' consolidation stage, whereas Hypothesis B assumes that creep contribution should be included throughout the consolidation and compression process. This question remains controversial among researchers. Mesri and Godlewski [5], Choi [6], Feng [7], Mesri and Vardhanabhuti [8], and Mesri [9], supporting Hypothesis A, believed that soil is compressed for two interrelated reasons: (*i*) the change of effective stress, (*ii*) the change of time. Meanwhile, Bjerrum [10], Stolle *et al.* [11], Vermeer and Neher [12], Nash and Ryde [13], Yin *et al.* [14], Leroueil [15], Leoni *et al.* [16], Karim *et al.* [17], Nash and Brown [18] used Hypothesis B to consider that the creep occurs during the consolidation stage. Navarro and Alonso [19] regarded the 'secondary compression' of clays as the rate of local water transfer process. Recently, researchers [20–22] have undertaken some efforts to the double porosity model for two scales of porosity in the soil fabric structure. Cosenza and Korošak [23] presented a heuristic approach that adopts two additional parameters of fractional order and fractional viscosity factor, to consider the 'secondary consolidation' of clayey soil as a result of pore water pressure diffusion from micro- to macro-pores. Borja and Choo [24] developed a framework of soil constitutive model to consider the pore water pressure dissipation in the macro- and micro-scale, and used this model to simulate the 'secondary compression' in one-dimensional (1D) consolidation, which agrees well with the experimental data. The double porosity theory provides the basis for understanding the soil consolidation behavior. The different porosity scales for 'primary consolidation' and 'secondary consolidation' reasonably explain that creep also occurs during consolidation stage. According to the definition, creep is a continuous deformation of soil under a constant load (or an incremental creep under an incremental constant load) [1, 14]. It is reasonable to say that creep always exists under the action of varying effective stress, which means that Hypothesis B is logically correct.

Based on Hypothesis B and the 'equivalent time' concept [10, 25, 26], Yin [2], Yin and Feng [3] presented a new simplified Hypothesis B method for the handy calculation of the consolidation settlement of a single soil layer exhibiting, considering different stress–strain states. Yin and Feng [3] verified the accuracy of this new simplified method by comparing calculated values with results from fully coupled finite element (FE) simulations. In reality, because of the geological history, a soil profile has layers more than one layer [27, 28]. The consolidation problem of multiple soil layers was extensively studied before. Schiffman and Stein [29] obtained a mathematical solution for a layered consolidation problem. US Department of the Navy [30] proposed a simplified procedure to convert multiple soil layers into one single soil layer. Details of this procedure will be presented later. Zhu and Yin [28, 31] presented an analytical solution and solution charts for double soil layers under the ramp loading with different depths, and demonstrated the different consolidation behaviors between the double soil layers and a simplified one single soil layer [30]. Meanwhile, Xie *et al.* [32] introduced an analytical solution for the two-layered soil with partially drained boundaries. Xie *et al.* [33] considered the nonlinear properties of double layered soils. Related problems such as double layered soils with vertical drains [34, 35], soft clayey soils reinforced by floating stone columns [36, 37], and double layered system for unsaturated soil [38] have been widely studied without considering creep.

This paper aims to generalize a new simplified Hypothesis B method [3] for a single soil layer to double soil layers for calculating consolidation settlement of soils with creep for different stress–strain states under instant loading. Examples with two different total thickness values (4 m and 8 m) and three different stress–strain states ($OCR = 1$, 1.5 and 2) are presented to illustrate the accuracy of this simplified Hypothesis B method when using Zhu and Yin method [28, 31] and US Navy method [30] for determination of the average degree of consolidation. The accuracy (or relative errors) of this simplified Hypothesis B method is examined by comparing calculated results with simulation results from a fully coupled FE software with an elastic visco-plastic constitutive model for the clayey soil used in the examples. As a benchmark comparison, the conventional Hypothesis A method with US Navy method for the average degree of consolidation has also been used to calculate consolidation settlements of the same cases.

DOI: 10.1002/nag

2. BRIEF REVIEW OF THE NEW SIMPLIFIED METHOD BASED ON HYPOTHESIS B FOR A SINGLE SOIL LAYER

Based on Hypothesis B and 'equivalent time' concept [25, 26, 39], Yin [2], Yin and Feng [3] proposed a new simplified Hypothesis B method for 1-D consolidation settlement prediction for one single layer of a clayey soil as follows:

$$\begin{aligned} S_{totalB} &= S_{"primary"} + S_{creep} \\ &= U_v S_f + \left[\alpha S_{creep,f} + (1-\alpha) S_{"secondary"}\right] \; for \;\; t \geq 1 \;\; day \quad \left(t \geq t_{EOP,field} \, for \;\; S_{"secondary"}\right) \end{aligned} \tag{1}$$

where $S_{"primary"} = U_v S_f$ denotes the settlement of 'primary' consolidation at any time t. U_v is the average degree of consolidation for the soil layer, and S_f represents the final settlement at the end of 'primary' consolidation. It is noted that $S_f = \varepsilon_f H$ where ε_f is the considering vertical strain and H is the thickness of a single soil layer. In Eq. (1), S_{creep} is the creep settlement during and after 'primary' consolidation. The subscript '*creep*' indicates that the settlement is related to creep. In Eq. (1), α is a constant parameter to reasonably consider the creep settlement during and after the consolidation, and its value should be in the range from 0 to 1. Referring to Figure 1, the effective stress–strain state is valid for the soil nearby the drainage boundary, while the effective stress path inside the clay away from the drainage boundary will be delayed because of the consolidation. For the soil nearby the drainage boundary, $S_{creep,f}$ in Eq. (1) is calculated at the final effective stress ignoring the coupling of the excess pore water pressure as the creep settlement and $S_{creep,f} = \varepsilon_{creep,f} H$ where $\varepsilon_{creep,f}$ is the corresponding final creep strain. In Eq. (1), $S_{"secondary"}$ is the 'secondary consolidation' settlement based on Hypothesis A for the soil far away from the drainage boundary, $S_{"secondary"} = \varepsilon_{"secondary"} H = \frac{C_{\alpha e}}{1+e_0} \log \frac{t}{t_{EOP,field}} H$, where $\varepsilon_{"secondary"}$ is the corresponding 'secondary' strain, $C_{\alpha e}$ is the 'secondary consolidation' coefficient, e_0 is the initial void ratio, and $t_{EOP,field}$ is the time at the End-Of-Primary (EOP) consolidation in the field and can be calculated using the time at $U_v = 98\,\%$. It is noted that

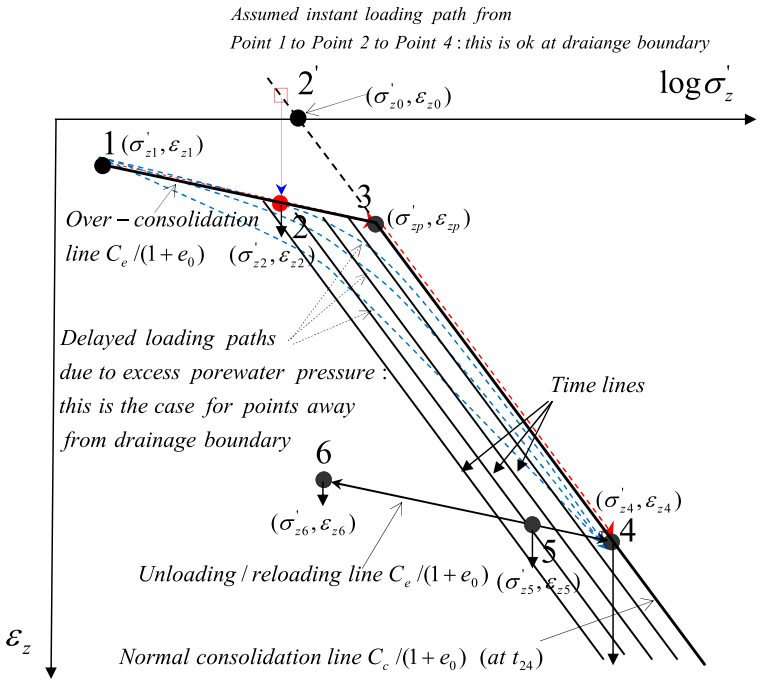

Figure 1. Relationship of vertical strain *versus* log (vertical effective stress) with different time lines and **stress–strain** states. [Colour figure can be viewed at wileyonlinelibrary.com]

DOI: 10.1002/nag

when $\alpha = 0$, Eq. (1) is reduced to the equation of Hypothesis A method: $S_{totalA} = U_v S_f + S_{"secondary"} for\ t \geq t_{EOP,field}$ for $S_{"secondary"}$. We use S_{totalA} to denote the settlement calculated using Hypothesis A method here, rather than still using S_{totalB}.

The key issue of Eq. (1) is how to accurately determine the creep strain under different stress–strain states including the normal consolidation and over-consolidation states in the new simplified Hypothesis B method. Figure 1 shows the relationship of vertical strain versus log(vertical effective stress) with different stress–strain states. The initial stress–strain state, *Point* 1 $\left(\sigma'_{z1}, \varepsilon_{z1}\right)$, and pre-consolidation stress–strain state, *Point* 3 $\left(\sigma'_{zp}, \varepsilon_{zp}\right)$, are already known. The slope of unloading–reloading line is $C_e/(1+e_0)$, and the slope of normal consolidation line is $C_c/(1+e_0)$, which are obtained from oedometer tests with duration of 24 h (1 day) as a common approach. When the initial point is at *Point* 1 and the final effective stress state is at *Point* 2 on the over-consolidation line, the final 'primary' consolidation and creep strains are calculated with the following equations [3]:

$$\begin{aligned} \varepsilon_f &= \varepsilon_{z2} = \frac{C_e}{1+e_o}\log\left(\frac{\sigma'_{z2}}{\sigma'_{z1}}\right) + \varepsilon_{z1} \\ \varepsilon_{creep,f} &= \frac{C_{ae}}{1+e_0}\log\left(\frac{t+t_{e2}}{t_0+t_{e2}}\right) \\ t_{e2} &= t_0 \times 10^{\left(\varepsilon_{z2}-\varepsilon_{zp}\right)\frac{(1+e_0)}{C_{ae}}}\left(\frac{\sigma'_{z2}}{\sigma'_{zp}}\right)^{-\frac{C_c}{C_{ae}}} - t_0 \quad for\ \ t \geq 1\ \ day. \end{aligned} \tag{2}$$

The t_0 is a material parameter and shall be taken as 1 (day) because $C_e/(1+e_0)$ and $C_c/(1+e_0)$ are obtained from oedometer tests with duration of 24 h (1 day). Eq. (2) is valid for time t equal to or larger than 1 day because the data points in Figure 1 all have 1-day duration already.

When the initial point is at *Point* 1 and the final effective stress state is at *Point* 4 on the normal consolidation line, the final 'primary' consolidation and creep strains are expressed as:

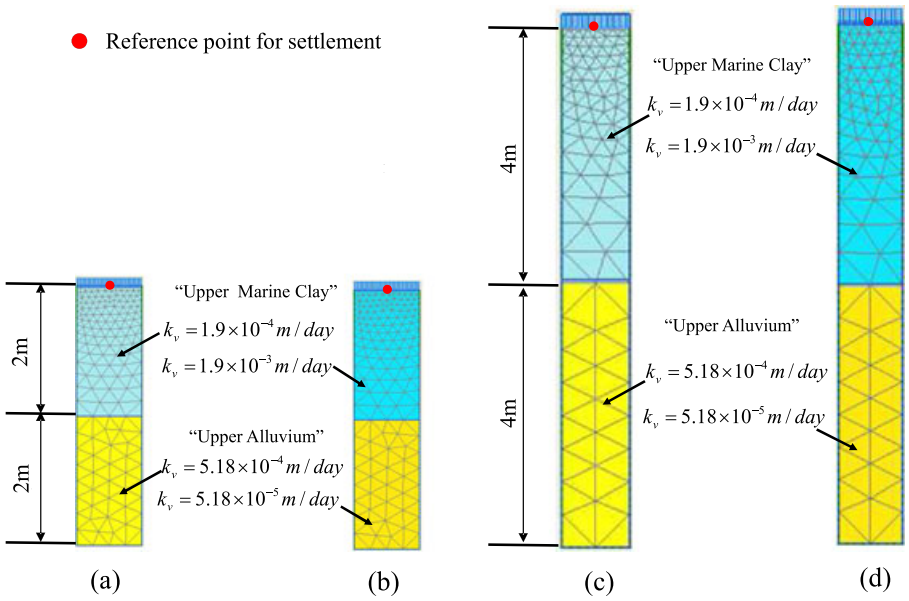

Figure 2. Profiles of double soil layers for Plaxis simulation with free drainage in the top and impermeable in the bottom: (a) *Case I* (4*m*), (b) *Case II* (4*m*), (c) *Case III* (8*m*), (d) ***Case IV* (8*m*).** [Colour figure can be viewed at wileyonlinelibrary.com]

DOI: 10.1002/nag

Table I. Values of parameters used in the new simplified Hypothesis B method and plaxis for double soil layers.

(a) Values of parameters in the new simplified Hypothesis B method

Case	Soil layer	e_o	$\gamma_{soil}\,(kN/m^3)$ s	OCR	C_e	C_c	$C_{\alpha e}$	$k_v(m/day)$	$t_0(day)$
Case I (4*m*)	'Upper Marine Clay'	2.65	15	1, 1.5, 2	0.0913	1.4624	0.0639	1.9×10^{-4}	1
CaseIII (8*m*)	'Upper Alluvium'	1	19.5	1, 1.5, 2	0.05	0.2993	0.016	5.18×10^{-4}	1
Case II (4*m*)	'Upper Marine Clay'	2.65	15	1, 1.5, 2	0.0913	1.4624	0.0639	1.9×10^{-3}	1
Case IV (8*m*)	'Upper Alluvium'	1	19.5	1, 1.5, 2	0.05	0.2993	0.016	5.18×10^{-5}	1

(b) Values of parameters used in Plaxis

Case	Soil layer	$\gamma_{soil}\,(kN/m^3)$	OCR	κ^*	λ^*	μ^*	$k_v(m/day)$	$c'(kPa)$	$\phi'(°)$
Case I (4*m*)	'Upper Marine Clay'	15	1, 1.5, 2	0.0217	0.174	0.0076	1.9×10^{-4}	0.1	25
CaseIII (8*m*)	'Upper Alluvium'	19.5	1, 1.5, 2	0.0217	0.065	0.00347	5.18×10^{-4}	0.1	30
Case I (4*m*)	'Upper Marine Clay'	15	1, 1.5, 2	0.0217	0.174	0.0076	1.9×10^{-3}	0.1	25
CaseIV (8*m*)	'Upper Alluvium'	19.5	1, 1.5, 2	0.0217	0.065	0.00347	5.18×10^{-5}	0.1	30

Note: λ^* is the modified compression index, $\lambda^* = \frac{C_c}{2.3(1+e_0)}$, κ^* is the modified swelling index, $\kappa^* \approx \frac{C_e}{2.3(1+e_0)}$, μ^* is the modified creep index, $\mu^* = \frac{C_{ae}}{2.3(1+e_0)}$, all used in Plaxis.

DOI: 10.1002/nag

$$\varepsilon_f = \varepsilon_{z4} = \left(\frac{C_e}{1+e_o}\log\left(\frac{\sigma'_{zp}}{\sigma'_{z1}}\right) + \varepsilon_{z1}\right) + \frac{C_c}{1+e_o}\log\left(\frac{\sigma'_{z4}}{\sigma'_{zp}}\right)$$
$$\varepsilon_{creep,f} = \frac{C_{\alpha e}}{1+e_0}\log\left(\frac{t}{t_0}\right) \quad for\ \ t \geq 1\ \ day. \tag{3}$$

We prefer to call $C_{\alpha e}$ a creep coefficient, rather than the 'secondary' consolidation coefficient because Eq. (2) and Eq. (3) consider creep occurs during and after 'primary' consolidation. Eq. (2) and Eq. (3) are derived by using the equivalent time t_e proposed by Yin and Graham [25, 26], Yin *et al.* [14].

3. A NEW SIMPLIFIED HYPOTHESIS B METHOD FOR CALCULATING CONSOLIDATION SETTLEMENT OF MULTIPLE LAYERS OF SOILS EXHIBITING CREEP

In many cases, there are more than one layer of soils in the field, and each stratum is influenced by the other layer [31]. To consider double-layered soil condition, a new simplified Hypothesis B method is proposed:

$$S_{totalB} = \sum_{i=1}^{n} S_{"primary"i} + \sum_{i=1}^{n} S_{creepi} = U_a \sum_{i=1}^{n} S_{fi} + \sum_{i=1}^{n}\left[\alpha S_{creep,fi} + (1-\alpha) S_{"secondary"i}\right]$$
$$= U_a \sum_{i=1}^{n} \varepsilon_{fi} H_i + \sum_{i}^{n}\left\{\left[\alpha \varepsilon_{creep,fi} + (1-\alpha)\varepsilon_{"secondary"i}\right] H_i\right\} \quad for\ t \geq 1day\ \left(t \geq t_{EOP,field}\ for\ \ S_{"secondary"i}\right) \tag{4}$$

where $\sum_{i=1}^{n} S_{"primary"i}$ is the 'primary' consolidation settlement of n soil layers, U_a and $\sum_{i=1}^{n} S_{fi}$ are the average degree of consolidation and the total 'primary' consolidation settlement of n soil layers, $\sum_{i=1}^{n} S_{creepi}$ is the total creep settlement of n soil layers, and $\sum_{i=1}^{n} S_{creep,fi}$ and $\sum_{i=1}^{n} S_{"secondary"i}$ are the total

Table II. Summary of calculated values of parameters used in the new simplified Hypothesis B method for double soil layers

Case	*OCR*	'Upper Marine Clay'			'Upper Alluvium'			$s_{f1}+s_{f2}$ (*m*)	*p*	*q*
		s_{f1} (*m*)	m_{v1} (kPa^{-1})	c_{v1} (m^2/day)	s_{f2} (*m*)	m_{v2} (kPa^{-1})	c_{v2} (m^2/day)			
(a) Calculated values of parameters for 4-m-thick double soil layers										
Case I (4*m*)	1	0.635	0.01588	0.00122	0.096	0.00239	0.02208	0.731	−0.22	0.62
	1.5	0.500	0.01258	0.00154	0.052	0.00130	0.04080	0.552	−0.31	0.67
	2	0.409	0.01023	0.00189	0.025	0.00064	0.08308	0.434	−0.42	0.74
Case I (4*m*)	1	0.635	0.01588	0.0122	0.096	0.00239	0.00221	0.731	−0.88	−0.40
	1.5	0.500	0.01258	0.0154	0.052	0.00130	0.00408	0.552	−0.90	−0.32
	2	0.409	0.01023	0.0189	0.025	0.00064	0.00831	0.434	−0.92	−0.20
(b) Calculated values of parameters for 8-m-thick double soil layers										
Case	*OCR*	'Upper Marine Clay'			'Upper Alluvium'			$s_{f1}+s_{f2}(m)$	*p*	*q*
		s_{f1} (*m*)	m_{v1} (kPa^{-1})	c_{v1} (m^2/day)	s_{f2} (*m*)	m_{v2} (kPa^{-1})	c_{v2} (m^2/day)			
Case III (8 *m*)	1	0.935	0.01169	0.00166	0.114	0.00142	0.03709	1.049	−0.27	0.65
	1.5	0.671	0.00839	0.00231	0.032	0.00032	0.16748	0.703	−0.51	0.79
	2	0.483	0.00604	0.00321	0.019	0.00024	0.22200	0.502	−0.51	0.79
Case IV (8*m*)	1	0.935	0.01169	0.0166	0.114	0.00143	0.00371	1.049	−0.89	−0.36
	1.5	0.671	0.00839	0.0231	0.032	0.00040	0.01307	0.703	−0.93	−0.14
	2	0.483	0.00604	0.0321	0.019	0.00024	0.02220	0.502	−0.94	−0.09

DOI: 10.1002/nag

Table III. Values of 'equivalent time' t_{e2} of all sub-layers of 'upper alluvium' with OCR = 2 for 8-m-thick double soil layers

No.(j)	Depth at the middle of each sub-layer (m)	$\sigma'_{z1,j}$ (kPa)	$\sigma'_{zp,j}$ (kPa)	$\sigma'_{zf,j}$ (kPa)	ε_{zp}	$\varepsilon_{zf,j}$	t_{e2}
1–8	Vary 0.25–3.75	1.25–18.75	2.5–37.5	21.25–38.75	0.0075	—	0
9	4.25	22.375	44.75	42.375	0.0075	0.00694	1.34
10	4.75	27.125	54.25	47.125	0.0075	0.00600	8.00
11	5.25	31.875	63.75	51.875	0.0075	0.00529	23.93
12	5.75	36.625	73.25	56.625	0.0075	0.00473	54.50
13	6.25	41.375	82.75	61.375	0.0075	0.00428	104.88
14	6.75	46.125	92.25	66.125	0.0075	0.00391	179.35
15	7.25	50.875	101.75	70.875	0.0075	0.00360	280.97
16	7.75	55.625	111.25	75.625	0.0075	0.00334	411.56

final creep settlement and the total 'secondary' consolidation settlement of n soil layers. Eq. (4) is an extension of Eq. (1) to consider multiple soil layers. Eq. (4) can be reduced to Eq. (1) when $n = 1$. In previous study, Yin and Feng [3] suggested α 0.8 for a single soil layer. In the study of this paper, the authors have found that α is related to OCR and can be taken as $\alpha = 0.4 + 0.2\text{OCR}$. For OCR = 1, 1.5, and 2, we have $\alpha = 0.6,\ 0.7,\ 0.8$. The verification of these α values can be seen in Figures 3–8 later with a comparison with FE simulation results. Eqs. (2) and (3) are also used to determine the final creep compression $\varepsilon_{creep,f}$ and then creep settlement $S_{creep,f}$ of a soil in each layer under different stress–strain states. Another important issue is how to correctly determine the average degree of consolidation, m_v for multiple soil layers.

In this paper, we use Eq. (4) to analyze a double soil layer system which was studied before by Zhu and Yin [28, 31], Xie *et al.* [27, 32] without considering creep. In this analysis, the solution derived by

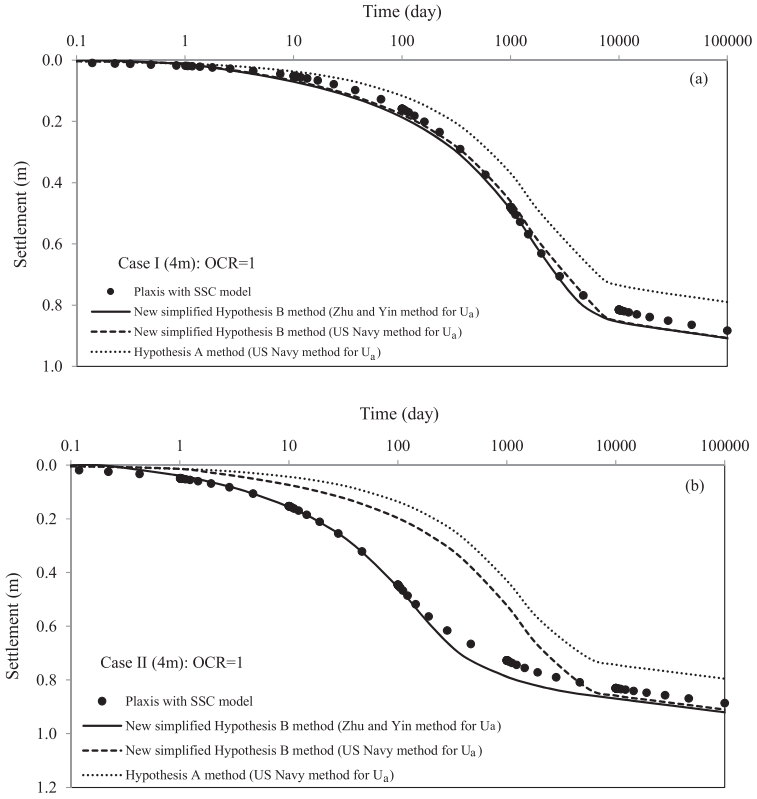

Figure 3. Comparison of FE simulation and the new simplified Hypothesis B method for 4-m-thick double soil layers with OCR = 1: (a) settlement–log(time) curves for *Case I ((4)m)*; (b) settlement–log(time) curves for *Case II ((4)m)*.

DOI: 10.1002/nag

Zhu and Yin [28, 31] for double soil layer consolidation analysis is adopted (denoted Zhu and Yin method) for calculating the average degree of consolidation m_v. Zhu and Yin [28, 31] provided charts for calculating the average degree of consolidation m_v. In the solution and charts, Zhu and Yin [28, 31] introduced two independent parameters (p, q), construction time factor (T_c) and time factor (T) for the consolidation settlement calculation. Key equations are summarized as follows:

$$
\begin{aligned}
p &= \frac{\sqrt{k_2 m_{v2}} - \sqrt{k_1 m_{v1}}}{\sqrt{k_2 m_{v2}} + \sqrt{k_1 m_{v1}}} \\
q &= \frac{H_1\sqrt{c_{v2}} - H_2\sqrt{c_{v1}}}{H_1\sqrt{c_{v2}} + H_2\sqrt{c_{v1}}} \\
\omega &= \frac{(1+q)}{2} \\
\xi &= \frac{(1-q)}{2} \\
T_c &= \frac{c_{v1}c_{v2}t_c}{\left(H_1\sqrt{c_{v2}} + H_2\sqrt{c_{v1}}\right)^2} \\
T &= \frac{c_{v1}c_{v2}t}{\left(H_1\sqrt{c_{v2}} + H_2\sqrt{c_{v1}}\right)^2}
\end{aligned}
\tag{5}
$$

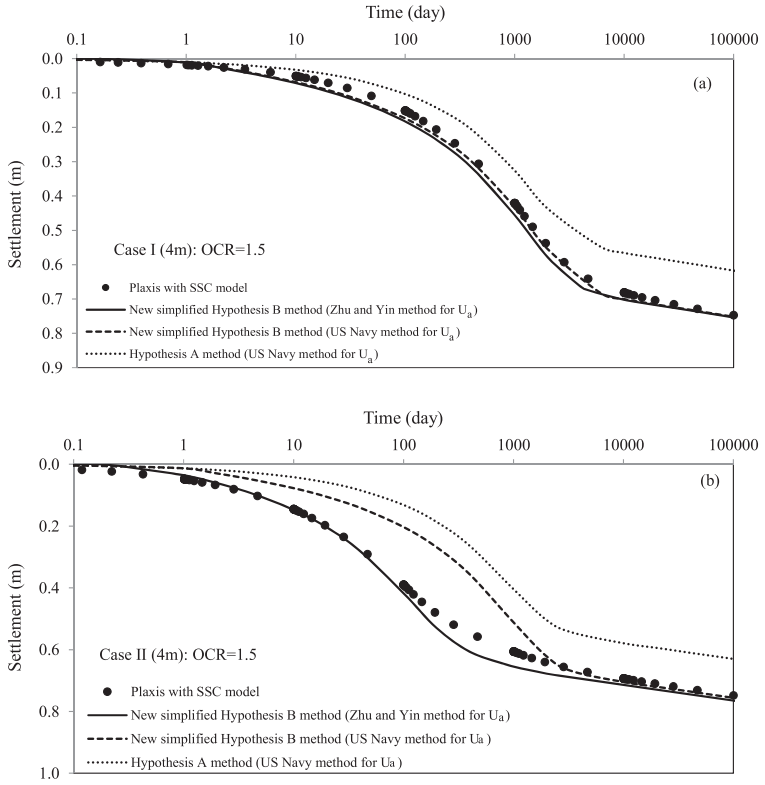

Figure 4. Comparison of FE simulation and the new simplified Hypothesis B method for 4-m-thick double soil layers with OCR = 1.5: (a) settlement–log(time) curves for *Case I (*(4)*m)*; (b) settlement–log(time) curves for *Case II (*(4)*m)*.

DOI: 10.1002/nag

$$U_a(T,\ T_c) = \begin{cases} \dfrac{T_c}{T} - \displaystyle\sum_{n=1}^{\infty} \frac{c_n}{\lambda_n^4 T_c}\left[1 - \exp\left(-\lambda_n^2 T\right)\right] & T \le T_c \\ 1 - \displaystyle\sum_{n=1}^{\infty} \frac{c_n}{\lambda_n^4 T_c}\left[1 - \exp\left(-\lambda_n^2 T_c\right)\right] \times \exp\left[-\lambda_n^2 (T - T_c)\right] & T \ge T_c \end{cases} \tag{6}$$

where λ_n is the root of the equation $sin\theta + psin(q\theta) = 0$ for both top and bottom drained condition (*condition1*) and the equation $cos\theta - pcos(q\theta) = 0$ for one side drained condition (*condition2*). Values of c_n are determined by the following equation:

$$c_n = \begin{cases} \dfrac{2\left[m_{v1} H_1 \xi \sin(\lambda_n \xi) + m_{v2} H_2 \omega \sin(\lambda_n \omega)\right]^2}{\omega^2 \xi^2 (m_{v1} H_1 + m_{v2} H_2)\left[m_{v1} H_1 \xi \sin^2(\lambda_n \xi) + m_{v2} H_2 \omega \sin^2(\lambda_n \omega)\right]} & for\ condition\ 1 \\ \dfrac{2\left[m_{v1} H_1 \xi \cos(\lambda_n \xi)\right]^2}{\omega^2 (m_{v1} H_1 + m_{v2} H_2)\left[m_{v1} H_1 \xi \cos^2(\lambda_n \xi) + m_{v2} H_2 \omega \sin^2(\lambda_n \omega)\right]} & for\ condition\ 2 \end{cases} . \tag{7}$$

Details of the derivation could be found in Zhu and Yin [28, 31], and the solution is valid for the uniform vertical stress under the ramp loading on double soil layers. The procedures of a step-by-step calculation are provided later.

US Department of the Navy [30] proposed a simplified procedure for consolidation analysis of multiple soil layers. For double soil layers, we can convert soil layer 2 to an equivalent thickness of soil layer 1, using:

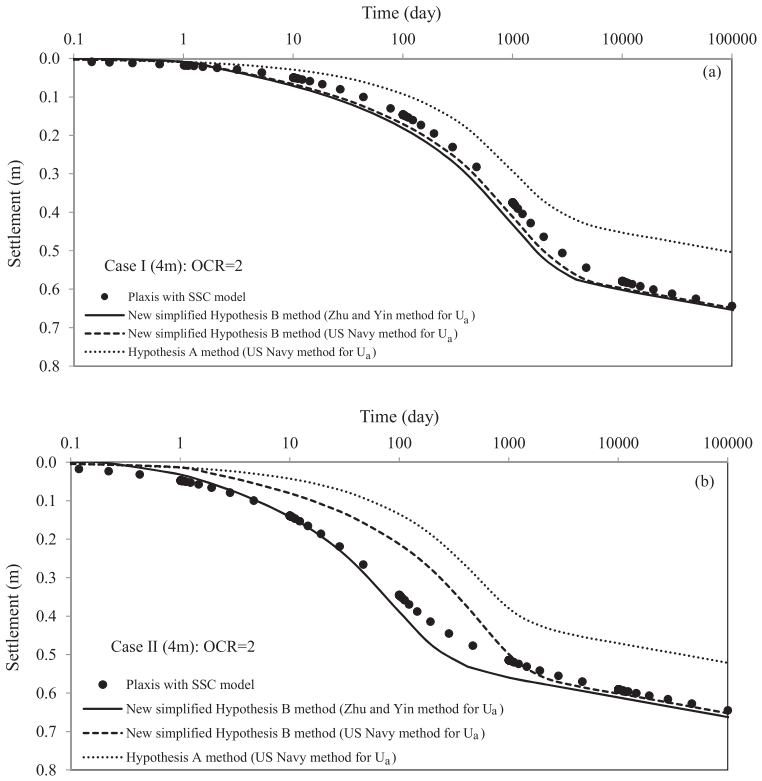

Figure 5. Comparison of FE simulation and the new simplified Hypothesis B method for 4-m-thick double soil layers with OCR = 2: (a) settlement–log(time) curves for *Case I ((*4*)m)*; (b) settlement–log(time) curves for *Case II ((*4*)m)*.

DOI: 10.1002/nag

$$H_2^{'} = H_2(c_{v1}/c_{v2})^{1/2}$$
$$T = \frac{c_{v1}t}{\left(H_1 + H_2^{'}\right)^2} \tag{8}$$

where H_2 is the height of the soil layer 2, $H_2^{'}$ is the equivalent thickness of soil layer 2 as if it is made up of soil layer 1, and c_{v1} and c_{v2} are the coefficients of consolidation for layers 1 and 2, respectively. T is the overall time factor of the whole deposit. After the conversion, the average degree of consolidation, U_a, can be determined as one single soil layer. This method is named as US Navy method in this paper.

4. FOUR CASES OF DOUBLE SOIL LAYERS AND FINITE ELEMENT MODELING APPROACH

In this section, we have selected the geologic profile of the Hong Kong International Airport (HKIA) in Lantau Island, Hong Kong as an example to apply the new simplified Hypothesis B method for consolidation analysis of double soil layers. The representative values of soil parameters are adopted for using this new simplified method to calculate the consolidation settlement of soils with creep. Plaxis (2D 2015 version) is also used to analyze the consolidation settlement of the same soil layers. The corresponding results will be presented and compared in the next section to verify the applicability and accuracy of the new simplified Hypothesis B method.

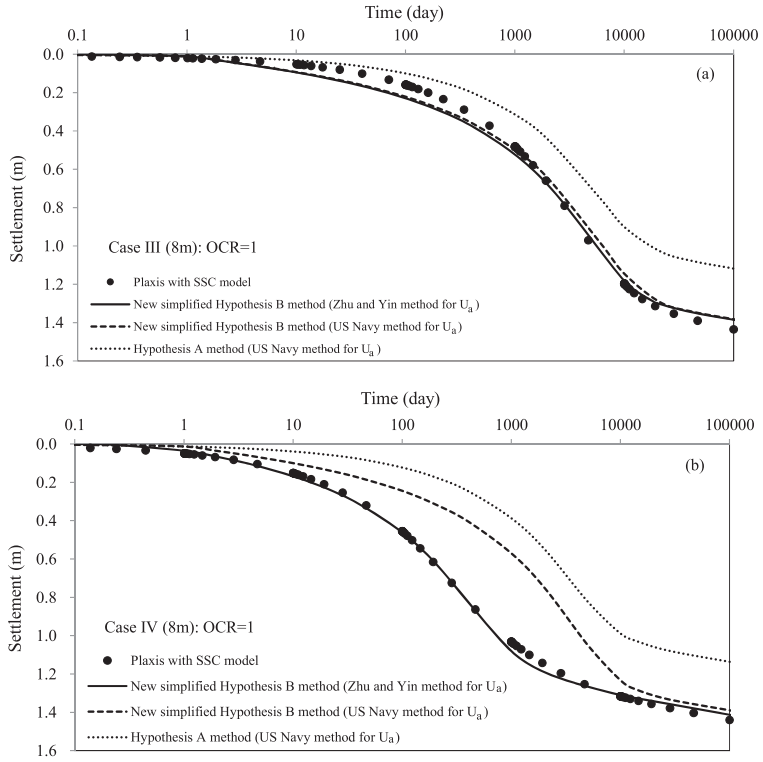

Figure 6. Comparison of FE simulation and the new simplified Hypothesis B method for 8-m-thick double soil layers with OCR = 1: (a) settlement–log(time) curves for *Case III (*(8)*m)*; (b) settlement–log(time) curves for *Case IV (*(8)*m)*.

DOI: 10.1002/nag

4.1. Description of the double soil layers

There is more than one soil layer at the site of HKIA [40, 41]. 'Upper Marine Clay' is at the top of the soil layer with 2 m–8 m in thickness and 'Upper Alluvium' layer underlays the 'Upper Marine Clay'. The base of 'Upper Alluvium' is regarded to be impermeable, and the top of 'Upper Marine Clay' is seabed and normally filled by sand so that the top is considered free drained [42]. Detailed description of 'Upper Marine Clay' can be found in [3, 43, 44]. The void ratio of 'Upper Alluvium' is 1. Both 'Upper Marine Clay' and 'Upper Alluvium' are considered to have three different OCR values ($OCR = 1$, 1.5 and 2) as a parametric study.

Figure 2 shows the profile of four cases of double soil layers. Table I presents values of all parameters of four cases of double soil layers used for consolidation analysis using the new simplified Hypothesis B method and FE modeling (FEM) using Plaxis (2D version 2015). The total thickness of *Case I* (4*m*) and *Case II* (4*m*) is 4 m with 2 m 'Upper Marine Clay' in the top followed by 2 m 'Upper Alluvium', the bottom of which is impermeable. Comparing to *Case I* (4*m*), the difference of *Case II* (4*m*) is that the permeability value of 'Upper Marine Clay' is increased by one order, and the permeability value of 'Upper Alluvium' is decreased by one order. The total thickness of *Case III* (8*m*) and *Case IV* (8*m*) is 8 m with 4 m 'Upper Marine Clay' in the top followed by 4 m 'Upper Alluvium', the bottom of which is impermeable. Comparing to *Case III* (8*m*), the difference of *Case IV* (8*m*) is that the permeability value of 'Upper Marine Clay' is increased by one order and the permeability value of 'Upper Alluvium' is decreased by one order. A vertical stress of 20*kPa* is assumed suddenly applied on the two layers in Figure 2 [3].

4.2. Description of a finite element modeling approach

In order to verify the accuracy of the new simplified Hypothesis B method for double soil layers, the FE software Plaxis (2D version 2015) is used for the numerical simulation adopting the soft soil creep (SSC) model [12, 45], which is, in fact, an non-linear Elastic Visco-Plastic constitutive

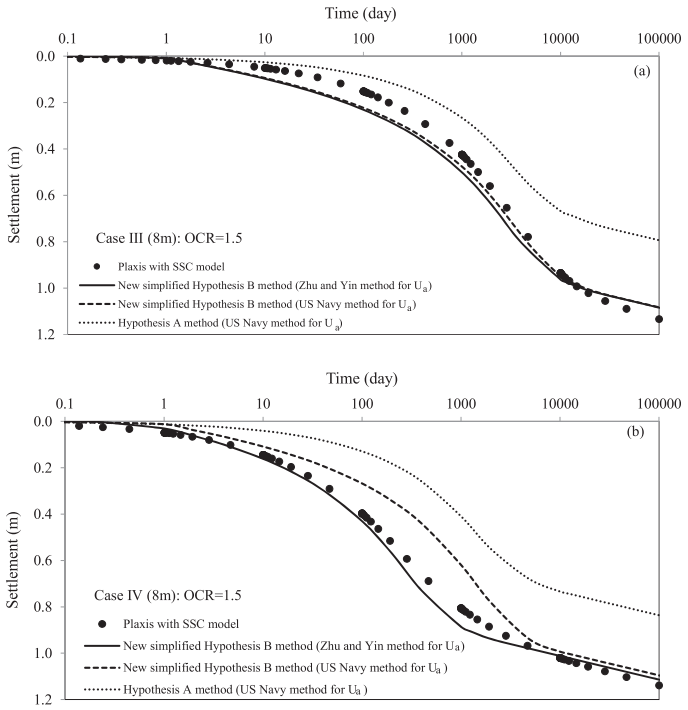

Figure 7. Comparison of FE simulation and the new simplified Hypothesis B method for 8-m-thick double soil layers with OCR = 1.5: (a) settlement–log(time) curves for *Case III (*(8)*m)*; (b) settlement–log(time) curves for *Case IV (*(8)*m)*.

DOI: 10.1002/nag

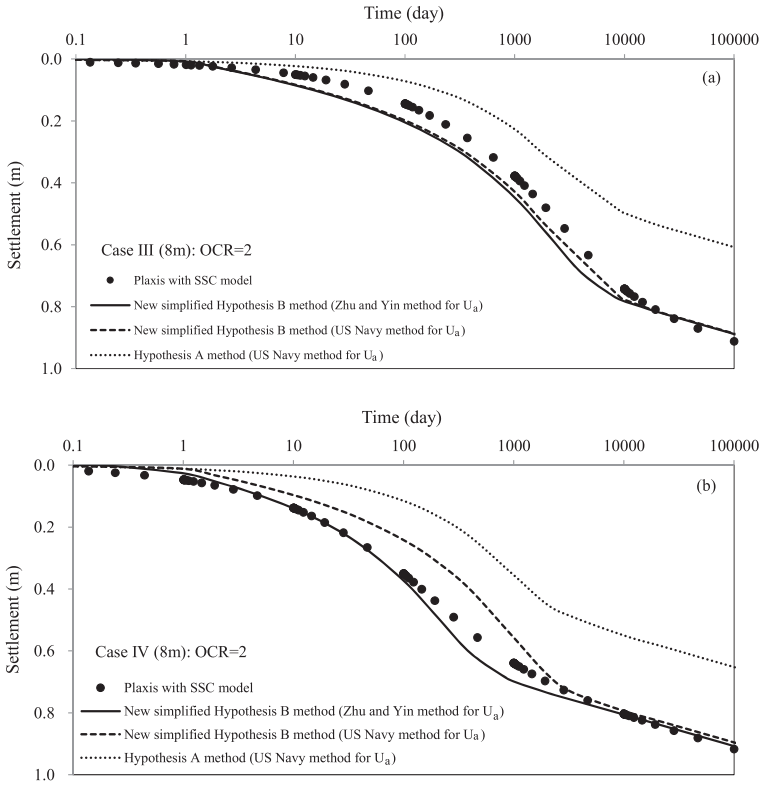

Figure 8. Comparison of FE simulation and the new simplified Hypothesis B method for 8-m-thick double soil layers with OCR = 2: (a) settlement–log(time) curves for *Case III (*(8)*m)*; (b) settlement–log(time) curves for *Case IV (*(8)*m)*.

model [46, 47]. A two-dimensional plane strain FE mesh with 15-node triangular elements is used in Plaxis simulation.

As illustrated in Figure 2, the top elements of the soil have free drainage, and the bottom elements are impermeable when conducting the consolidation analysis. The left and right vertical boundaries in Figure 2 are impermeable and are confined to have vertical movements only. A vertical stress of 20*kPa* is instantly applied on the top of all FE simulation models, and the loading period is up to 100 000 days to make sure that consolidation is totally completed in all simulation cases. The monitoring point for the settlement is at the top surface of the FE model, as illustrated in Figure 2. The definition of the SSC parameters can be found in the Plaxis manual (2D version 2015), and values of parameters used in Plaxis are listed in Table I. The initial pre-consolidation stress plays an important role in the ground settlement prediction when adopting the SSC model [45]. When considering OCR value effects, OCR values of 'Upper Marine Clay' and 'Upper Alluvium' are set to be 1, 1.5, and 2. Initial stress–strain condition before adding the vertical loading and consolidation is generated with the in-situ K_0 condition.

5. APPLICATION AND VERIFICATION OF THE NEW SIMPLIFIED HYPOTHESIS B METHOD FOR CONSOLIDATION ANALYSIS OF DOUBLE SOIL LAYERS WITH CREEP

This section presents the detailed procedures of applying the new simplified Hypothesis B method for consolidation analysis of four cases of double layers of soils exhibiting creep and calculated results.

5.1. Procedures of applying the new simplified Hypothesis B method for consolidation settlement calculations

In order to calculate the consolidation settlement of soils with creep, the initial and final effective stress states should be first determined. It is suggested that the total thickness of 4 m or 8 m shall be divided

DOI: 10.1002/nag

Table IV. Relative error values for Hypothesis A method and the new simplified Hypothesis B methods using Zhu and Yin method for U_a and US Navy method for U_a.

(a) Relative error values of parameters for 4-m-thick double soil layers

Case	OCR	Time (day)	S_{Plaxis} (m)	US Navy method for U_a					Zhu and Yin method for U_a		
				U_a(%)	S_{totalA} (m)	S_{totalA} *relative error*(%)	S_{totalB} (m)	S_{totalB} *relative error*(%)	U_a(%)	S_{totalB} (m)	S_{totalB} *relative error*(%)
Case I (4*m*)	1	1000	0.479	50	0.369	23.0	0.461	3.9	54.0	0.487	1.5
		7500	0.797	98	0.716	10.1	0.835	4.7	98.8	0.842	5.7
		100 000	0.883	100	0.788	10.7	0.907	2.7	100	0.908	2.8
	1.5	730	0.373	50	0.278	25.5	0.380	1.9	54.1	0.402	7.8
		5580	0.650	98	0.544	16.3	0.678	4.2	98.9	0.684	5.2
		100 000	0.747	100	0.619	17.2	0.753	0.7	100	0.754	0.9
	2	550	0.321	50	0.217	32.3	0.325	1.2	53.9	0.346	7.8
		4200	0.536	98	0.426	20.4	0.570	6.4	98.9	0.579	8.0
		100 000	0.643	100	0.505	21.5	0.649	0.8	100	0.653	1.5
Case II (4*m*)	1	725	0.701	50	0.366	47.8	0.454	35.3	92.9	0.767	9.4
		5525	0.813	98	0.717	11.9	0.831	2.2	100	0.856	5.3
		100 000	0.886	100	0.795	10.2	0.910	2.7	100	0.920	3.9
	1.5	445	0.554	50	0.279	49.7	0.373	32.7	92.7	0.609	9.9
		3375	0.662	98	0.544	17.8	0.670	1.2	100	0.690	4.3
		100 000	0.748	100	0.630	15.8	0.756	1.0	100	0.765	2.2
	2	262	0.439	50	0.218	50.4	0.313	28.8	88.7	0.484	10.3
		2000	0.543	98	0.426	21.5	0.557	2.6	100	0.576	6.0
		100 000	0.645	100	0.521	19.1	0.652	1.1	100	0.662	2.7

(b) Relative error values of parameters for 8-m-thick double soil layers

Case	OCR	Time (day)	S_{Plaxis} (m)	US Navy method for U_a					Zhu and Yin method for U_a		
				U_a (%)	S_{totalA} (m)	S_{totalA} *relative error*(%)	S_{totalB} (m)	S_{totalB} *relative error*(%)	U_a (%)	S_{totalB} (m)	S_{totalB} *relative error*(%)
Case III (8*m*)	1	2800	0.789	50	0.526	33.3	0.737	6.6	54.0	0.778	1.5
		21 260	1.314	98	1.028	21.7	1.293	1.6	98.9	1.305	0.7
		100 000	1.435	100	1.118	22.1	1.383	3.7	100	1.385	3.5
	1.5	1750	0.543	50	0.352	35.1	0.580	6.7	51.5	0.590	8.5
		13 400	0.981	98	0.689	29.7	0.980	0.1	99.0	0.989	0.8
		100 000	1.134	100	0.792	30.1	1.080	4.5	100	1.085	4.3
	2	1230	0.429	50	0.251	41.4	0.460	7.3	51.1	0.465	8.5
		9450	0.734	98	0.492	32.9	0.773	5.2	99.0	0.779	6.0
		100 000	0.912	100	0.606	33.5	0.887	2.8	100	0.888	2.6
Case IV (8*m*)	1	1850	1.137	50	0.526	53.7	0.726	36.1	93.5	1.181	3.9
		14 050	1.339	98	1.028	23.2	1.282	4.2	100	1.326	1.0
		100 000	1.440	100	1.136	21.1	1.390	3.5	100	1.413	1.9
	1.5	740	0.759	50	0.352	53.6	0.552	27.2	92.1	0.848	11.7
		5650	0.981	98	0.690	29.7	0.953	2.9	100	0.987	0.6
		100 000	1.139	100	0.830	27.1	1.094	4.0	100	1.114	2.2
	2	475	0.558	50	0.251	55.0	0.428	23.4	88.2	0.621	11.2
		3630	0.743	98	0.492	33.7	0.739	0.5	100	0.761	2.5
		100 000	0.917	100	0.648	29.3	0.895	2.4	100	0.907	1.1

into a number of sub-layers with 0.5-m thickness in order to calculate the final primary settlement S_{fi} more accurately for each soil type layer. Second, values of the initial effective stress ($\sigma'_{z1,j}$), that is, $Point\ 1\ \left(\sigma'_{z1}, \varepsilon_{z1}\right)$ in Figure 1, pre-consolidation stress state ($\sigma'_{zp,j}$), and final effective stress ($\sigma'_{zf,j}$) for each sub-layer j after loading are calculated below:

DOI: 10.1002/nag

$$\begin{aligned}\sigma'_{z1,j} &= \left(\gamma_{soil,j} - \gamma_w\right) z_j \\ \sigma'_{zp,j} &= OCR \times \sigma'_{z1,j} \\ \sigma'_{zf,j} &= \sigma'_{z1,j} + \Delta\sigma'_z\end{aligned} \tag{9}$$

where z_j is the sub-layer middle location, $\gamma_{soil,j}$ is the saturated weight of the soil in the sub-layer, as listed in Table I, γ_w is water unit weight, taken as 9.81 kN/m^3, and $\Delta\sigma'_z$ is the vertical loading, taken as 20 kPa in the calculation. In Eq. (9), we introduce a new index 'j' for sub-layers (up to a total of m sub-layers) of 0.5 m thick only for each soil type. This index 'j' is different from the index 'i' in Eq. (4) which is for layers of different soils.

It should be noted that the unit weight of 'Upper Alluvium' is different from that of 'Upper Marine Clay' soil and the initial effective stress should be determined carefully for each layer in Figure 2. As shown in Figure 1, the initial effective stress state is at $Point\ 1\ \left(\sigma'_{z1}, \varepsilon_{z1}\right)$ for $OCR = 1.5\ or\ 2$, and at $Point\ 3\ \left(\sigma'_{zp}, \varepsilon_{zp}\right)$ for $OCR = 1$. Assuming the initial strain is zero for all four cases. Final effective stress state is at $Point\ 4\ \left(\sigma'_{z4}, \varepsilon_{z4}\right)$ after the loading of 20 kPa for all the sub-layers of 'Upper Marine Clay' with two different thicknesses 2 m or 4 m and OCR values. After the loading of 20 kPa, the final effective stress state after the stress increment is at $Point\ 4\ \left(\sigma'_{z4}, \varepsilon_{z4}\right)$ for all sub-layers of 'Upper Alluvium' with $OCR = 1$, but at $Point\ 2\ \left(\sigma'_{z2}, \varepsilon_{z2}\right)$ for some sub-layers of 'Upper Alluvium' when 8-m layer when $OCR = 1.5\ or\ 2$ and 4-m soil layer with $OCR = 2$. All these final effective stresses can be calculated using the parameter values in Table I.

Third, Eq. (3) is used after the stress increment of 20 kPa to determine 'primary' consolidation final settlement $S_{fi,j}$, for each sub-layer j of 0.5 m thick with $OCR = 1$ of a soil type layer i. Because all the sub-layers of 'Upper Marine Clay' and 'Upper Alluvium' are at $Point\ 4\ \left(\sigma'_{z4}, \varepsilon_{z4}\right)$ for final effective stress state, Eq. (3) is used for $S_{fi,j}$. When the final effective stress state is at $Point\ 2\ \left(\sigma'_{z2}, \varepsilon_{z2}\right)$, Eq. (2) is adopted for some sub-layers of 'Upper Alluvium'. The total final 'primary' consolidation settlements of 'Upper Marine Clay' and 'Upper Alluvium' can be obtained by summing those of all sub-layers. Afterwards, the total final 'primary' consolidation settlement S_{fi}, the *coefficient of volume compressibility*, m_{vi}, and the *coefficient of consolidation,* c_{vi}, for the whole 'Upper Marine Clay' or the whole 'Upper Alluvium' can be obtained as follows:

$$S_{fi} = \sum_{j=1}^{m} S_{fi,j} \qquad m_{vi} = \frac{1}{H_i \Delta\sigma'_z} S_{fi} \qquad c_{vi} = \frac{k_{vi}}{m_{vi}\gamma_w} \tag{10}$$

where H_i is the total thickness of 'Upper Marine Clay' or 'Upper Alluvium'. Calculated values of S_{fi}, m_{vi}, and c_{vi} for 'Upper Marine Clay' and 'Upper Alluvium' are listed in Table II.

Fourth, the factors for double soil layers, p and q, can be calculated with Eq. (5) by substituting the values of m_v and c_v, and the corresponding values are also listed in Table II. Take *Case I*(4*m*) with $OCR = 1$ as an example: $H_1 = H_2 = 2m$, $c_{v1} = 0.00122$ m^2/day, and $c_{v2} = 0.02208$ m^2/day in Table II, the time factor, T, after a loading time of 100 days with one-way drainage condition could be determined as follows:

$$T = \frac{c_{v1}c_{v2}t}{\left(H_1\sqrt{c_{v2}} + H_2\sqrt{c_{v1}}\right)^2} = \frac{0.0012 \times 0.02208 \times 100}{4\left(\sqrt{0.02208} + \sqrt{0.0012}\right)^2} = 0.02. \tag{11}$$

From the solution charts for one-way drainage condition [31], the average degree of consolidation U_a is 18% for $p = -0.3$ and $q = 0.62$ (from solution charts in Zhu and Yin [28, 31]) and is 13% for $p = 0.3$ and $q = 0.62$. It is noted that $T_c = 0$ because the loading is suddenly applied. With the help of the interpolation method for $p = -0.22$ in Table II, the average degree of consolidation U_a at time of 100 days and for $p = -0.22$ and $q = 0.62$ could be obtained:

DOI: 10.1002/nag

$$U_a = \frac{[0.3-(-0.22)]\times 18\% + [(-0.22)-(-0.3)]\times 13\%}{[0.3-(-0.3)]} = 17.3\%. \quad (12)$$

Similarly, the average degree of consolidation, U_a, for double soil layers in other different times or other conditions can also be determined.

In order to compare with the US Navy method [30], the average degree of consolidation, U_a, is also calculated by transferring the 'Upper Alluvium' into 'Upper Marine Clay' soil considering the difference of coefficient of consolidation, c_v, with Eq. (8). Then, the average degree of consolidation, U_a, could be easily determined as one equivalent single layer.

Last, for 'Upper Marine Clay', the creep compression $\varepsilon_{creep,f}$ is calculated by adopting Eq. (3) when the final effective stress state is in a normal consolidation state. Eq. (2) shall be used for calculating the creep compression $\varepsilon_{creep,f}$ when the final effective stress state of some sub-layers is in over-consolidation state. The equivalent times, t_{e2}, in Eq. (2) shall also be calculated first using the third row equation in Eq. (2) for a few sub-layers of 'Upper Alluvium' with 8 m and listed in Table III for $OCR = 2$. Values of $t_{EOP,field}$ are determined to be the time when the average degree of consolidation is 98% for double soil layers.

5.2. Comparison of results from the new simplified Hypothesis B method, FE simulations, and Hypothesis A method

The FE software Plaxis (2015 version) is used to simulate the same four cases of double soil layers, and results are used to verify the accuracy of calculated results using the new simplified Hypothesis B method. Because the conventional Hypothesis A method is still used by some people but the limitations of this method are not well understood, it is also good to know the difference between the new simplified Hypothesis B method and conventional Hypothesis A method. The limitations of this method are not well understood. It is also good to know the difference between the new simplified Hypothesis B method and conventional Hypothesis A method. Therefore, the conventional Hypothesis A method with US Navy method for the average degree of consolidation has also been used to calculate consolidation settlements of the same cases.

Curves of the new simplified Hypothesis B method are compared with curves from FE simulations with a SSC model and from Hypothesis A method in Figures 3–8 for different layer thickness and OCR values. Dot symbols are results from the Plaxis FE simulations. Solid lines represent calculation results of the new simplified Hypothesis B method with Zhu and Yin method for U_a. Dashed lines are the calculation results of the new simplified Hypothesis B method with US Navy method for U_a. Dotted lines are the calculation results of the Hypothesis A method with US Navy method for U_a.

a. *Case I*(4*m*) and *Case II*(4*m*)

A comparison of FE simulation results with SSC model and the new simplified Hypothesis B method using Zhu and Yin method and US Navy method is shown in Figure 3 for 4-m-thick double soil layers with $OCR = 1$ ($\alpha = 0.6$). For *Case I*(4*m*), it can be observed that calculated results of the new simplified Hypothesis B method using US Navy method and Zhu and Yin method for U_a are almost the same as illustrated in Figure 3(a) and are all very close to FE simulation results. The calculated curves with Zhu and Yin method for U_a are overlapped by those with US Navy method for U_a when the 'primary' consolidation is completed. For *Case II*(4*m*), there is an obvious gap between the calculated results using Zhu and Yin method for U_a and those adopting US Navy method for U_a. It is seen clearly from Figure 3(b) that calculated curves of the new simplified Hypothesis B method using Zhu and Yin method for U_a are in a good agreement with FE simulation results. However, the obvious difference between FE simulation results and calculated results using US Navy method is observed during the consolidation stage. After the consolidation stage, results of the new simplified Hypothesis B method using both Zhu and Yin method and US Navy method are very close to FE simulation results. By comparing the results between the new

DOI: 10.1002/nag

simplified Hypothesis B method using Zhu and Yin method, US Navy method, and FE simulation results, it can be deduced that US Navy method predicts the wrong average degree of consolidation, U_a, for double soil layers in *Case II*(4*m*). It is seen from Figure 3 that Hypothesis A method gives much less settlement compared to results from the FE simulation and the new simplified Hypothesis B method.

Yin and Feng [3] defined the parameter, *relative error*, to evaluate the accuracy of the new simplified Hypothesis B method at a certain time *t*. The *relative error* is defined as:

$$relative\ \ error = |(S_{totalB} - S_{Plaxis})/S_{Plaxis}| \times 100\% \tag{13}$$

where S_{Plaxis} is the predicted settlement from Plaxis at time *t*. In this paper, we take two times at $U_a = 50\,\%$, $U_a = 80\,\%$ (from Hypothesis A method using US Navy method for U_a) and time of 100 000 days. S_{totalB} is the total settlement calculated from the new simplified Hypothesis B method. Eq. (3) can also be used to calculate *relative error* for Hypothesis A method, in which S_{totalB} is replaced by S_{totalA}. As a result, values of *relative error* for all double soil layer conditions are listed in Table IV(a).

Figure 4 shows the comparison of settlement–log(time) curves from FE simulation, the new simplified Hypothesis B method, and Hypothesis A method for 4 m double layers of soil profile with $OCR = 1.5$ ($\alpha = 0.7$). Figure 5 shows the comparison of settlement–log(time) curves from FE simulation, the new simplified Hypothesis B method, and Hypothesis A method for 4-m double layers of soil profile with $OCR = 2$ ($\alpha = 0.8$). Similar characteristics are observed for the new simplified Hypothesis B method with Zhu and Yin method and US Navy method for U_a in the two cases in Figures 4 and 5.

For 4-m thick double soil layer with $OCR = 1$, 1.5, and 2, it can be observed in Table IV(a) that the values of *relative error* are from 0.9% to 10.3% for the new simplified Hypothesis B method using Zhu and Yin method for U_a and from 0.7% to 35.5% for the new simplified Hypothesis B method using US Navy method for U_a. However, values of *relative error* are from 10.1% to 50.4% for the Hypothesis A method with US Navy method for U_a. The Hypothesis A method underestimates the consolidation settlement a lot.

b. *Case III*(8*m*) and *Case IV*(8*m*)

For 8-m-thick double layers of soil profile, Figures 6, 7, and 8 show comparisons of curves from the FE simulation, the new simplified Hypothesis B method with Zhu and Yin method and US Navy method for U_a, and from Hypothesis A method with US Navy method for U_a for $OCR = 1$, 1.5, and 2, respectively. Characteristics of these curves are similar to those in Figures 3, 4, and 5. In overall, the curves from the new simplified Hypothesis B method with Zhu and Yin method for U_a are closer to the dot lines from the Plaxis FE simulations than those from other two simple methods. Again, Hypothesis A method underestimates the settlement a lot.

All values of the *relative error* are listed in Table IV(b). In both cases of *Case III*(8*m*) and *Case IV*(8*m*) with $OCR = 1$, 1.5, and 2, it can be observed in Table IV(b) that the values of *relative error* are from 0.7% to 11.7% for the new simplified Hypothesis B method using Zhu and Yin method for U_a and 0.1% to 36.1% for the new simplified Hypothesis B method using US Navy method for U_a. The values of *relative error* are from 21.1% to 55.0% for the Hypothesis A method with US Navy method for U_a. Again, the Hypothesis A method underestimates the consolidation settlement a lot.

Some errors are caused by the approximation of US Navy method for estimating U_a. Zhu and Yin [31] found that errors of US Navy method are very significant in some simplification cases of double soil layers which are converted into one single soil layer. In order to predict the long-term consolidation settlement as accurately as possible, Zhu and Yin method is recommended for calculating U_a of a double soil layer profile.

6. CONCLUSIONS

Based on Hypothesis B and the 'equivalent time' concept [25, 26], a new simplified method is presented to calculate the consolidation settlement of double layers of soils with creep for different

DOI: 10.1002/nag

stress–strain states. Two idealized soil layers with different total thickness values (4 m and 8 m) and three different OCR values are considered for consolidation analysis to illustrate the applicability of this new simplified Hypothesis B method. Zhu and Yin method and US Navy method are adopted to obtain the average degree of consolidation for double soil layers. Four cases of the consolidation of the double soil profile have been analyzed using a FE method with an elastic visco-plastic constitutive model, the new simplified Hypothesis B method, and Hypothesis A method. Results are presented and discussed. Main conclusions are drawn as follows:

a. It is found that the curves from the new simplified Hypothesis B method adopting Zhu and Yin method for U_a are generally in good agreement with results from FE simulation. The *relative error* of this new method with Zhu and Yin method for U_a is from 0.9% to 8.5% for *Case I*(4*m*) and *Case III*(8*m*), and from 1.0% to 11.7% for *Case II*(4*m*) and *Case III*(8*m*).
b. Curves from the new simplified Hypothesis B method adopting US Navy method for U_a are close to those from the new method with Zhu and Yin method U_a in *Case I*(4*m*) and *Case III*(8*m*) as well as those from the FE simulations. The differences and *relative errors* are big in *Case II*(4*m*) and *Case IV*(8*m*). The *relative error* of this new method adopting US Navy method for U_a is from 0.1% to 7.3% for *Case I*(4*m*) and *Case III*(8*m*), and from 0.5% to 36.1% for *Case II*(4*m*) and *Case III*(8*m*).
c. The consolidation settlements are all underestimated by using Hypothesis A method adopting US Navy method for U_a in all cases. The *relative error* of the Hypothesis A method adopting US Navy method for U_a is from 10.1% to 55.0% for all four cases.
d. According to the study in this paper, this new simplified Hypothesis B method adopting Zhu and Yin method for calculating the average degree of consolidation is the most accurate method for calculating the consolidation settlements of double layers of soils exhibiting creep.

ACKNOWLEDGEMENTS

The work in this paper is supported by a research grant (project no. 51278442) from National Natural Science Foundation of China (NSFC), two general research fund (GRF) projects (PolyU 152196/14E and PolyU 152796/16E) from Research Grants Council (RGC) of Hong Kong Special Administrative Region Government of China, and grants (4-BCAW, G-YM28, G-YN97, B-Q43L) from The Hong Kong Polytechnic University, China.

REFERENCES

1. Mitchell KJ, Soga K. *Fundamentals of Soil Behavior* (3rd). John Wiley & Sons, Inc.: New York, 2005.
2. Yin J-H. From constitutive modeling to development of laboratory testing and optical fiber sensor monitoring technologies. *Chinese Journal of Geotechnical Engineering* 2011; **33**(1):1–15.
3. Yin J-H, Feng W-Q. A new simplified method and its verification for calculation of consolidation settlement of a clayey soil with creep. *Canadian Geotechnical Journal* 2016. doi: 10.1139/cgj-2015-0290.
4. Ladd CC, Foott R, Ishihara K, Schlosser F, Poulos HG. Stress–deformation and strength characteristics. State of the Art Report, Proceeding 9th of ISMFE, Tokyo, 1977; **2**:421–494.
5. Mesri G, Godlewski PM. Closure of "time and stress–compressibility interrelationship". *Journal of the Geotechnical Engineering Division* 1979; **105**(1):106–113.
6. Choi, Y-K. Consolidation behavior of natural clays. University of Illinois at Urbana-Champaign, 1982.
7. Feng, T-W. Compressibility and permeability of natural soft clays and surcharging to reduce settlements. Diss. University of Illinois at Urbana-Champaign, 1991.
8. Mesri G, Vardhanabhuti B. Closure of 'Secondary compression' by Mesri and Vardhanabhuti (2005). *Journal of Geotechnical and Geoenviromental Engineering* 2006; **132**:817–818.
9. Mesri G. Effects of friction and thickness on long-term consolidation behavior of Osaka Bay clays. *Soils and Foundations* 2009; **49**(5):823–824.
10. Bjerrum L. Engineering geology of Norwegian normally-consolidated marine clays as related to settlements of buildings. *Geotechnique* 1967; **17**(2):83–118.
11. Stolle DFE, Vermeer PA, Bonnier PG. A consolidation model for a creeping clay. *Canadian Geotechnical Journal* 1999; **36**(4):754–759.
12. Vermeer, P A, and Neher H P. A soft soil model that accounts for creep. Proceedings of the International Symposium "Beyond 2000 in Computational Geotechnics: 10 Years of PLAXIS International", Balkema. 1999: 249–261.

13. Nash DFT, Ryde SJ. Modelling consolidation accelerated by vertical drains in soils subject to creep. *Geotechnique* 2001; **51**(3):257–273.
14. Yin J-H, Zhu J-G, Graham J. A new elastic visco-plastic model for time-dependent behaviour of normally and over-consolidated clays: theory and verification. *Canadian Geotechnical Journal* 2002; **39**(1):157–173.
15. Leroueil, S. The Isotache approach. Where are we 50 years after its development by Professor Šuklje? 2006 Prof. Šuklje's Memorial Lecture. Proceedings of the XIII Danube-European Conference on Geotechnical Engineering, Ljubljana, Slovenia. 2006(2): 55–88.
16. Leoni M, Karstunen M, Vermeer PA. Anisotropic creep model for soft soils. *Geotechnique* 2008; **58**(3):215–226.
17. Karim MR *et al.* Predicting the long-term performance of a wide embankment on soft soil using an elastic-viscoplastic model. *Canadian Geotechnical Journal* 2010; **47**(2):244–257.
18. Nash D, Brown M. Influence of destructuration of soft clay on time-dependent settlements: comparison of some elastic viscoplastic models. *International Journal of Geomechanics* 2015; **15**:A4014004, 1–19.
19. Navarro V, Alonso Pérez de Agreda E. Secondary compression of clays as a local dehydration process. *Geotechnique* 2001; **51**(10):859–869.
20. Khalili N, Witt R, Laloui L, Koliji A. Effective stress in double porous media with two immiscible fluids. *Geophysical Research Letters* 2005; **32**(15). doi:10.1029/2005GL023766.
21. Gray WG, Schrefler BA. Analysis of the solid phase stress tensor in multiphase porous media. *International Journal for Numerical and Analytical Methods in Geomechanics* 2007; **31**:541–581.
22. Koliji A, Vulliet L, Laloui L. New basis for the constitutive modelling of aggregated soils. *Acta Geotechnica* 2008; **3**:61–69.
23. Cosenza P, Korošak D. Secondary consolidation of clay as an anomalous diffusion process. *International Journal for Numerical and Analytical Methods in Geomechanics* 2014; **38**(12):1231–1246.
24. Borja RI, Choo J. Cam-Clay plasticity, Part VIII: A constitutive framework for porous materials with evolving internal structure. *Computer Methods in Applied Mechanics and Engineering* 2016; **309**:653–679.
25. Yin J–H, Graham J. Viscous–elastic–plastic modelling of one-dimensional time-dependent behaviour of clays. *Canadian Geotechnical Journal* 1989; **26**(2):199–209.
26. Yin J-H, Graham J. Equivalent times and one-dimensional elastic viscoplastic modelling of time-dependent stress–strain behaviour of clays. *Canadian Geotechnical Journal* 1994; **31**(1):42–52.
27. Xie K-H. Theory of one dimensional consolidation of double-layered ground and its applications [J]. *Chinese Journal of Geotechnical Engineering* 1994; **5**:24–35.
28. Zhu G-F, Yin J-H. Consolidation of double soil layers under depth-dependent ramp load. *Geotechnique* 1999; **49** (3):415–421.
29. Schiffmann RL, Stein JR. One-dimensional consolidation of layered systems. *Journal of Soil Mechanics & Foundations Div.* 1970; **96**:1499–1504.
30. US Department of the Navy. *Soil Mechanics Design Manual 7.1. NAVFAC DM-7.1*. US Department of the Navy: Arlington, Va., 1982.
31. Zhu G-F, Yin J-H. Solution charts for the consolidation of double soil layers. *Canadian Geotechnical Journal* 2005; **42**(3):949–956.
32. Xie K-H, Xie X-Y, Gao X. Theory of one dimensional consolidation of two-layered soil with partially drained boundaries. *Computers and Geotechnics* 1999; **24**(4):265–278.
33. Xie K-H, Xie X-Y, Jiang W. A study on one-dimensional nonlinear consolidation of double-layered soil. *Computers and Geotechnics* 2002; **29**(2):151–168.
34. Tang X-W, Onitsuka K. Consolidation of double-layered ground with vertical drains. *International Journal for Numerical and Analytical Methods in Geomechanics* 2001; **25**(14):1449–1465.
35. Wang X-S, Jiao JJ. Analysis of soil consolidation by vertical drains with double porosity model. *International Journal for Numerical and Analytical Methods in Geomechanics* 2004; **28**(14):1385–1400.
36. Han J, Ye S-L. A theoretical solution for consolidation rates of stone column-reinforced foundations accounting for smear and well resistance effects. *The International Journal Geomechanics* 2002; **2**(2):135–151.
37. Wang G-C. Consolidation of soft clay foundations reinforced by stone columns under time-dependent loadings. *Journal of Geotechnical and Geoenvironmental Engineering* 2009; **135**(12):1922–1931.
38. Zhou W-H, Zhao L-S, Li X-B. A simple analytical solution to one-dimensional consolidation for unsaturated soils. *International Journal for Numerical and Analytical Methods in Geomechanics* 2014; **38**(8):794–810.
39. Yin J-H, Graham J. Elastic visco-plastic modelling of one-dimensional consolidation. *Geotechnique* 1996; **46**(3):515–527.
40. Koutsoftas DC, Foott R, Handfelt LD. Geotechnical investigations offshore Hong Kong. *Journal of Geotechnical Engineering* 1987; **113**(2):87–105.
41. Handfelt LD, Koutsoftas DC, Foott R. Instrumentation for test fill in Hong Kong. *Journal of Geotechnical Engineering* 1987; **113**(2):127–146.
42. Degago SA *et al.* Use and misuse of the isotache concept with respect to creep hypotheses A and B. *Geotechnique* 2011; **61**(10):897–908.
43. Zhu G-F, Yin J-H, Graham J. Consolidation modelling of soils under the test embankment at Chek Lap Kok International Airport in Hong Kong using a simplified finite element method. *Canadian Geotechnical Journal* 2001; **38**(2):349–363.
44. Pyrah IC. One-dimensional consolidation of layered soils. *Geotechnique* 1996; **46**(3):555–560.

DOI: 10.1002/nag

45. Waterman D, Broere W. Practical application of the Soft Soil Creep model. *Plaxis Bulletin* 2011; **15**:1–15.
46. Yin J-H, Graham J. Elastic visco-plastic modelling of the time-dependent stress–strain behavior of soils. *Canadian Geotechnical Journal* 1999; **36**(4):736–745.
47. Yin J-H. Fundamental issues on constitutive modelling of the time-dependent stress–strain behaviour of geomaterials. *International Journal of Geomechanics* 2015; **15**(5):A4015002-1-A4015002-9.

DOI: 10.1002/nag

Acta Geotechnica
https://doi.org/10.1007/s11440-021-01318-2

RESEARCH PAPER

A general simple method for calculating consolidation settlements of layered clayey soils with vertical drains under staged loadings

Jian-Hua Yin[1] · Ze-Jian Chen[1] · Wei-Qiang Feng[2]

Received: 10 May 2021 / Accepted: 19 July 2021

Abstract
It is well known that the calculation of consolidation settlements of clayey soils shall consider creep compression in both "primary" consolidation and so-called secondary consolidation periods. Rigorous Hypothesis B method is a coupled method and can consider creep compression in the two periods. But this method needs to solve a set of nonlinear partial differential equations with a proper elastic viscoplastic (EVP) constitutive model so that this method is not easy to be used by engineers. Recently, Yin and his coworkers have proposed a simplified Hypothesis B method for single and two layers of soils. But this method cannot consider complicated loadings such as loading, unloading and reloading. This paper proposes and verifies a general simple method with a new logarithmic function for calculating consolidation settlements of viscous clayey soils without or with vertical drains under staged loadings such as loading, unloading and reloading. This new logarithmic function is suitable to cases of zero or very small initial effective stress. Equations of this simple method are derived for complicated loading conditions. This method is then used to calculate consolidation settlements of clayey soils in three typical cases: Case 1 is a single soil layer without vertical drains under loading only; Case 2 is a two-layered soil profile with vertical drains subjected to loading, unloading and reloading; and Case 3 is a real case of a test embankment on seabed of four soil layers installed with vertical drains under three stages of loading. Settlements of all three cases using the new general simple methods are compared with values calculated using rigorous fully coupled finite element method (FEM) with an elastic viscoplastic (EVP) constitutive model (Cases 1 and 2) and measured data for Case 3. It is found that the calculated settlements are in good agreement with values from FEM and/or measured data. It is concluded that the general simple method is suitable for calculating consolidation settlements of layered viscous clayey soils without or with vertical drains under complicated loading conditions with good accuracy and also easy to use by engineers using spreadsheet calculation.

Keywords Clayey soil · Consolidation · Creep · Elastic viscoplastic · Settlement · Time-dependent

1 Introduction

In recent decades, many geotechnical structures have been constructed on clayed soil ground, especially on seabed with layered clayey soils and other soil types in many coastal cities in the world. One typical example is two artificial islands (5.10 km^2 for runway one and 5.45 km^2 for runway 2) of Kansai International Airport in Osaka, Japan. Runway one was constructed starting in December 1986 and was open in September 1994. Runway two was constructed in May 1999 and was open in August 2007. The excessive settlements have been a problematic issue [1]. In Hong Kong, a total area of 74 km^2 was reclaimed on seabed since 1887 to 2020. Recently, three large artificial

✉ Jian-Hua Yin
cejhyin@polyu.edu.hk

Ze-Jian Chen
ze-jian.chen@connect.polyu.hk

Feng Wei-Qiang
fengwq@sustech.edu.cn

[1] Department of Civil and Environmental Engineering, The Hong Kong Polytechnic University, Hung Hom, Kowloon, Hong Kong, China

[2] Department of Ocean Science and Engineering, Southern University of Science and Technology, Shenzhen, China

Published online: 04 January 2022

islands were constructed on seabed as part of Hong Kong–Zhuhai–Macao link project. In near future, more marine reclamations will be constructed on seabed in Hong Kong waters. Excessive settlements, especially long-term settlements have been and will be a big concern. It is well known that settlements of saturated clayey soils are caused by dissipation of excessive pore water pressure in voids of soils and also by viscous deformation of soil skeleton. The stress–strain behaviour of the skeleton of clayey soils is time-dependent due to the viscous nature of the skeleton [6, 12, 19, 24]. Methods for calculating settlements of saturated clayey soils shall consider the coupling process of dissipation of excessive pore water pressure and viscous deformation of soil skeleton.

Terzaghi [29] first presented a theory and equations for analysis of the consolidation of soil in one-dimensional (1D) straining (oedometer condition). But this theory cannot consider viscous deformation of soil skeleton. Later, improved methods were proposed, including methods based on Hypothesis A [20, 21] and other methods based on Hypothesis B [2, 3, 6, 10, 11, 19, 15, 16]. Hypothesis A method assumes no creep compression during the "primary" consolidation period, and the creep compression occurs only in the "secondary" compression starting at t_{EOP} which is the time at End-Of-Primary consolidation. Yin and Feng [35] and Feng and Yin [9] pointed out that Hypothesis A method normally underestimates the total settlements due to ignoring creep compression in the "primary" consolidation period.

Hypothesis B is a coupled consolidation analysis using a proper constitutive relationship for the time-dependent stress–strain behaviour of clayey soils. Hypothesis B method needs to solve a set of two partial equations: (i) an equation derived based on mass continuity condition using Darcy's law and (i) a constitutive equation such Yin and Graham's [37] 1D elastic viscoplastic model (1D EVP) [38]. Yin and Graham [38] used a finite difference method to solve this set of equations. The computed settlements and excessive pore water pressures were in good agreement with measured data from tests done by Berre and Iversen [5]. Yin and Graham [38] also found that Hypothesis A method underestimated total settlements. Nash and Ryde [22, 23] also used Hypothesis B method adopting 1D EVP model [37] to analyse the consolidation settlement of an embankment on soft ground with vertical drains. Their computed settlements were in good agreement with measured values.

Hypothesis B method needs to solve a set of nonlinear partial different equations, and a computer program is needed. This method is difficult to be used by practicing engineers without such computer program and without a good knowledge of nonlinear constitutive model. To overcome this limitation, Yin and Feng [35] and Feng and Yin [9] proposed a decoupled simplified Hypothesis B method for calculating settlements due to both excessive porewater pressure dissipation and also due to creep compression during and after the "primary" consolidation period. The calculated settlements are in close agreement with measured data and computed values using the fully coupled Hypothesis B method with the aid of computer software. However, this simplified method is neither suitable for complicated loading such as staged unloading and reloading, nor for multiple layers of soils with vertical drains. In this paper, authors propose and verify a general simplified Hypothesis B method (also called a general simple method) for calculating consolidation settlements of layered clayey soils with or without vertical drains under staged loadings including loading, unloading and reloading. Such loading process is commonly used in practice. In addition, a new logarithmic function, which has definition at zero stress, is used in this method for calculating settlements of soils at very small vertical effective stress.

2 Formulation of a general simple method for calculating consolidation settlements of multi-layered soils exhibiting creep under staged loading

2.1 Formulation of a general simplified Hypothesis B method

Figure 1 shows a soil profile with n-layers of soils with corresponding thicknesses $(H_1, H_2, \ldots H_n)$ and depths $(z_1, z_2, \ldots z_n)$. The total thickness of this profile is H. A vertical drain with smear zone is shown in Fig. 1, where $d_d = 2r_d$ is the diameter of a drain equal to twice radius r_d of the drain, $d_s = 2r_s$ is the diameter of a smear zone equal to twice radius r_s of the smear zone, $d_e = 2r_e$ is the diameter of an equivalent unit cell equal to twice radius r_e of the cell. It is noted that vertical drains are installed all in the same triangular pattern or the same square pattern and are subjected a uniform surcharge over all vertical drains. Therefore, deformation of soils in all unit cells is approximately in the vertical direction. Thus, soils in each unit cell are assumed to be in 1D straining on average. 1D straining constitutive models can be used, for example 1D EVP model [36, 37]. If a horizontal soil profile has no vertical drains, then $d_d = d_s = 0$ and $d_e = \infty$ in Fig. 1, which is also suitable for multi-layered soils without vertical drains.

Authors propose a general simplified Hypothesis B method for calculating consolidation settlement of multi-layered viscous soils with or without vertical drains under any loading condition for the soil profile under uniform

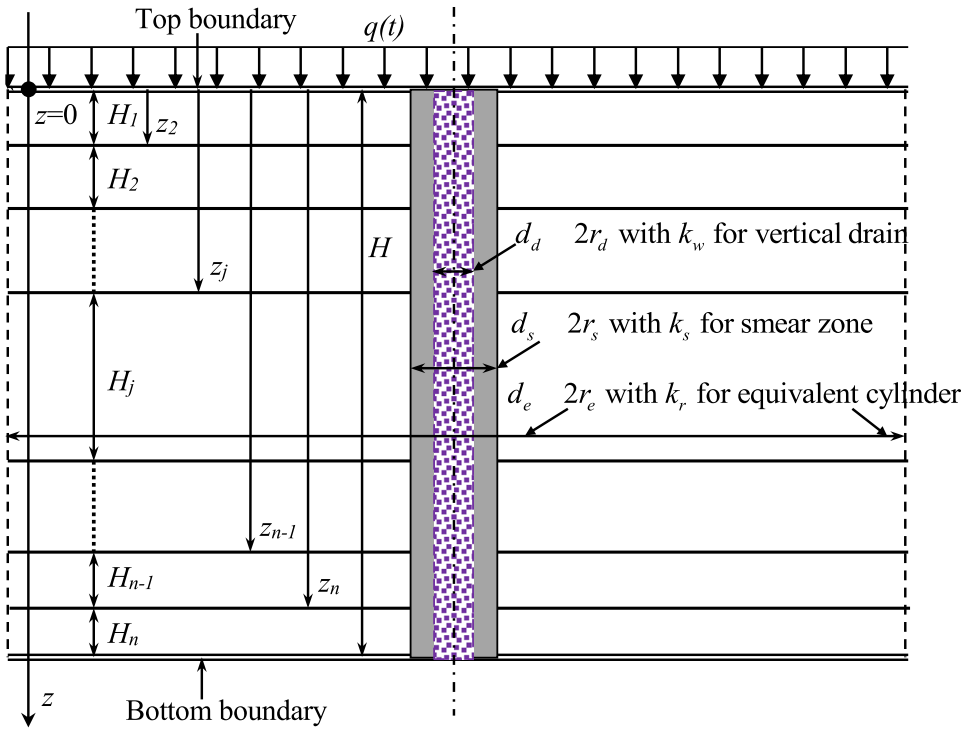

Fig. 1 A soil profile of *n*-layers with vertical drain subjected to uniform surcharge *q(t)* with time

surcharge *q(t)* in Fig. 1. Formulation of this general simple method is presented below:

$$S_{\text{total}B} = S_{\text{primary}} + S_{\text{creep}} = \sum_{j=1}^{j=n} U_j S_{fj} + \sum_{j=1}^{j=n} S_{\text{creep}j}$$
$$= U \sum_{j=1}^{j=n} S_{fj} + \sum_{j=1}^{j=n} \left[\alpha U_j^{\beta} S_{\text{creep},fj} + \left((1 - \alpha U_j^{\beta}) S_{\text{creep,dj}} \right) \right] \quad (1)$$
$$\text{for all } t \geq t_{\text{EOP,lab}} \left(t \geq t_{\text{EOP,field}} \text{for } S_{\text{creep},dj} \right)$$

The formulation in Eq. (1) is a de-coupled simplified Hypothesis B method. The "de-coupled" means that "primary" consolidation settlement S_{primary} is separated from creep settlement S_{creep}. The separation of "primary" consolidation from "secondary" compression for a laboratory test is shown in Fig. 2. A normal soil specimen in oedometer test has 20 mm in thickness with double drainage so that the value of $t_{\text{EOP,lab}}$ in Fig. 2 is small with tens of minutes only. $t_{\text{EOP,field}}$ in Eq. (1) is the End-Of-Primary (EOP) time for soil layers in the field. The value of $t_{\text{EOP,field}}$ may vary from a few years to tens of years depending on the thickness and permeability of soils in the field. $t_{24\text{hrs}}$ in Fig. 2 is the time with duration of 24 h in an oedometer test, normally larger than $t_{\text{EOP,lab}}$ with $t_{\text{EOP,lab}} < t_{24\text{hrs}} < t_{\text{EOP,field}}$ normally true. In practical application, $t_{\text{EOP,lab}}$ will be replaced by the time t_0, which is conveniently adopted as 24 h with conventional oedometer tests. The compression indices are calculated using test data from the same duration of 24 h as t_0. It shall be pointed out that in Eq. (1), the items of $S_{\text{creep},dj}$ will be zero for $t \leq t_{\text{EOP,field}}$ and will become positive $t > t_{\text{EOP,field}}$.

In Eq. (1), "primary" consolidation settlement S_{primary} shall be calculated for multiple soil layers with or without a vertical drain:

$$S_{\text{primary}} = \sum_{j=1}^{j=n} U_j S_{fj} = U \sum_{j=1}^{j=n} S_{fj} \quad (2)$$

where U_j is combined average degree of consolidation for *j*-layer and U is combined average degree of consolidation for all multiple soil layers with or without a vertical drain:

$$U_j = 1 - (1 - U_{vj})(1 - U_{rj}) \quad (3a)$$

$$U = 1 - (1 - U_v)(1 - U_r) \quad (3b)$$

Equation (3) is called Carrillo's (1942) formula where U_{vj} and U_{rj} or U_v and U_r are average degree of vertical consolidation and radial consolidation for *j*-layer or multiple soil layers. If there is no vertical drain, $U_{rj} = U_r = 0$, from (3), $U_j = U_{vj}$ or $U = U_v$. For multiple soil layers, the superposition of the average degree of consolidation for each layer is not valid since the continuation condition at each interface of two layers must be satisfied. S_{fj} is the final "primary" consolidation at End-Of-Primary (EOP)

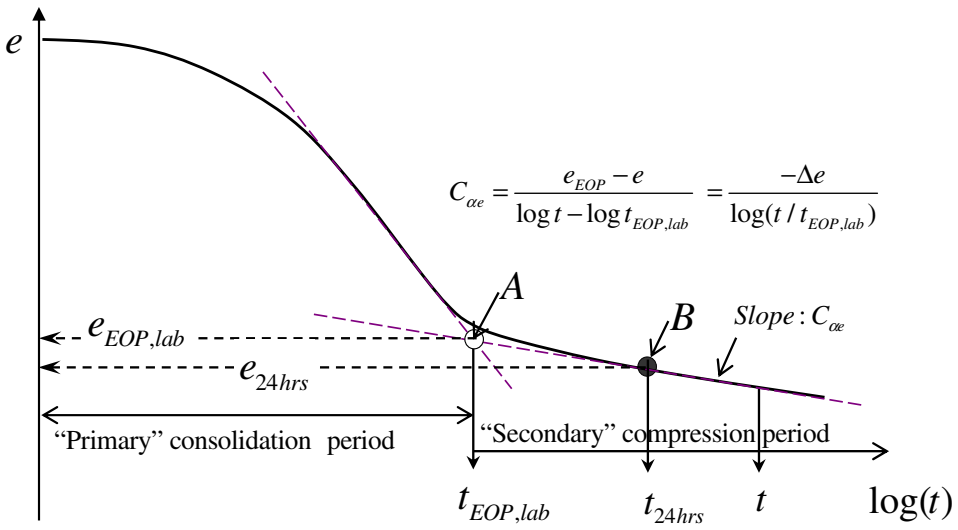

Fig. 2 Curve of void ratio *versus* log (time) and "secondary" compression coefficient

consolidation for *j*-layer. S_{fj} can be calculated using the coefficient of volume compressibility m_v or compression indexes C_c, C_r of *j*-layer. More details on calculations of S_{fj} and U are presented in the next section.

In Eq. (1), $S_{\text{creep}j}$ is creep settlement of soil skeleton in *j*-layer and is equal to:

$$S_{\text{creep}j} = \alpha U_j^{\beta} S_{\text{creep},fj} + \left(1 - \alpha U_j^{\beta}\right) S_{\text{creep},dj} \quad \text{for all } t \geq t_{\text{EOP,lab}} \left(t \geq t_{\text{EOP,field}} \text{ for } S_{\text{creep},dj}\right) \tag{4a}$$

Equation (4a) can also be written as:

$$S_{\text{creep}j} = \begin{cases} \alpha U_j^{\beta} S_{\text{creep},fj} & \text{for } t \geq t_{\text{EOP,lab}} \\ \alpha U_j^{\beta} S_{\text{creep},fj} + \left(1 - \alpha U_j^{\beta}\right) S_{\text{creep},dj} & t \geq t_{\text{EOP,field}} \end{cases} \tag{4b}$$

where U_j is from Eq. (3a) with value from 0 to 1 only and β is a power index with value from 0 to 1. Yin [33] used a parameter $\alpha = 1$ without U_j^{β}. But this over-predicted total consolidation settlement. Yin and Feng [35] and Feng and Yin [9] used $\alpha = 0.8$ without U_j^{β} and gave results in close agreement with measured data and values from rigorous fully coupled consolidation modelling. In this paper, a general term of αU_j^{β} is suggested. See more examples later in this paper on more accurate prediction results.

$S_{\text{creep},fj}$ in Eqs. (1) or (4) is creep settlement of *j*-layer under the "final" vertical effective stress after load increased, ignoring the excess porewater pressure. $S_{\text{creep},dj}$ in Eqs. (1) or (4) is "delayed" creep settlement of *j*-layer under the "final" vertical effective stress ignoring the excess porewater pressure. $S_{\text{creep},dj}$ starts for $t \geq t_{\text{EOP,field}}$, in other words, is "delayed" by time of $t_{\text{EOP,field}}$ to occur. $t_{\text{EOP,field}}$ is the End-Of-Primary (EOP) of consolidation for field condition of *j*-layer. More discussion on $S_{\text{creep},fj}$ and $S_{\text{creep},dj}$ is in later section.

2.2 *Calculation of S_{fj}*

In Eq. (2), the total primary consolidation settlement S_{primary} is sum of settlements S_{fj} of all sub-layers multiplied by an over-all average degree of consolidation U. This section presents methods and solutions for calculating S_{fj}. In the following calculations, in order to make all equations and text in following paragraphs concise, the layer index "*j*" is removed, keeping in minds that these equations are for one soil layer.

If the coefficient of volume compressibility m_v is used and vertical effective stress increment $\Delta\sigma_z'$ and thickness H are known for a soil *j*-layer, S_f for *j*-layer is:

$$S_f = m_v \Delta\sigma_z' H \tag{5}$$

It is noted that m_v is not a constant, depending on vertical effective stress, and shall be used with care. For clayey soils or soft soils, it is better to use C_c and C_r to calculate S_f for higher accuracy. An oedometer test is normally done on the same specimen in multi-stages. According to British Standard 1377 [7], the standard duration for each load shall normally last for 24 h. In this paper, the indexes C_r, C_c and pre-consolidation stress point $(\sigma_{zp}', \varepsilon_{zp})$ are all determined from the standard oedometer test with duration of 24 h (1 day), that is, $t_{24\text{hrs}} = 1$ day, for each load and for each layer. The idealized relationship between the vertical strain and the log (effective stress) is shown in Fig. 3 with loading, unloading and reloading states.

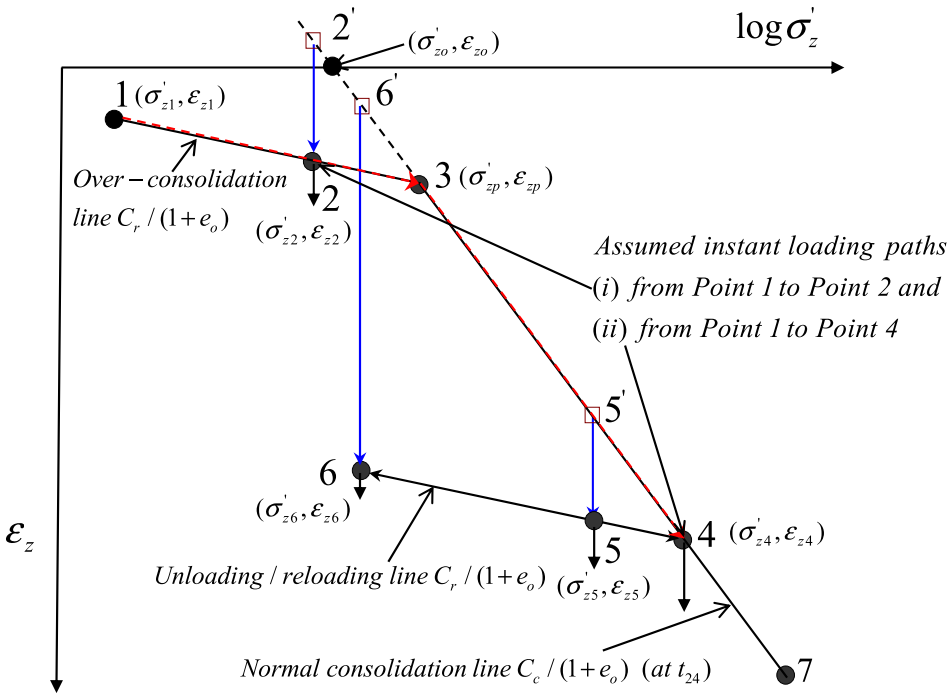

Fig. 3 Relationship of strain (or void ratio) and log(effective stress) with different consolidation states

Yin and Graham [36,37] and Yin [31] pointed out limitations of using a logarithmic function for fitting creep curve of log(time) and strain, when time is zero. In 1D EVP model, Yin and Graham [36,37] introduced a time parameter t_o in a logarithmic function to care creep starting from time zero. In many real cases, the vertical effective stress σ'_z is zero or very near zero, for example, σ'_z at surface or near surface of seabed soils or soil ground. If a normal logarithmic function is used for fitting compression curve of log(effective stress) and strain, when the stress is zero, the strain is infinite. To overcome this problem, a unit stress σ'_{unit} is added to the logarithmic function in this paper and was also in Yin's a nonlinear logarithmic-hyperbolic function in [32]. Adding σ'_{unit} in linear logarithmic stress function is particularly necessary for very soft soils in a soil ground with initial effective stress zero at the top of the surface. For example, the initial vertical effective stress at the top surface in soft Hong Kong Marine Clay (HKMC) in seedbed is zero.

As shown in Fig. 3 and assuming stresses in each layer are uniform, the final settlements S_f for j-layer in Eq. (2) for six cases are calculated as follows by adding σ'_{unit1} and σ'_{unit2} in a new logarithmic stress function for elastic compression (OCL) and elastic–plastic (NCL) compression separately.

(i) Loading from point 1 to point 2 with OCR $= \sigma'_{zp}/\sigma'_{z1}$ and point 2 in OCL:

$$S_{f,1-2} = \varepsilon_{z,1-2}H = \frac{C_r}{1+e_o}\log\left(\sigma'_{z2}+\sigma'_{\text{unit1}}/\sigma'_{z1}+\sigma'_{\text{unit1}}\right)H \tag{6a}$$

The $\varepsilon_{z,1-2}$ is the vertical strain increase due to stress increases from σ'_{z1} to σ'_{z2}. The OCR is over-consolidation ratio, and OCL is an over-consolidation line. If σ'_{unit1} is zero, (6a) goes back to conventional logarithmic stress function. The value of σ'_{unit1} is from 0.001 kPa to 1 kPa. For very soft soils, σ'_{unit1} takes values close to 0.01 kPa. Similar strain increase symbols are used in the following equations. Equation (6a) can avoid singularity problem at initial stress zero ($\sigma'_{z1} = 0$) and is good for very soft soils, such as slurry under self-weight consolidation.

(ii) Loading from point 1 to point 4 with OCR $= \sigma'_{zp}/\sigma'_{z1} > 1$ and point 4 in NCL:

$$S_{f,1-4} = \varepsilon_{z,1-4}H = \left[C_r/1+e_o\log\left(\sigma'_{zp}+\sigma'_{\text{unit1}}\Big/\sigma'_{z1}+\sigma'_{\text{unit1}}\right) + \frac{C_c}{1+e_o}\log\left(\sigma'_{z4}+\sigma'_{\text{unit2}}\Big/\sigma'_{zp}+\sigma'_{\text{unit2}}\right)\right]H \tag{6b}$$

NCL is a normal consolidation line. Adding

σ'_{unit1} and σ'_{unit2} in Eq. (6b) can avoid singularity problem at initial stress zero ($\sigma'_{z1} = \sigma'_{zp} = 0$).

(iii) Loading from point 3 to point 4 with OCR $= \sigma'_{zp}/\sigma'_{z3} = 1$ and point 4 in NCL:

$$S_{f,3-4} = \varepsilon_{z,3-4}H = C_c/1 + e_o \log\left(\sigma'_{z4} + \sigma'_{\text{unit2}} \Big/ \sigma'_{zp} + \sigma'_{\text{unit2}}\right)H \tag{6c}$$

(iv) Unloading from point 4 to point 6:

$$S_{f,4-6} = \varepsilon_{z,4-6}H = C_r/1 + e_o \log\left(\sigma'_{z6} + \sigma'_{\text{unit1}} \Big/ \sigma'_{z4} + \sigma'_{\text{unit1}}\right)H \tag{6d}$$

(v) Reloading from point 6 to point 5:

$$S_{f,6-5} = \varepsilon_{z,6-5}h = C_r/1 + e_o \log\left(\sigma'_{z5} + \sigma'_{\text{unit1}} \Big/ \sigma'_{z6} + \sigma'_{\text{unit1}}\right)h \tag{6e}$$

(vi) Reloading from point 6 to point 7:

$$S_{f,6-7} = \varepsilon_{z,6-7}H = \left[C_r/1 + e_o \log\left(\sigma'_{z4} + \sigma'_{\text{unit1}} \Big/ \sigma'_{z6} + \sigma'_{\text{unit1}}\right) + \frac{C_c}{1+e_o} \log\left(\sigma'_{z7} + \sigma'_{\text{unit2}} \Big/ \sigma'_{z4} + \sigma'_{\text{unit2}}\right)\right]H \tag{6f}$$

However, the initial stresses and stress increments in a clayey soil layer are not uniform; Eq. (6) cannot be used. There are two approaches to consider this non-uniform stress as below.

(a) Dividing j-layer into sub-layers

A general method is to divide this soil layer into sub-layers with smaller thickness, say, 0.25 m to 0.5 m, which has been adopted by previous studies [35, 40]. The stresses and parameters in each sub-layer are considered uniform and constant. The final settlement S_f for j-layer is sum of settlements of all sub-layers [9, 35]. For each sub-layer with uniform stresses, equations in Eqs. (6a–6f) can be used depending on the initial and final stress points. This method is flexible and valid for complicated cases in which vertical stress and pre-consolidation pressure may not be uniform.

(b) Special case of constant parameters C_c, C_r and linear changes of initial stresses, stress increments, and pre-consolidation pressure for j-layer

For a clayey soil layer of thickness H, C_c, C_r are often constant, but stresses may vary with depth z. Figure 4

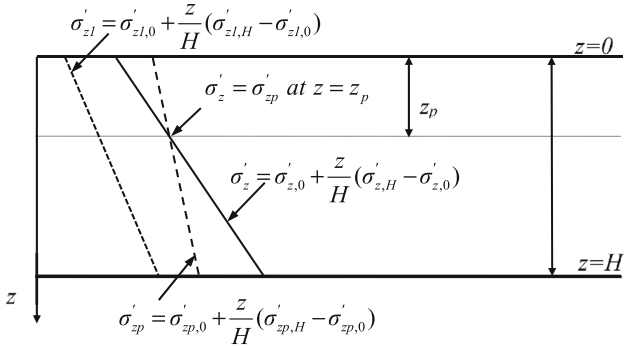

Fig. 4 Linear changes of initial vertical effective stress (σ'_{z1}), total vertical effective stress (σ'_z), vertical pre-consolidation stress (σ'_{zp}) for a soil layer

shows linear changes of initial vertical effective stress, total vertical effective stress, vertical pre-consolidation stress for a soil layer. Linear changes are in following equations:

$$\sigma'_{z1} = \sigma'_{z1,0} + \frac{z}{H}\left(\sigma'_{z1,H} - \sigma'_{z1,0}\right) \tag{7a}$$

$$\sigma'_{zp} = \sigma'_{zp,0} + \frac{z}{H}\left(\sigma'_{zp,H} - \sigma'_{zp,0}\right) \tag{7b}$$

$$\sigma'_z = \sigma'_{z4,0} + \frac{z}{H}\left(\sigma'_{z4,H} - \sigma'_{z4,0}\right) \tag{7c}$$

where σ'_{z1} is the initial vertical effective stress. It is noted that the increase of pre-consolidation stress (or pressure) σ'_{zp} may not be as fast as the total vertical effective stress σ'_z as shown in Fig. 4. Therefore, there is a point which $\sigma'_{zp} = \sigma'_z$ at depth z_p. Let us consider a general case of loading from point 1 to point 4, the calculation of settlements of j-layer for four different cases are in following.

(i) Normal consolidation case: OCR $= \sigma'_{zp}/\sigma'_{z1} = 1$.

In this case, initial effective stress σ'_{z1} and pre-consolidation stress σ'_{zp} are the same, after the stress increase, $\sigma'_z > \sigma'_{zp} = \sigma'_{z1}$. In this case, $S_{f,1-4}$ is:

$$S_{f,1-4} = \int_{z=0}^{z=H} \varepsilon_{z,1-4}dz = \int_{z=0}^{z=H} \frac{C_c}{1+e_o} \log\left(\sigma'_z + \sigma'_{\text{unit2}} \Big/ \sigma'_{zp} + \sigma'_{\text{unit2}}\right)dz \tag{8a}$$

Substituting Eq. (6) into the above equation:

$$S_{f,1-4} = \int_{z=0}^{z=H} \frac{C_c}{(1+e_o)\ln(10)} \ln\left[\frac{\sigma'_{z4,0} + \frac{z}{H}\left(\sigma'_{z4,H} - \sigma'_{z4,0}\right) + \sigma'_{\text{unit2}}}{\sigma'_{z1,0} + \frac{z}{H}\left(\sigma'_{z1,H} - \sigma'_{z1,0}\right) + \sigma'_{\text{unit2}}}\right] dz$$

$$= \frac{C_c}{(1+e_o)\ln(10)} \left\{ \int_{z=0}^{z=H} \ln\left[\sigma'_{z4,0} + \frac{z}{H}\left(\sigma'_{z4,H} - \sigma'_{z4,0}\right) + \sigma'_{\text{unit2}}\right] dz - \int_{z=0}^{z=H} \ln\left[\sigma'_{z1,0} + \frac{z}{H}\left(\sigma'_{z1,H} - \sigma'_{z1,0}\right) + \sigma'_{\text{unit2}}\right] dz \right\}$$

Let us introduce a new variable $x = \sigma'_{z4,0} + \frac{z}{H}\left(\sigma'_{z4,H} - \sigma'_{z4,0}\right) + \sigma'_{\text{unit2}}$ and $y = \sigma'_{z1,0} + \frac{z}{H}\left(\sigma'_{z1,H} - \sigma'_{z1,0}\right) + \sigma'_{\text{unit2}}$; we have $dz = \left[H/\left(\sigma'_{z4,H} - \sigma'_{z4,0}\right)\right]dx$ and $dz = \left[H/\left(\sigma'_{z1,H} - \sigma'_{z1,0}\right)\right]dy$. Noting that for $z = 0$ and H, we have $x_{z=0} = \sigma'_{z4,0} + \sigma'_{\text{unit2}}$ and $x_{z=H} = \sigma'_{z4,H} + \sigma'_{\text{unit2}}$; $y_{z=0} = \sigma'_{z1,0} + \sigma'_{\text{unit2}}$ and $y_{z=H} = \sigma'_{z1,H} + \sigma'_{\text{unit2}}$. The above equation can be written as:

$$S_{f,1-4} = \frac{C_c}{(1+e_o)\ln(10)} \left\{ \int_{x=\sigma'_{z4,0}+\sigma'_{\text{unit2}}}^{x=\sigma'_{z4,H}+\sigma'_{\text{unit2}}} \frac{H}{\left(\sigma'_{z4,H} - \sigma'_{z4,0}\right)} \ln x dx - \int_{y=\sigma'_{z1,0}+\sigma'_{\text{unit2}}}^{y=\sigma'_{z1,H}+\sigma'_{\text{unit2}}} \frac{H}{\left(\sigma'_{z1,H} - \sigma'_{z1,0}\right)} \ln y dy \right\}$$

Since $\int \ln x dx = x\ln x - x$ and $\int \ln y dy = y\ln y - y$, the above equation becomes:

$$S_{f,1-4} = \frac{C_c}{(1+e_o)\ln(10)} \left\{ \frac{H}{\left(\sigma'_{z4,H} - \sigma'_{z4,0}\right)} [x\ln x - x]_{x=\sigma'_{z4,0}+\sigma'_{\text{unit2}}}^{x=\sigma'_{z4,H}+\sigma'_{\text{unit2}}} - \frac{H}{\left(\sigma'_{z1,H} - \sigma'_{z1,0}\right)} [y\ln y - y]_{y=\sigma'_{z1,0}+\sigma'_{\text{unit2}}}^{y=\sigma'_{z1,H}+\sigma'_{\text{unit2}}} \right\}$$

From above, we have:

$$S_{f,1-4} = \frac{C_c}{(1+e_o)\ln(10)} \left\{ \frac{H}{(\sigma'_{z4,H} - \sigma'_{z4,0})} [(\sigma'_{z4,H} + \sigma'_{\text{unit2}}) \ln(\sigma'_{z4,H} + \sigma'_{\text{unit2}}) - (\sigma'_{z4,H} + \sigma'_{\text{unit2}}) - ((\sigma'_{z4,0} + \sigma'_{\text{unit2}}) \ln(\sigma'_{z4,0} + \sigma'_{\text{unit2}}) - (\sigma'_{z4,0} + \sigma'_{\text{unit2}}))] - \frac{H}{(\sigma'_{z1,H} - \sigma'_{z1,0})} [(\sigma'_{z1,H} + \sigma'_{\text{unit2}}) \ln(\sigma'_{z1,H} + \sigma'_{\text{unit2}}) - (\sigma'_{z1,H} + \sigma'_{\text{unit2}}) - ((\sigma'_{z1,0} + \sigma'_{\text{unit2}}) \ln(\sigma'_{z1,0} + \sigma'_{\text{unit2}}) - (\sigma'_{z1,0} + \sigma'_{\text{unit2}}))] \right\} \quad (8b)$$

(ii) Over-consolidation case: $\text{OCR} = \sigma'_{zp}/\sigma'_{z1} > 1$ and $\sigma'_z \geq \sigma'_{zp}$ for $0 \leq z \leq H$.

Figure 4 shows a case commonly encountered in the field. Initially, the soil is over-consolidated with $\text{OCR} = \sigma'_{zp}/\sigma'_{z1} > 1$. After increased loading $\Delta\sigma'_z = \sigma'_z - \sigma'_{z1}$, we have and $\sigma'_z \geq \sigma'_{zp}$ for $0 \leq z \leq H$. In this case, we have:

$$S_{f,1-4} = \int_{z=0}^{z=H} \varepsilon_{z,1-4} dz = \int_{z=0}^{z=H} \left[\frac{C_r}{1+e_o} \log\left(\frac{\sigma'_{zp} + \sigma'_{\text{unit1}}}{\sigma'_{z1} + \sigma'_{\text{unit1}}}\right) + \frac{C_c}{1+e_o} \log\left(\frac{\sigma'_z + \sigma'_{\text{unit2}}}{\sigma'_{zp} + \sigma'_{\text{unit2}}}\right)\right] dz \quad (8c)$$

Substituting equations in (6) for $\sigma'_{z1}, \sigma'_{zp}, \sigma'_z$ into (8c) and using the same method in (i), the integration of above equation is:

$$
\begin{aligned}
S_{f,1-4} = {} & \frac{C_r}{(1+e_o)\ln(10)}\left\{\frac{H}{(\sigma'_{zp,H}-\sigma'_{zp,0})}[(\sigma'_{zp,H}+\sigma'_{\text{unit1}})\right. \\
& \ln(\sigma'_{zp,H}+\sigma'_{\text{unit1}}) - (\sigma'_{zp,H}+\sigma'_{\text{unit1}}) - \\
& ((\sigma'_{zp,0}+\sigma'_{\text{unit1}})\ln(\sigma'_{zp,0}+\sigma'_{\text{unit1}}) - (\sigma'_{zp,0}+\sigma'_{\text{unit1}}))] \\
& - \frac{H}{(\sigma'_{z1,H}-\sigma'_{z1,0})}[(\sigma'_{z1,H}+\sigma'_{\text{unit1}})\ln(\sigma'_{z1,H}+\sigma'_{\text{unit1}}) \\
& - (\sigma'_{z1,H}+\sigma'_{\text{unit1}}) - ((\sigma'_{z1,0}+\sigma'_{\text{unit1}})\ln(\sigma'_{z1,0}+\sigma'_{\text{unit1}}) \\
& \left. - (\sigma'_{z1,0}+\sigma'_{\text{unit1}}))]\right\} + \\
& \frac{C_c}{(1+e_o)\ln(10)}\left\{\frac{H}{(\sigma'_{z4,H}-\sigma'_{z4,0})}[(\sigma'_{z4,H}+\sigma'_{\text{unit2}})\right. \\
& \ln(\sigma'_{z4,H}+\sigma'_{\text{unit2}}) - (\sigma'_{z4,H}+\sigma'_{\text{unit2}}) - \\
& ((\sigma'_{z4,0}+\sigma'_{\text{unit2}})\ln(\sigma'_{z4,0}+\sigma'_{\text{unit2}}) - (\sigma'_{z4,0}+\sigma'_{\text{unit2}}))] \\
& - \frac{H}{(\sigma'_{zp,H}-\sigma'_{zp,0})}[(\sigma'_{zp,H}+\sigma'_{\text{unit2}})\ln(\sigma'_{zp,H}+\sigma'_{\text{unit2}}) \\
& - (\sigma'_{zp,H}+\sigma'_{\text{unit2}}) - ((\sigma'_{zp,0}+\sigma'_{\text{unit2}})\ln(\sigma'_{zp,0}+\sigma'_{\text{unit2}}) \\
& \left. -(\sigma'_{zp,0}+\sigma'_{\text{unit2}}))]\right\}
\end{aligned}
\tag{8d}
$$

(iii) Over-consolidation case: $\text{OCR} = \sigma'_{zp}/\sigma'_{z1} > 1$ and $\sigma'_z < \sigma'_{zp}$ for $0 \le z \le z_p$.

Figure 4 shows a case in which $\text{OCR} = \sigma'_{zp}/\sigma'_{z1} > 1$, but $\sigma'_z < \sigma'_{zp}$ for $0 \le z \le z_p$ and $\sigma'_z \ge \sigma'_{zp}$ for $z_p \le z \le H$. In this case, the settlement calculation shall consider depth z_p:

$$
\begin{aligned}
S_{f,1-4} = {} & \int_{z=0}^{z=H} \varepsilon_{z,1-4}\,dz \\
= {} & \begin{cases}
\displaystyle\int_{z=0}^{z=z_p} \frac{C_r}{1+e_o}\log\left(\frac{\sigma'_z+\sigma'_{\text{unit1}}}{\sigma'_{z1}+\sigma'_{\text{unit1}}}\right)dz & \text{for } 0 \le z \le z_p \\
\displaystyle\int_{z=z_p}^{z=H} \left[\frac{C_r}{1+e_o}\log\left(\frac{\sigma'_{zp}+\sigma'_{\text{unit1}}}{\sigma'_{z1}+\sigma'_{\text{unit1}}}\right)\right. & \\
\left. + \frac{C_c}{1+e_o}\log\left(\frac{\sigma'_z+\sigma'_{\text{unit2}}}{\sigma'_{zp}+\sigma'_{\text{unit2}}}\right)\right]dz & \text{for } z_p \le z \le H
\end{cases}
\end{aligned}
\tag{8e}
$$

Linear equations in Eq. (6) for $\sigma'_{z1}, \sigma'_{zp}, \sigma'_z$ can be substituted into Eq. (8e). Analytical integration solution can be obtained using the same method in (i) and is not presented here. Equations like Eq. (8) can be obtained for other loading, unloading, and reloading cases with linear changes of stresses and are not discussed here.

In many calculations, m_v is needed, for example, in Eq. (5) and $c_v = k_v/(m_v\gamma_w)$ and $c_r = k_r/(\gamma_w m_v)$ in order to calculate U_v and U_r. If indexes C_r, C_c and pre-consolidation stress point $(\sigma'_{zp}, \varepsilon_{zp})$ are used to calculate final settlements in Eqs. (6, 7 and 8), the coefficient of vertical volume compressibility m_v can be back-calculated as.

(i) For the case of Eq. (6b) in normal loading:

$$
m_{v,1-4} = \frac{S_{f,1-4}}{H(\sigma'_{z4}-\sigma'_{z1})} \tag{9a}
$$

(ii) For the case of Eq. (6d) in unloading:

$$
m_{v,4-6} = \frac{S_{f,4-6}}{H(\sigma'_{z4}-\sigma'_{z6})} \tag{9b}
$$

In Eqs. (9a) and (9b), settlements and stress increments are known so that m_v corresponding to the same stress increment can be calculated. In Eq. (9b), $S_{f,4-6}$ and $(\sigma'_{z4} - \sigma'_{z6})$ are both negative so that $m_{v,4-6}$ is positive. The calculation method for m_v in Eqs. (9a) and (9b) can be applied to other different loading stages.

2.3 Calculation of U_j and U

In Eqs. (1) and (2), an average degree of consolidation U_j for j-layer or over-all average degree of consolidation U is needed. The basic definition of U_j for j-layer is:

$$
\begin{aligned}
U_j = \frac{S_j(t)}{S_{fj}} = {} & \frac{\int_{z=0}^{z=H_j} m_{vj}\Delta\sigma'_{zj}(t)\,dz}{\int_{z=0}^{z=H_j} m_{vj}\Delta\sigma'_{zjf}\,dz} = \frac{\int_{z=0}^{z=H_j}[u_{eij}-u_{ej}(t)]\,dz}{\int_{z=0}^{z=H_j} u_{eij}\,dz} \\
= {} & 1 - \frac{\int_{z=0}^{z=H_j} u_{ej}(t)\,dz}{\int_{z=0}^{z=H_j} u_{eij}\,dz}
\end{aligned}
\tag{10a}
$$

where S_{fj} is the final settlement for j-layer using m_{vj} and $\Delta\sigma'_{zjf}$, calculated using Eq. (5). It is noted that the final vertical effective stress increment $\Delta\sigma'_{zjf}$ is equal to the initial excess pore water pressure u_{eij} for j-layer. $u_{ej}(t)$ is the excess pore water pressure at time t for j-layer. Equation (10a) can be written as:

$$U_j = 1 - \frac{\frac{1}{H_j}\int_{z=0}^{z=H_j} u_{ej}(t)dz}{\frac{1}{H_j}\int_{z=0}^{z=H_j} u_{eij}dz} = 1 - \frac{\overline{u}_{ej}(t)}{\overline{u}_{eij}} \tag{10b}$$

where $\overline{u}_{eij}$ and $\overline{u}_{ej}$ are the average initial and current excess porewater pressures, respectively, t for j-layer. The over-all average degree of consolidation U is:

$$U = \frac{S_{\text{primary}}}{S_f} = \frac{\sum_{j=1}^{j=n} S_j(t)}{\sum_{j=1}^{j=n} S_{fj}} = \frac{\sum_{j=1}^{j=n}\int_{z=0}^{z=H_j} m_{vj}\Delta\sigma'_{zj}(t)dz}{\sum_{j=1}^{j=n}\int_{z=0}^{z=H_j} m_{vj}\Delta\sigma'_{zjf}dz} = 1 - \frac{\sum_{j=1}^{j=n} m_{vj}\int_{z=0}^{z=H_j} u_{ej}(t)dz}{\sum_{j=1}^{j=n} m_{vj}\int_{z=0}^{z=H_j} u_{eij}dz} \tag{11a}$$

From Eq. (10a), $\overline{u}_{ej}(t) = (1 - U_j)\overline{u}_{eij}$. Using this relation, (11a) can be written:

$$U = 1 - \frac{\sum_{j=1}^{j=n} m_{vj}\frac{H_j}{H_j}\int_{z=0}^{z=H_j} u_{ej}(t)dz}{\sum_{j=1}^{j=n} m_{vj}\frac{H_j}{H_j}\int_{z=0}^{z=H_j} u_{eij}dz} = 1 - \frac{\sum_{j=1}^{j=n} m_{vj}H_j\overline{u}_{ej}(t)}{\sum_{j=1}^{j=n} m_{vj}H_j\overline{u}_{eij}} = 1 - \frac{\sum_{j=1}^{j=n} m_{vj}H_j(1-U_j)\overline{u}_{eij})}{\sum_{j=1}^{j=n} m_{vj}H_j\overline{u}_{eij}} = 1 - \frac{\sum_{j=1}^{j=n} m_{vj}H_j\overline{u}_{eij} - \sum_{j=1}^{j=n} m_{vj}H_jU_j\overline{u}_{eij}}{\sum_{j=1}^{j=n} m_{vj}H_j\overline{u}_{eij}} = \frac{\sum_{j=1}^{j=n} m_{vj}H_j\overline{u}_{eij}U_j}{\sum_{j=1}^{j=n} m_{vj}H_j\overline{u}_{eij}} \tag{11b}$$

Attention shall be paid to the definition and differences of U_j and U. The following paragraphs summarize existing solutions for U_v, U_r, U_j and U.

The early analytical solutions were obtained by Terzaghi [29] for a single soil layer with thickness H under suddenly applied load for 1-D straining. Charts of these solutions can be found in Craig's Soil Mechanics Knappett [17]. For double drainage with linear excess pore water pressure u_e distribution or one-way drainage with uniform u_e distribution, the following appreciate equation is good and simple to calculate U_v:

$$\begin{cases} \text{For } U_v < 0.6: \quad T_v = \dfrac{\pi}{4}U_v^2, \quad U_v = \sqrt{\dfrac{4T_v}{\pi}} \\ \text{For } U_v \geq 0.6: \quad T_v = -0.944\log(1-U_v) - 0.085, \\ U_v = 1 - 10^{-\frac{T_v+0.085}{0.933}} \end{cases} \tag{12a}$$

If we assume that when $U_v = 98\%$, $u_e \approx 0$; time at $U_v = 98\%$ is selected as time at EOP in the field $t_{\text{EOP,field}}$. We have:

$$T_v = -0.944\log(1-U_v) - 0.085 = 0.150 \tag{12b}$$

$$t_{\text{EOP,field}} = \frac{T_v d^2}{c_v} = \frac{1.50d^2}{c_v} \tag{12c}$$

where d is the maximum drainage path of a soil layer, if double drainage, $d = H/2$, c_v is the coefficient of vertical consolidation.

To consider ramp loading as shown in Fig. 4, a simple correction method for U_v proposed by Terzaghi [29] can be used. Solutions to 1-D consolidation under depth-dependent ramp load and to special 1-D consolidation problems can be found in Zhu and Yin [41, 48] Solutions to double soil layers without vertical drains under ramp load can be found in Zhu and Yin [43]. Solutions to 2-D consolidation of a single soil layer with vertical drains under ramp load were obtained by Zhu and Yin [45 , 46 , 47]. Solutions to 2-D consolidation of a single soil layer with vertical drains without well resistance under suddenly applied load were obtained by Barron [4]. Hansbo [14] presented analytical solution to consolidation problem of a soil with vertical drains considering both smear zone and well resistance under suddenly applied load under equal vertical strain assumption.

Solutions to consolidation problem of a stratified soil with vertical and horizontal drainage under ramp loading were obtained by Walker and Indraratna [26] and Walker et al. [27] using a spectral method. The main partial differential equation for the average excess pore water pressure $\overline{u}$ using spectral method is:

$$\frac{m_v}{\overline{m}_v}\frac{\partial\overline{u}}{\partial t} = -\left[dT_r\frac{\eta}{\overline{\eta}}\overline{u} - dT_v\left(\frac{\partial}{\partial Z}\left(\frac{k_v}{\overline{k}_v}\right)\frac{\partial\overline{u}}{\partial Z} + \frac{k_v}{\overline{k}_v}\frac{\partial^2\overline{u}}{\partial Z^2}\right)\right] + \frac{m_v}{\overline{m}_v}\frac{\partial\overline{\sigma}}{\partial t} + dT_r\frac{\eta}{\overline{\eta}}w \tag{13a}$$

where $\eta = \frac{k_r}{r_e^2\mu}$, $\mathrm{d}T_v = \frac{\overline{c}_v}{H^2}$, $\mathrm{d}T_r = \frac{2\overline{\eta}}{\gamma_w\overline{m}_v}$, $\overline{c}_v = \frac{\overline{k}_v}{\gamma_w\overline{m}_v}$, $Z = \frac{z}{H}$. Vertical and horizontal drainages are considered simultaneously in Eq. (13a). All parameters are explained below:

$\overline{u}$: averaged excess pore water pressure (averaged along radial coordinate r) at depth Z, a function of time t and Z.

$\overline{\sigma}$: average total stress (averaged along r) at depth Z, a function of time t and Z.

w: water pressure applied on the vertical drains, varying with depth Z, which is zero without vacuum pre-loading pressure.

r_w: unit weight of water.

k_r: the horizontal permeability coefficient of the undisturbed soil, a function of Z.

m_v: coefficient of volume compressibility (assumed the same in smear and undisturbed zone), calculated using total incremental strain resulted from primary consolidation under total stress increment, and a function of Z.

Parameters k_v, m_v and η can be depth-dependent in a piecewise linear way or kept constant within each layer. $\overline{k}_v$, $\overline{m}_v$ and $\overline{\eta}$ are convenient reference values at certain depth; for example, values $k_{v,j=1}$, $m_{v,j=1}$ and $\eta_{j=1}$ of layer 1. If so, $\overline{c}_v = \overline{k}_v/\gamma_w \overline{m}_v = k_{v,j=1}/\gamma_w m_{v,j=1} = c_{v,j=1}$. $\overline{\eta} = \overline{k}_r/r_e^2\mu = k_{r,j=1}/r_e^2\mu = \eta_{j=1}$. All the parameters in Eq. (13a) have been normalized and may be different for different soil layers. (No layer index is used here to make presentation concise.) Normalized parameters in Eq. (13a) are: $m_v/\overline{m}_v$, $\eta/\overline{\eta}$, $k/\overline{k}_v$.

The parameter $\eta = k_r/(r_e^2\mu)$ is related to radial permeability k_r, equivalent radius r_e of cylinder cell, and μ. If there is no horizontal drainage in a soil layer, $k_r = 0$ to that $\eta = 0$. This is useful for consolidation analysis of soils with partially penetrating vertical drains. All soil layers below vertical drains have $\eta = 0$. Walker and Indraratna [26] and Walker et al. [27] discussed that their method can also simulate the effect of using long and short drains in unison. For example, in lower soil layers where only long drains are installed, η shall have smaller value than that of upper soil layers where both short and long drains are present.

μ inside η is a dimensionless drain geometry/smear zone parameter. Expressions for μ can be taken as the following by considering effects of smear zone, well resistance, or approximation [14]:

$$\mu = \frac{n^2}{n^2-1}\left(\ln\frac{n}{s} - \frac{3}{4} + \frac{k_r}{k_s}\ln s\right) + \frac{s^2}{n^2-1}\left(1 - \frac{s^2}{4n^2}\right) + \frac{k_r}{k_s}\frac{1}{n^2-1}\left(\frac{s^4-1}{4n^2} - s^2 + 1\right) + \pi z(2l-z)\frac{k_r}{q_w}\left(1 - \frac{1}{n^2}\right) \tag{13b}$$

In (13b), $T_r = \frac{c_r t}{r_e^2}$, $n = \frac{r_e}{r_d}$, $s = \frac{r_s}{r_d}$. $q_w = k_w \pi r_w^2$ is the specific discharge capacity of drain (vertical hydraulic gradient $i = 1$). z is the vertical coordinate in Fig. 1 and l is the length of drain when closed at bottom or a half of drain when bottom is open. If hydraulic resistance of vertical drains is zero, this means $q_w = k_w \pi r_d^2 \Rightarrow \infty$. (13b) can be simplified:

$$\mu = \frac{n^2}{n^2-1}\left(\ln\frac{n}{s} - \frac{3}{4} + \frac{k_r}{k_s}\ln s\right) + \frac{s^2}{n^2-1}\left(1 - \frac{s^2}{4n^2}\right) + \frac{k_r}{k_s}\frac{1}{n^2-1}\left(\frac{s^4-1}{4n^2} - s^2 + 1\right) \tag{13c}$$

Walker and Indraratna [28] also provided an expression for μ considering parabolic smear zone permeability but ignoring smear zone:

$$\mu = \ln\frac{n}{s} - \frac{3}{4} + \frac{\kappa(s-1)^2}{(s^2 - 2\kappa s + \kappa)}\ln\frac{s}{\sqrt{\kappa}} - \frac{s(s-1)\sqrt{\kappa(\kappa-1)}}{2(s^2-2\kappa s+\kappa)}\ln\left(\frac{\sqrt{\kappa}+\sqrt{\kappa-1}}{\sqrt{\kappa}-\sqrt{\kappa-1}}\right) \tag{13d}$$

where κ is the ratio of undisturbed horizontal permeability k_r to smear zone permeability k_{so} at the drain/soil interface, (at $r = r_d$, $k_s = k_{s0}$). At $r = r_s$, $k_s = k_r$.

Walker and Indraratna [26] provided an Excel spreadsheet calculation program implemented with VBA program named SPECCON to enable convenient adoption of this method for consolidation analysis of multiple soils layers with or without vertical drains. After inputted all parameters and load $\overline{\sigma}$, this program gives excess pore water pressure at time t $\overline{u}_{ej}(t)$ for j-layer and $\overline{u}_e(t)$ for all layers together. The combined average degree of consolidation U_j for each j-layer is calculated using Eq. (10a). The overall combined average degree of consolidation U for all layers shall be calculated using Eq. (11a) or Eq. (11b). Once U_j and U with time t are known, total "primary" consolidation settlement S_{primary} can be calculated using Eq. (2).

2.4 Calculation of S_{creep}, $S_{\text{creep}j}$, $S_{\text{creep},fj}$ and $S_{\text{creep},dj}$

In Eqs. (1) or (4b), the total creep settlement S_{creep} of all layers together is sum of $S_{\text{creep}j}$ for all layers. This is a simple superposition. The key items for calculating $S_{\text{creep}j}$ are $S_{\text{creep},fj}$ and $S_{\text{creep},dj}$.

(a) Calculation of $S_{\text{creep},fj}$ for different stress–strain states

Creep settlement $S_{\text{creep},fj}$ of j-layer is calculated as creep compression under the "final" vertical effective stress ignoring coupling of excess porewater pressure nor any ramp loading process. This is an ideal case in order to decouple this consolidation problem. To consider creep compression occurred in "primary" consolidation starting from time zero, the void ratio e due to creep is [36, 37]:

$$e = e_o - C_{\alpha e}\log\frac{t_o + t_e}{t_o} \tag{14}$$

where $C_{\alpha e}$ is a creep parameter; t_o is another creep parameter; t_e is "equivalent time" defined by Yin and Graham [36, 37] and e_o is the initial void ratio at $t_e = 0$. In this study, $C_{\alpha e}$ is considered constant as a common practice in engineering. Yin [32] proposed a nonlinear creep model which considers the creep limit with time and the decreasing trend of $C_{\alpha e}$ with effective stress, which shows advantages in very long-term settlement calculations [8]. For settlement calculation of settlements of most soft soils in a normal service life (say 50 years) of a geotechnical structure, it is still reliable and convenient to adopt constant values of $C_{\alpha e}$ to avoid lengthy equations as much as

possible [9, 35]. According to the "equivalent time" concept [31, 33, 34, 36, 37], the total strain ε_z at any stress–strain state in Fig. 3 can be calculated by the following equation:

$$\varepsilon_z = \varepsilon_{zp} + \frac{C_c}{V}\log\frac{\sigma_z^{'}}{\sigma_{zp}^{'}} + \frac{C_{\alpha e}}{V}\log\frac{t_o + t_e}{t_o} \tag{15}$$

where $\varepsilon_{zp} + \frac{C_c}{V}\log\frac{\sigma_z^{'}}{\sigma_{zp}^{'}}$ is the strain on the normal consolidation line (NCL) under stress $\sigma_z^{'}$ (also called "reference time line" and noting initial specific volume $V = 1 + e_o$) and $\frac{C_{\alpha e}}{V}\log\frac{t_o+t_e}{t_o}$ is the creep strain occurring from the NCL under the same stress $\sigma_z^{'}$. The above equation is valid for any 1-D loading path. The calculation of $S_{\text{creep},fj}$ is dependent on the final stress–strain state $(\sigma_z^{'}, \varepsilon_z)$. To make presentation concise, in the following equations, layer index j, are removed.

(i) The final stress–strain point is on an NCL line, for example at point 4

The final creep settlement for any point on NCL line is:

$$S_{\text{creep},f} = \frac{C_{\alpha e}}{1 + e_o}\log\left(\frac{t_o + t_e}{t_o}\right)H \quad \text{for } t_e \geq 0 \tag{16a}$$

For a suddenly applied load kept for a duration time t, we have $t_e = t - t_o$. Submitting the above relation into (16a), we have:

$$S_{\text{creep},f} = \frac{C_{\alpha e}}{1 + e_o}\log\left(\frac{t}{t_o}\right)H \quad \text{for} \quad t \geq 1 \text{ day} \tag{16b}$$

Noting $t_o = 1$ day since C_r and C_c are determined using data with 1-day duration. In (16a), if $t = 1$ day, from $t_e = t - t_o$, $t_e = 1 - 1 = 0$. This means that at time $t = 1$ day, creep settlement $S_{\text{creep},f}$ on NCL is zero. According to elastic viscoplastic (EVP) modelling theory [36, 37], the compression strain rate is the sum of elastic strain rate and viscoplastic strain rate. The NCL line in Fig. 3, in fact, has included both elastic strain and viscoplastic strain (or creep strain). The creep settlement in (16a) is additional creep compression starting from 1 day or below NCL.

(ii) The final stress–strain point is on an OCL line, for example at point 2

Consider a sudden load increase from point 1 to point 2, which is kept unchanged with a duration time t. The final creep settlement for any point, for example point 2, on over-consolidation line (OCL) is:

$$S_{\text{creep},f} = \frac{C_{\alpha e}}{1 + e_o}\log\left(\frac{t_o + t_e}{t_o + t_{e2}}\right)H \quad \text{for } t_e \geq t_{e2} \tag{16c}$$

(16c) can be re-written with $\Delta\varepsilon_{z\text{creep}}$ included:

$$S_{\text{creep},f} = \left[\frac{C_{\alpha e}}{1 + e_o}\log\left(\frac{t_o + t_e}{t_o}\right) - \frac{C_{\alpha e}}{1 + e_o}\log\left(\frac{t_o + t_{e2}}{t_o}\right)\right]H = \Delta\varepsilon_{z\text{creep}}H$$

Referring to Fig. 3, it is seen that $\frac{C_{\alpha e}}{1+e_o}\log\left(\frac{t_o+t_{e2}}{t_o}\right)$ is the strain from point $2^{'}$ to point 2, while $\frac{C_{\alpha e}}{1+e_o}\log\left(\frac{t_o+t_e}{t_o}\right)$ is the strain from point $2^{'}$ to a point below point 2 downward. The increased strain for further creep done from point 2 is $\Delta\varepsilon_{z\text{creep}}$, which is used to calculate creep settlement $S_{\text{creep},f}$ under loading at point 2. It is noted that the relationship between t_e and the creep duration time t under the stress $\sigma_{z2}^{'}$ is $t_e = t_{e2} + t - t_o$. t_{e2} here or in (16c) can be calculated below. Using Eq. (15), at point 2 of $(\sigma_{z2}^{'}, \varepsilon_{z2})$, we have:

$$\varepsilon_{z2} = \varepsilon_{zp} + \frac{C_c}{V}\log\frac{\sigma_{z2}^{'}}{\sigma_{zp}^{'}} + \frac{C_{\alpha e}}{V}\log\frac{t_o + t_{e2}}{t_o}$$

From the above, we have:

$$\log\frac{t_o + t_{e2}}{t_o} = (\varepsilon_{z2} - \varepsilon_{zp})\frac{V}{C_{\alpha e}} - \frac{C_c}{C_{\alpha e}}\log\frac{\sigma_{z2}^{'}}{\sigma_{zp}^{'}}$$

$$t_{e2} = t_o \times 10^{(\varepsilon_{z2}-\varepsilon_{zp})\frac{V}{C_{\alpha e}}}\left(\frac{\sigma_{z2}^{'}}{\sigma_{zp}^{'}}\right)^{-\frac{C_c}{C_{\alpha e}}} - t_o \tag{16d}$$

It is seen from (16d) that the equivalent time t_{e2} at point 2 is uniquely related to the stress–strain state point $(\sigma_{z2}^{'}, \varepsilon_{z2})$. Substituting $t_e = t_{e2} + t - t_o$ into (16c), we have:

$$S_{\text{creep,f}} = \frac{C_{\alpha e}}{1 + e_o}\log\left(\frac{t + t_{e2}}{t_o + t_{e2}}\right)H \quad t \geq 1 \text{ day} \tag{16e}$$

If we consider unloading from point 4 to point 6 in Fig. 3, using the same approach above, we can derive the following equations:

$$t_{e6} = t_o \times 10^{(\varepsilon_{z6}-\varepsilon_{zp})\frac{V}{C_{\alpha e}}}\left(\frac{\sigma_{z6}^{'}}{\sigma_{zp}^{'}}\right)^{-\frac{C_c}{C_{\alpha e}}} - t_o \tag{16f}$$

$$S_{\text{creep},f} = \frac{C_{\alpha e}}{1 + e_o}\log\left(\frac{t_o + t_e}{t_o + t_{e6}}\right)H = \frac{C_{\alpha e}}{1 + e_o}\log\left(\frac{t + t_{e6}}{t_o + t_{e6}}\right)H \quad t \geq 1 \text{ day} \tag{16g}$$

Reloading from point 6 to point 5:

$$t_{e5} = t_o \times 10^{(\varepsilon_{z5}-\varepsilon_{zp})\frac{V}{C_{\alpha e}}}\left(\frac{\sigma_{z5}^{'}}{\sigma_{zp}^{'}}\right)^{-\frac{C_c}{C_{\alpha e}}} - t_o \tag{16h}$$

$$S_{\text{creep},f} = \frac{C_{\alpha e}}{1 + e_o}\log\left(\frac{t_o + t_e}{t_o + t_{e5}}\right)H = \frac{C_{\alpha e}}{1 + e_o}\log\left(\frac{t + t_{e5}}{t_o + t_{e5}}\right)H \quad t \geq 1 \text{ day} \tag{16i}$$

(b) Calculation of $S_{\text{creep},dj}$ for different stress–strain states.

$S_{\text{creep},dj}$ is called "delayed" creep settlement of j-layer under the "final" vertical effective stress ignoring the excess porewater pressure. $S_{\text{creep},dj}$ starts for $t \geq t_{\text{EOP,field}}$, that is, is "delayed" by time of $t_{\text{EOP,field}}$. The selection of time at EOP is subjective since the separation of "primary" consolidation from "secondary" compressions is not scientific and subjective. In the general simple method, the time at $U_j = 98\%$ is considered to be the time at EOP, that is, $t_{\text{EOP,field}}$ for field condition for j-layer [35]. Equation (12c) or other solutions for U_j can be used to calculate $t_{\text{EOP,field}}$ for a single-layer case. Equations for calculating $S_{\text{creep},dj}$ for different "final" stress–strain state are presented below. The layer index j is removed in following equations.

(i) The final stress–strain point is on an NCL line, for example at point 4.

Equation (16a) is the final creep settlement for any point on NCL line for $t_e \geq 0$ or $t \geq 1$ day:

$$S_{\text{creep},f} = \frac{C_{\alpha e}}{1+e_o}\log\left(\frac{t_o+t_e}{t_o}\right)H \quad t_e \geq 0$$

$S_{\text{creep},d}$ is delayed by $t_{\text{EOP,field}}$:

$$\begin{aligned} S_{\text{creep},d} &= \frac{C_{\alpha e}}{1+e_o}\log\left(\frac{t_o+t_e}{t_o}\right)H \\ &\quad - \frac{C_{\alpha e}}{1+e_o}\log\left(\frac{t_o+t_{e,\text{EOP,field}}}{t_o}\right)H \\ &= \frac{C_{\alpha e}}{1+e_o}\log\left(\frac{t_o+t_e}{t_o+t_{e,\text{EOP,field}}}\right)H \quad \text{for } t_e \geq t_{e,\text{EOP,field}} \end{aligned} \tag{17a}$$

Noting $\because t_e = t - t_o \quad \therefore t_{e,\text{EOP,field}} = t_{\text{EOP,field}} - t_o$. Substituting these time relations into (17a):

$$S_{\text{creep},d} = \frac{C_{\alpha e}}{1+e_o}\log\left(\frac{t}{t_{\text{EOP,field}}}\right)H \quad \text{for } t \geq t_{\text{EOP,field}} \tag{17b}$$

In (17b) $S_{\text{creep},d}$ is calculated for $t \geq t_{\text{EOP,field}}$, that is, "delayed" by time $t_{\text{EOP,field}}$.

(ii) The final stress–strain point is on an OCL line, for example at point 2.

The final creep settlement at point 2 is:

$$S_{\text{creep},f} = \frac{C_{\alpha e}}{1+e_o}\log\left(\frac{t+t_{e2}}{t_o+t_{e2}}\right)H$$

for $t_e \geq t_{e2}$ or $t \geq t_o = 1$ day

$S_{\text{creep},d}$ is delayed by $t_{\text{EOP,field}}$:

$$\begin{aligned} S_{\text{creep},d} &= \frac{C_{\alpha e}}{1+e_o}\log\left(\frac{t+t_{e2}}{t_o+t_{e2}}\right)H \\ &\quad - \frac{C_{\alpha e}}{1+e_o}\log\left(\frac{t_{\text{EOP,field}}+t_{e2}}{t_o+t_{e2}}\right)H \\ S_{\text{creep},d} &= \frac{C_{\alpha e}}{1+e_o}\log\left(\frac{t+t_{e2}}{t_{\text{EOP,field}}+t_{e2}}\right)H \quad \text{for } t \geq t_{\text{EOP,field}} \end{aligned} \tag{18a}$$

When $t = t_{\text{EOP,field}}$, $S_{\text{creep},d}$ in (18a) is zero.

Using the same approach, at point 6:

$$S_{\text{creep},d} = \frac{C_{\alpha e}}{1+e_o}\log\left(\frac{t+t_{e6}}{t_{\text{EOP,field}}+t_{e6}}\right)H \quad \text{for } t \geq t_{\text{EOP,field}} \tag{18b}$$

at point 5:

$$S_{\text{creep},d} = \frac{C_{\alpha e}}{1+e_o}\log\left(\frac{t+t_{e5}}{t_{\text{EOP,field}}+t_{e5}}\right)H \quad \text{for } t \geq t_{\text{EOP,field}} \tag{18c}$$

3 Consolidation settlements of a clay layer with OCR = 1 or 1.5 from general simple method and fully coupled consolidation analyses

In this section, consolidation settlements of an idealized horizontal layer of Hong Kong Marine Clay (HKMC) are calculated using the simplified Hypothesis B method and two fully coupled finite element (FE) consolidation models. This HKMC layer has 4 m in thickness and is free drained on the top surface and impermeable at the bottom. Overconsolidation ratio (OCR) is OCR = 1 or 1.5. Two FE programs are used for fully coupled consolidation analysis of the HKMC layer: one is software "Consol" developed by Zhu and Yin [42, 44] and the other one is Plaxis software (2D 2015 version) Plaxis [25]. In the "Consol" analysis, a 1D EVP model [36, 37] is used for the consolidation modelling. In Plaxis software (2D 2015 version), a soft soil creep (SSC) model is adopted in the FE simulations. SSC model is in fact a 3D EVP model [30]. The structure and parameters of this SSC model are almost the same as a 3D EVP model proposed by Yin [31] and Yin and Graham [39].

Values of all parameters used in FE consolidation simulation are listed in Table 2. In all FE simulations, a vertical stress of 20 kPa is assumed to be instantly applied on the top surface and kept constant for a period of 18,250 days (50 years). Since HKMC layer is in seabed, the initial vertical effective stress is zero at the top of the HKMC layer surface. Therefore, the unit stress σ'_{unit1} or σ'_{unit2} in Eq. (6) cannot be zero. The best value of

σ'_{unit1} or σ'_{unit2} shall be determined by oedometer compression test data at very small vertical effective stress. Here we may assume that σ'_{unit1} or σ'_{unit2} takes values from 0.0 1 to 1 kPa and discuss difference of calculated settlement values.

(a) Normally consolidated HKMC layer with H = 4 m and OCR = 1.

The integrated Eq. (8b) is used to calculate the final "primary" settlement $S_{f,1-4}$. The values of all parameters are listed in Table 1. The values of all stresses are $\sigma'_{z1,0} = 0$, $\sigma'_{z1,H} = 20.76$kPa, $\sigma'_{z4,0} = 20$, $\sigma'_{z4,H} = 40.76$kPa. $S_{f,1-4}$ is:

$$(40.76 - 20)$$

Using above equation with σ'_{unit2} = 0.01 kPa, it is found that $S_{f,1-4}$ = 0.944 m; if σ'_{unit2} = 0.1 kPa, $S_{f,1-4}$ = 0.928 m; if σ'_{unit2} = 0.5 kPa, $S_{f,1-4}$ = 0.879 m; if σ'_{unit2} = 1 kPa, $S_{f,1-4} = 0.834$ m. This means that the final "primary" settlement $S_{f,1-4}$ is sensitive to the value of σ'_{unit2}. In this example, we select σ'_{unit2} = 0.1 kPa so that the final "primary" settlement $S_{f,1-4}$ is 0.928 m.

The calculation of average m_v and c_v is below:

$$\Delta\varepsilon_{z,1-4} = S_{f,1-4} = 0.928/4 = 0.232$$

$$m_v = \Delta\varepsilon_{z,1-4}/\Delta\sigma'_{z,1-4} = 0.232/20 = 0.0116 \quad (1/\text{kPa})$$

$$c_v = k/(\gamma_w m_v) = 1.9 \times 10^{-4}/(9.81 \times 0.0116) = 1.670 \times 10^{-3}\ (m^2/\text{day}) = 0.610\ (m^2/\text{year})$$

As explained, a thick layer can be divided into small sub-layers. The stresses and values of soil parameters in each sub-layer are assumed be constant. In this case, simple equations in Eq. (6b) can be used to calculate that the final "primary" settlement $S_{f,1-4}$ for each sub-layer. This layer of 4 m can be divided into 2, 4, or 8 sub-layers with thickness of 2 m, 1 m, and 0.5 m, respectively. The final "primary" settlement $S_{f,1-4}$ calculated is 0.743 m, 0.831 m, 0.881 m and 0.910 m sub-layers with thickness of 4 m, 2 m, 1 m, and 0.5 m, respectively. Values of S_f, m_v and c_v for sub-layer thickness of 0.5 m for OCR = 1 are listed in Table 2. ε_{zp} in Table 2 is the vertical strain in each sub-layer (0.5 m here) from the initial effective stress σ'_{zi} to pre-consolidation pressure σ'_{zp} and $\bar{\varepsilon}_{zp}$ is average of all ε_{zp} values. Since OCR = 1, $\sigma'_{zp} = \sigma'_{zi}$, the strain ε_{zp} and $\bar{\varepsilon}_{zp}$ are zero. $\Delta\varepsilon_z$ is the strain increase in each sub-layer for loading from σ'_{zp} to current stress σ'_z. $\Delta\bar{\varepsilon}_z$ is average of all $\Delta\varepsilon_z$ values. $(\bar{\varepsilon}_{zp} + \Delta\bar{\varepsilon}_z)$ is total vertical strain. Summary of values of S_f, m_v and c_v for different numbers of sub-layers for OCR = 1 is listed in Table 3 including S_f obtained by more accurate integration method. It is seen from Table 3 that the more sub-layers (or the smaller thickness of the sub-layers), the more accurate are these S_f, m_v and c_v. A thickness of 0.5 m is considered as appropriate since the relative error of S_f is only $\frac{0.928-0.910}{0.928} \times 100\% = 1.9\%$ of the integrated one.

In this example, the general simplified Hypothesis B method in Eq. (1) together with other equations on relevant parameters is used to calculate the total settlement $S_{\text{total}B}$

Table 1 Values of parameters for the upper marine clay of Hong Kong

(a) Values of basic property

$V = 1 + e_o$	w_i(kN/m^3)	OCR	w_i(%)
3.65	15	1 or 1.5	100

(b) Values of parameters used in Consol software

κ/V	λ/V	ψ/V	t_o(day)	k_v(m/day)	σ'_{zo}* (kPa)
0.01086	0.174	0.0076	1	1.90×10^{-4}	1

(c) Values of parameters used in PLAXIS

κ^*	λ^*	μ^*	t_o(day)	k_v(m/day)	OCR	φ'(kPa	φ'(deg)
0.02172	0.174	0.0076	1	1.90×10^{-4}	1 or 1.5	0.1	30

(d) Values of parameters used in the simplified Hypothesis B method

C_e $[C_e = \kappa\ln(10)]$	C_c $[C_c = \lambda\ln(10)]$	$C_{\alpha e}$ $[C_{\alpha e} = \psi\ln(10)]$	V	t_o(day)	k_v(m/day)
0.0913	1.4624	0.0639	3.65	1	1.90×10^{-4}

*: σ'_{zo} is the value of the effective vertical stress when the vertical strain of the reference time line is zero ($\varepsilon_{zo} = 0$). Further details can be found in Zhu and Yin [44].

Table 2 Calculation of S_f, m_v and c_v for sub-layer thickness of 0.5 m for OCR = 1

Mid sub-layer depth (m)	σ'_{zi} (kPa)	$\sigma'_z = \sigma'_{zi} + \Delta\sigma'_z$ (kPa)	$\sigma'_{zp} = \sigma'_{zi}$ (kPa)	ε_{zp}	$\Delta\varepsilon_z$	m_v(1/kPa)	$c_v = \frac{k_v}{\gamma_w m_v}$(m^2/day)
0.25	1.2975	21.2975	1.2975	0	0.4748	0.01137	1.704E-03
0.75	3.8925	23.8925	3.8925	0	0.3120		
1.25	6.4875	26.4875	6.4875	0	0.2428		
1.75	9.0825	29.0825	9.0825	0	0.2012		
2.25	11.6775	31.6775	11.6775	0	0.1727		
2.75	14.2725	34.2725	14.2725	0	0.1517		
3.25	16.8675	36.8675	16.8675	0	0.1355		
3.5	18.1650	38.1650	18.1650	0	0.1287		
				$\bar{\varepsilon}_{zp} =$ 0			
				Total strain $(\bar{\varepsilon}_{zp} + \Delta\bar{\varepsilon}_z)$:	0.2274		
				Settlement S_f (m)	0.9097		

Table 3 Summary of S_f, m_v and c_v for different numbers of sub-layers for OCR = 1

Number of sub-layers	Vertical strain ε_z after loading	m_v(1/kPa)	$c_v = \frac{k_v}{\gamma_w m_v}$(m^2/day)	$S_f = \varepsilon_z \times H$ (m)	S_f from integration (m)
1	0.1858	0.0093	2.086E-03	0.743	0.928
2	0.2077	0.0104	1.866E-03	0.831	0.928
4	0.2202	0.0110	1.760E-03	0.881	0.928
8	0.2274	0.0114	1.704E-03	0.910	0.928

using $\alpha = 0.8$ and $\beta = 0$ (denoted B Method 1), $\beta = 0.3$ (denoted B Method 2), and $\beta = 1$(denoted B Method 3). B Method 1 using $\alpha = 0.8$ and $\beta = 0$ is in fact the method published by Yin and Feng [35]. The calculated curves of settlements with log(time) from the simplified Hypothesis B method are shown in Fig. 5a for time up to 100 years. At the same time, Hypothesis A method and two fully coupled finite element models are used to calculate the curves of settlements with log(time), which are also shown in Fig. 5a for comparison. It is seen from Fig. 5a that, when $\alpha = 0.8$ and $\beta = 0.3$ m, B Method 2 gives curves much closer to the curves from the two finite element models of "Consol" by Zhu and Yin [42, 44] and Plaxis software (2D 2015 version). Values of parameters used in Consol software are listed in Table 1b and those of Plaxis in Table 1c. As shown in Fig. 5a, again, Hypothesis A method underestimates the total settlement for the time period.

(b) Over-consolidated HKMC layer with H = 4 m and OCR = 1.5

Equation (8d) from integration is used to calculate the final "primary" settlement $S_{f,1-4}$. Values of all parameters are listed in Table 1. Values of all stresses are $\sigma'_{z1,0} = 0$, $\sigma'_{z1,H} = 20.76$ kPa, $\sigma_{zp,0}{}' = 0$, $\sigma'_{zp,H} = 31.14$ kPa $\sigma'_{z4,0} = 20$, $\sigma'_{z4,H} = 40.76$ kPa. $S_{f,1-4}$ is:

$$S_{f,1-4} = \frac{0.0913}{3.656\ln(10)}\left\{\frac{4}{(31.14-0)}[(31.14+\sigma'_{\text{unit1}})\ln(31.14+\sigma'_{\text{unit1}}) - (31.14+\sigma'_{\text{unit1}}) - ((0+\sigma'_{\text{unit1}})\ln(0+\sigma'_{\text{unit1}}) - (0+\sigma'_{\text{unit1}}))] - \frac{4}{(20.76-0)}[(20.76+\sigma'_{\text{unit1}})\ln(20.76+\sigma'_{\text{unit1}}) - (20.76+\sigma'_{\text{unit1}}) - ((0+\sigma'_{\text{unit1}})\ln(0+\sigma'_{\text{unit1}}) - (0+\sigma'_{\text{unit1}}))]\right\} + \frac{1.4624}{3.65\ln(10)}\left\{\frac{4}{(40.76-20)}[(40.76+\sigma'_{\text{unit2}})\ln(40.76+\sigma'_{\text{unit2}}) - (40.76+\sigma'_{\text{unit2}}) - ((20+\sigma'_{\text{unit2}})\ln(20+\sigma'_{\text{unit2}}) - (20+\sigma'_{\text{unit2}}))] - \frac{4}{(40.76-0)}[(31.14+\sigma'_{\text{unit2}})\ln(31.14+\sigma'_{\text{unit2}}) - (31.14+\sigma'_{\text{unit2}}) - ((0+\sigma'_{\text{unit2}})\ln(0+\sigma'_{\text{unit2}}) - (0+\sigma'_{\text{unit2}}))]\right\}$$

Using above equation with $\sigma'_{\text{unit1}} = \sigma'_{\text{unit2}} = 0.01$ kPa, we find $S_{f,1-4} = 0.681$ m; if $\sigma'_{\text{unit1}} = \sigma'_{\text{unit2}} = 0.1$ kPa,

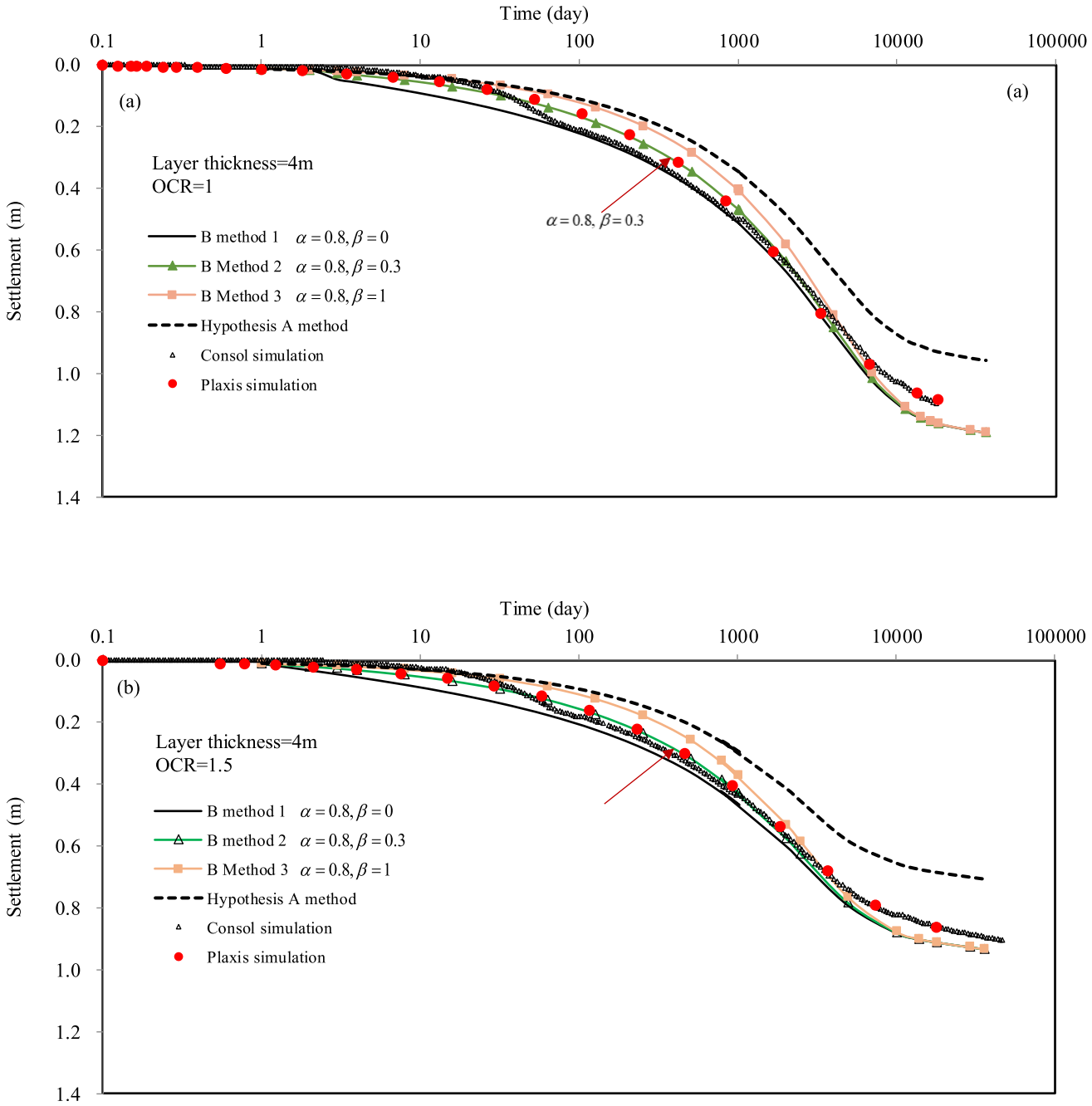

Fig. 5 Comparison of curves of settlements with log(time) from the simplified Hypothesis B method, Hypothesis A method, and two fully coupled finite element modellings – **a** h = 4 m and OCR = 1 and **b** h = 4 m and OCR = 1.5

$S_{f,1-4}$ = 0.669 m; if $\sigma'_{\text{unit1}} = \sigma'_{\text{unit2}}$ = 0.5 kPa, $S_{f,1-4}$ = 0.635 m; if $\sigma'_{\text{unit1}} = \sigma'_{\text{unit2}}$ = 1 kPa, $S_{f,1-4}$ = 0.604 m. This means that the final "primary" settlement $S_{f,1-4}$ is sensitive to the value of σ'_{unit1} and σ'_{unit2}. In this example, we select $\sigma'_{\text{unit1}} = \sigma'_{\text{unit2}}$ = 0.1 kPa so that the final "primary" settlement $S_{f,1-4}$ is 0.669 m. The calculation of average m_v and c_v is below:

$$\Delta\varepsilon_{z,1-4} = S_{f,1-4} = 0.669/4 = 0.167$$

$$m_v = \Delta\varepsilon_{z,1-4}/\Delta\sigma'_{z,1-4} = 0.167/20 = 0.00837 \quad (1/\text{kPa})$$

$$c_v = k/(\gamma_w m_v) = 1.9 \times 10^{-4}/(9.81 \times 0.00837)$$
$$= 2.316 \times 10^{-3}\ (\text{m}^2/\text{day}) = 0.845\ (\text{m}^2/\text{year})$$

This 4-m-thick layer can be divided into small sub-layers. The stresses and values of soil parameters in each sub-layer are assumed be constant. In this case, simple

Table 4 Calculation of S_f, m_v and c_v for sub-layer thickness of 0.5 m for OCR = 1.5

Mid sub-layer depth (m)	σ'_{zi} (kPa)	$\sigma'_z = \sigma'_{zi} + \Delta\sigma'_z$ (kPa)	$\sigma'_{zp} = \sigma'_{zi}$ (kPa)	ε_{zp}	$\Delta\varepsilon_z$	m_v(1/kPa)	$c_v = \frac{k_v}{\gamma_w m_v}$(m^2/day)
0.25	1.2975	21.2975	1.94625	0.004141	0.4084	0.00808	2.399E-03
0.75	3.8925	23.8925	5.83875	0.004312	0.2429		
1.25	6.4875	26.4875	9.73125	0.004348	0.1731		
1.75	9.0825	29.0825	13.62375	0.004364	0.1313		
2.25	11.6775	31.6775	17.51625	0.004373	0.1026		
2.75	14.2725	34.2725	21.40875	0.004378	0.0816		
3.25	16.8675	36.8675	25.30125	0.004382	0.0653		
3.75	19.4625	39.4625	29.19375	0.004385	0.0523		
				$\bar{\varepsilon}_{zp}$ = 0.004335	$\Delta\bar{\varepsilon}_z$ = 0.1572		
				Total strain $(\bar{\varepsilon}_{zp} + \Delta\bar{\varepsilon}_z)$:	0.1615		
				Settlement S_f (m):	0.6461		

Table 5 Summary of S_f, m_v and c_v for different numbers of sub-layers for OCR = 1.5

Number sub-layers	Vertical strain ε_z after loading	m_v (1/kPa)	$c_v = \frac{k_v}{\gamma_w m_v}$(m^2/day)	$S_f = \varepsilon_z \times H$ (m)	S_f from integration (m)
1	0.1207	0.006036	3.210E-03	0.483	0.669
2	0.1432	0.007158	2.707E-03	0.573	0.669
4	0.1562	0.00781	2.481E-03	0.625	0.669
8	0.1615	0.008076	2.399E-03	0.646	0.669

equations in (6b) can be used to calculate that the final "primary" settlement $S_{f,1-4}$ in each sub-layer. This layer of 4 m can divided into 2, 4, or 8 sub-layers with thickness of 2 m, 1 m, and 0.5 m, respectively. The final "primary" settlement $S_{f,1-4}$ calculated is 0.487 m, 0.573 m, 0.625 m, and 0.646 m sub-layers with thickness of 4 m, 2 m, 1 m, and 0.5 m, respectively. Values of S_f, m_v and c_v for sub-layer thickness of 0.5 m for OCR = 1.5 are listed in Table 4. The meanings of ε_{zp}, $\bar{\varepsilon}_{zp}$, $\Delta\varepsilon_z$, $\Delta\bar{\varepsilon}_z$, and $(\bar{\varepsilon}_{zp} + \Delta\bar{\varepsilon}_z)$ are the same as those in Table 2. Summary of values of S_f, m_v and c_v for different number of sub-layers for OCR = 1.5 is listed in Table 5 including S_f obtained by more accurate integration method. It can be seen that the relative error of S_f with sub-layer thickness of 0.5 m is only $\frac{0.669-0.646}{0.669} \times 100\% = 3.4\%$.

The simplified Hypothesis B method in (1) together with other equations on relevant parameters is used to calculate the total settlement S_{totalB} using $\alpha = 0.8$ and $\beta = 0$ (denoted B Method 1), $\beta = 0.3$ (denoted B Method 2) and $\beta = 1$ (denoted B Method 3) for OCR = 1.5. The calculated curves of settlements with log(time) from the simplified Hypothesis B method are shown in Fig. 5b for time up to 100 years. At the same time, Hypothesis A method and two fully coupled finite element models are used to calculate the curves of settlements with log(time), which are also shown in Fig. 5b for comparison. It is seen from Fig. 5b that when $\alpha = 0.8$ and $\beta = 0.3$ m, B Method 2 gives curves much closer to the curves from the two finite element models of "Consol" by Zhu and Yin [42, 43, 44] and Plaxis software (2D 2015 version). Again, Hypothesis A method underestimates the total settlement.

4 Consolidation settlements of layered soils with vertical drains under staged loading–unloading-reloading from general simple method and fully coupled consolidation analysis

4.1 Description of soil conditions

In this section, easy use and accuracy of the general simple method are demonstrated through calculation of

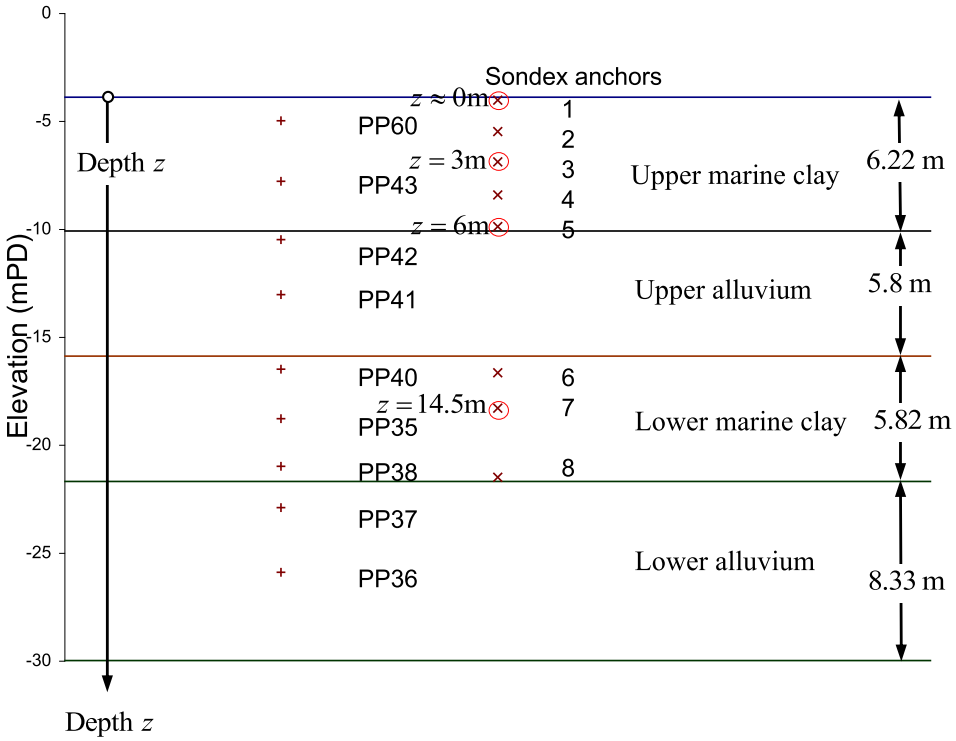

Fig. 6 Soil profile and settlement monitoring points of a test embankment at Chek Lap Kok for Hong Kong International Airport project in 1980s

consolidation settlements of a multiple-layered soil under multi-staged loadings with comparison with values from fully coupled FE simulations. The soil profile is modified from a real case in Hong Kong [18, 49] as shown in Figs. 6 and 7. This section only studies the first two layers, namely upper marine clay of 6.22 m thick and upper alluvium of 5.80 m thick. To make the consolidation analysis more accurate and to record accumulated settlement at different depths, the upper marine clay layer is divided into two layers by Sondex anchor 3, forming a total of three layers

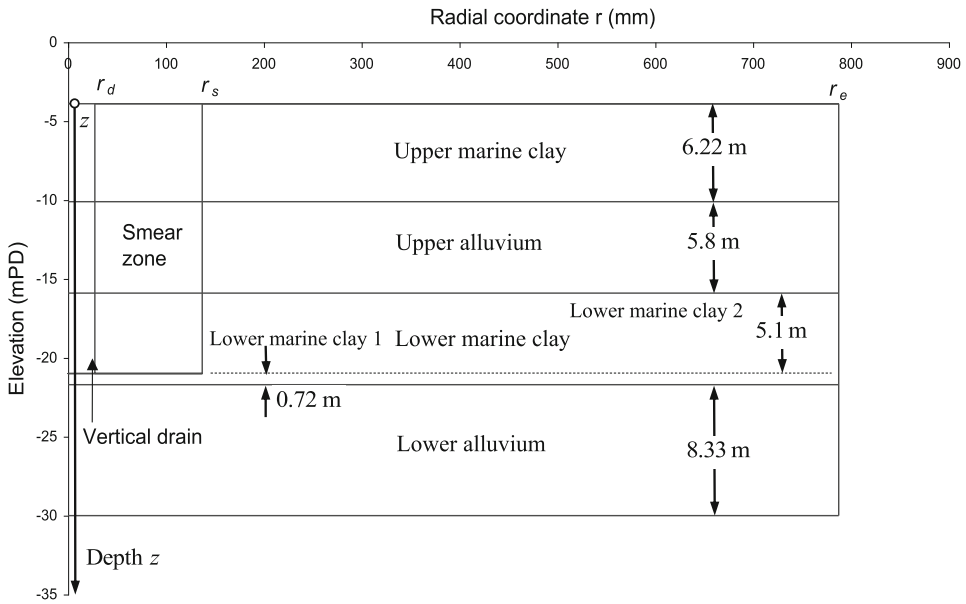

Fig. 7 Soil profile including a vertical drain and a smear zone of a test embankment at Chek Lap Kok for Hong Kong International Airport project in 1980s

of soils. Properties of upper marine clay and upper alluvium can be found in Table 6.

Prefabricated vertical drains (PVDs) with a spacing of 1.5 m in triangular pattern were inserted in the soils. The radius of influence zone of each PVD was $r_e = 0.525d = 0.7875$m for triangular pattern. The width of PVD was $b = 100$ mm, thickness was $t = 7$ mm, and equivalent radius is calculated as $r_d = (b + t)/4 + t/10 = 27.45$ mm [40]. The installation of PVDs normally causes a smear zone around the vertical drains as shown in Fig. 7. We assume that radius of this smear zone $r_s = 5r_d = 137.25$ mm, in which the soils were disturbed and the horizontal permeability k_r became k_s with values listed in Table 6. Other properties such as OCR and compression indices of the smear zone remain the same as the undisturbed region.

There are four stages of loadings to be applied on top of the soils, including two stages of loading, one stage of unloading and the final stage of reloading. The magnitude of vertical load (p_1, p_2, p_3, p_4), construction time $(t_{c1}, t_{c2}, t_{c3}, t_{c4})$ and loading stage duration (t_1, t_2, t_3, t_4) are shown in Fig. 8a. This type of staged loading is very close to the real case of reclamation process from loading (filling to a designed level), increasing loading (surcharging fill), unloading by removing part of surcharging fill, and reloading again due to construction of superstructures on reclaimed land. The final stage of loading (superstructures) may last for 50 years (18,250 days) after completion of reclamation construction. To validate the general simplified Hypothesis B method, a fully coupled finite element (FE) analysis is conducted in Plaxis 2D (2015) for this case. A soft soil creep (SSC) model [30], which is mostly similar to the 3D EVP model by Yin and Graham [39], is adopted as the constitutive model for the two clayey soils in Fig. 7. The parameters used in the FE model for the two soils are the same as those in Table 6. Accumulated settlements at settlement monitoring points 1, 3 and 5 (depths of 0 m, 3 m, and 6 m, respectively) are calculated using the general simple method and the FE model and are plotted with total elapsed time. Excess pore pressures at the centre of each layer and at the middle between r_d and r_e are calculated by the FE model during the whole consolidation process.

4.2 Consolidation settlement calculation by general simple method under staged loadings

This section shows details with steps how to use the general simple method to calculate consolidation settlements of Case 2 under staged loading–unloading–reloading. The total consolidation settlements are summation of "primary" consolidation settlement and creep settlements in Eq. (1). For four stages of loading, details of calculations are presented below.

4.3 Stage 1

As shown in Fig. 8a, for Stage 1 under $p_1 = 52$kPa, the stress–strain state will move from point i $(\sigma'_{zi}, \varepsilon_{zi})$ to point 1 $(\sigma'_{z1}, \varepsilon_{z1})$ as in Fig. 8b. The calculation method of S_f is similar to the case of load increment from point 1 to 2 or point 1 to 4 in Fig. 3. Due to the nonlinear strain–stress relationship of soils and non-uniform stress distribution, each j-layer (j = 1, 2, 3 for 3 layers) is divided into several sub-layers (say N sub-layers) with a thickness of h_n (0.5 m or less) to calculate S_f and m_v. Within each sub-layer, initial effective stress σ'_{zi} can be considered as constant. The final vertical effective stress at Stage 1 is calculated as $\sigma'_{z1} = \sigma'_{zi} + p_1$ for each sub-layer. The settlement for each j-layer will be the superposition of settlements of all sub-layers ($n = 1 \ldots N$). Therefore, S_{fj1} and m_{vj1} for j-layer with thickness H_j in Stage 1 (sub-index "$_1$" for Stage 1; later "$_2$", "$_3$", "$_4$" for Stages 2, 3, and 4) are calculated in the following equations:

$$S_{fj1} = \sum_{n=1}^{n=N} \begin{cases} \dfrac{C_r}{1+e_o}\log\left(\dfrac{\sigma'_{z1}+\sigma'_{\text{unit1}}}{\sigma'_{zi}+\sigma'_{\text{unit1}}}\right)h_n, & \text{if } \sigma'_{z1} \le (\sigma'_{zi} + \text{POP}) \\ \left[\dfrac{C_r}{1+e_o}\log\left(\dfrac{\sigma'_{zi}+POP+\sigma'_{\text{unit1}}}{\sigma'_{zi}+\sigma'_{\text{unit1}}}\right) + \dfrac{C_c}{1+e_o}\log\left(\dfrac{\sigma'_{z1}+\sigma'_{\text{unit2}}}{\sigma'_{zi}+POP+\sigma'_{\text{unit2}}}\right)\right]h_n, & \text{if } \sigma'_{z1} > (\sigma'_{zi} + \text{POP}) \end{cases} \tag{19a}$$

$$m_{vj1} = \frac{\varepsilon_{z1} - \varepsilon_{zi}}{p_1} = \frac{S_{fj1}}{H_j p_1} \tag{19b}$$

where n is index for sub-layers within j-layer ($n = 1 \ldots N$), h_n is thickness of a sub-layer ($h_n \le 0.5$m), POP in Table 6 is called pre-over-consolidation pressure

Table 6 Parameters of soils and vertical drains for HKIA Chek Lap Kok Test Embankment

Main layer	Upper marine clay	Upper alluvium	Lower marine clay 1		Lower marine clay 2		Lower alluvium	
Case 2 and Case 3 layers	3 layers used in Case 2 (j = 1,2,3)		8 layers used in Case 3 (3 layers in Case 2 j = 1,2,3) + (5 layers here j = 4,5,6,7,8)					
Layer	1	2	3	4	5	6	7	8
H_j (m)	3.01	3.21	5.8	2.47	2.63	0.72	4.165	4.165
POP (kPa)	17		350	150		150	200	
γ (kN/m^3)	14.22		19.13	18.15		18.15	19.72	
$V = 1 + e_o$	3.65		2.06	2.325		2.325	2.06	
κ	0.0396		0.0224	0.0353		0.0353	0.0020	
λ	0.5081		0.1339	0.3030		0.3030	0.0087	
ψ	0.0078		0.0035	0.0061		0.0061	0.0000	
$C_r = C_e$	0.0913		0.0515	0.0814		0.0814	0.0046	
C_c	1.1699		0.3083	0.6977		0.6977	0.0200	
$C_{\alpha e}$	0.0180		0.0080	0.0140		0.0140	0.0000	
t_o (year)	0.0027		0.0027	0.0027		0.0027	0.0027	
k_v (m/yr)	0.03469		0.09461	0.00394		0.00394	0.1577	
$k_r = k_h$ (m/yr)	0.06307		0.18922	0.00978		0.00978	0.3155	
Drain spacing S (m)	1.5		1.5	1.5		No drain	No drain	
Drain pattern	Triangular		Triangular	Triangular		No drain	No drain	
$r_d = r_w$ (m)	0.0275		0.0275	0.0275		No drain	No drain	
r_s/r_d	5		5	5		No drain	No drain	
k_r/k_s	1.82		2.00	2.48		No drain	No drain	

(after [49] and POP $= \sigma'_{zp} - \sigma'_{zi}$. Equation (19) is valid for the final state $(\sigma'_{z1}, \varepsilon_{z1})$ in either over-consolidation (OC) state or normal consolidation (NC) state.

Values of S_{f1} and m_{v1} for three layers $(H_j, j = 1, 2, 3)$ under Stage 1 are calculated using Eq. (19) and listed in Table 7. After this, a Microsoft Excel spreadsheet with macros based on a spectral method developed by Walker and Indraratna [26] is used to calculate the average excess porewater pressure $\overline{u}_{ej}$ for j-layer using known values of k_v, k_r, and k_s in Table 6 and the calculated m_{vj1} in Table 7. The average degree of consolidation U_{j1} for j-layer for Stage 1 is then calculated using Eq. (10b). Using calculated values of U_{j1} and S_{fj1}, the "primary" consolidation settlement $S_{\text{primary}1}$ in Stage 1 is calculated as:

$$S_{\text{primary}} = \sum_{j=1}^{3} S_{\text{primary},j} = \sum_{j=1}^{3} U_{j1} S_{fj1} \tag{20}$$

To calculate creep settlement $S_{\text{creep}1}$ during Stage 1, the equivalent time in Yin and Graham's 1D EVP model should be determined according to the final stress–strain state $(\sigma'_{z1}, \varepsilon_{z1})$ for each sub-layer. If the soil is in normal consolidation state (*i.e.* $\sigma'_{z1} \geq (\sigma'_{zi} + \text{POP})$), equivalent time t_{e1} at the "final" effective stress σ'_{z1} in Stage 1 is zero. If the soil is in OC state (*i.e.* $\sigma'_{z1} < (\sigma'_{zi} + \text{POP})$), t_{e1} should be calculated as:

$$t_{e1} = t_o \times 10^{(\varepsilon_{z1} - \varepsilon_{zp})\frac{V}{C_{\alpha e}}} \left(\frac{\sigma'_{z1}}{\sigma'_{zp}}\right)^{-\frac{C_c}{C_{\alpha e}}} - t_o \tag{21}$$

where $\varepsilon_{z1} = \varepsilon_{zi} + S_{fj1}/H_j$ is the "final" strain without creep at Stage 1. In fact, Eq. (21) is also valid for NC state. The value of t_{e1} is calculated for each sub-layer h_n. Therefore, $S_{\text{creep},fj1}$, $S_{\text{creep},dj1}$, $S_{\text{creep}j1}$ and total settlement $S_{\text{total}Bj1}$ for each j-layer, no matter the "final" stress–strain point is in OC or NC state, can be calculated using the following equations:

$$S_{\text{creep},fj1} = \sum_{n=1}^{n=N} \frac{C_{\alpha e}}{1 + e_o} \log \frac{t_{e1} + t}{t_{e1} + t_o} h_n \text{ for } t_o \leq t \leq t_1 \tag{22a}$$

$$S_{\text{creep},dj1} = \sum_{n=1}^{n=N} \frac{C_{\alpha e}}{1 + e_o} \log \frac{t_{e1} + t}{t_{e1} + t_{\text{EOP,field}}} h_n \quad \text{for } t_{\text{EOP,field}} \leq t \leq t_1 \tag{22b}$$

$$S_{\text{creep}j1} = \alpha U_{j1}^{\beta} S_{\text{creep},fj1} + \left(1 - \alpha U_{j1}^{\beta}\right) S_{\text{creep},dj1} \tag{22c}$$

$$S_{\text{total}Bj1} = U_{j1} S_{fj1} + \left[\alpha U_{j1}^{\beta} S_{\text{creep},fj1} + \left(1 - \alpha U_{j1}^{\beta}\right) S_{\text{creep},dj1}\right] \tag{22d}$$

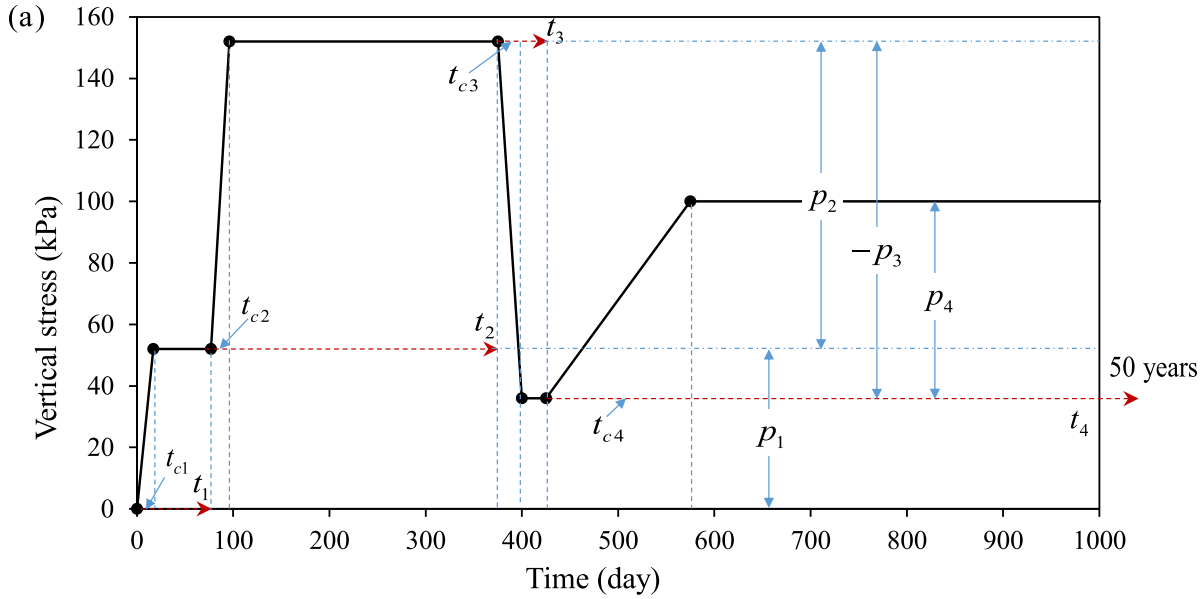

	Stage 1	Stage 1	Stage 1	Stage 2	Stage 2	Stage 3	Stage 3	Stage 4	Stage 4
Time (day)	0	17	77	96	375	400	425	575	18675
Stage pressure (kPa)	0	52	52	152	152	36	36	100	100
t_c and stage ending time t_1,t_2,t_3,t_4 (day)	$t_{c1}=17$, $t_1=77$			$t_{c2}=19$, $t_2=298$		$t_{c3}=25$, $t_3=50$		$t_{c4}=150$, $t_4=18520$	

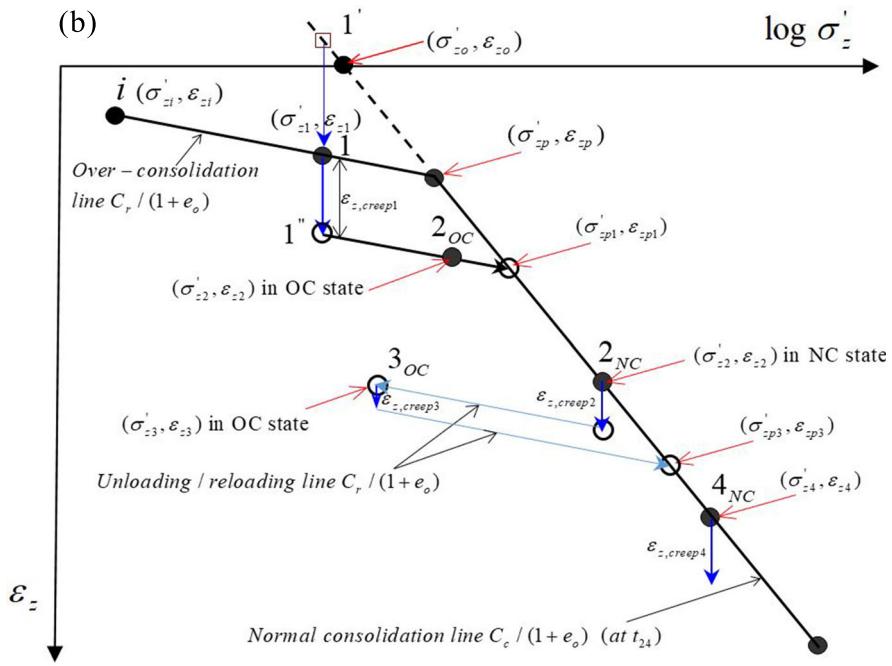

Fig. 8 **a** Construction time, stage time and vertical pressures of four staged loadings from loading, to unloading and reloading and **b** state points in vertical strain-log(effective stress) space

Table 7 Values of S_{fj} and m_{vj} for three soil layers under four stages calculated using the general simple method

Stage No., S_{fj} or m_{vj}	Layer 1 (j = 1)	Layer 2 (j = 2)	Layer 3 (j = 3)
1: S_{fj1} (m)	0.4291	0.3035	0.0415
2: S_{fj2} (m)	0.4157	0.3796	0.0409
3: S_{fj3} (m)	− 0.0428	− 0.0380	− 0.0509
4: S_{fj4} (m)	0.02989	0.02573	0.03296
1: m_{vj1} (1/kPa)	0.0027415	0.0018185	0.0001375
2: m_{vj2} (1/kPa)	0.0013810	0.0011825	0.0000704
3: m_{vj3} (1/kPa)	0.0001227	0.0001022	0.0000756
4: m_{vj4} (1/kPa)	0.0001342	0.0001083	0.0000768

In this case, Eq. (22d) is used to calculate $S_{\text{total}Bj1}$ for j-layer in Stage 1 with $\alpha = 0.8$ and $\beta = 0.3$. Using Eq. (1), the total settlement $S_{\text{total}B1}$ of 3 layers in Stage 1 is

$$S_{\text{total}B1} = \sum_{j=1}^{j=3} S_{\text{total}Bj1} = \sum_{j=1}^{j=3} U_{j1} S_{fj1} + \left[\alpha U_{j1}^{\beta} S_{\text{creep},fj1} + \left(1 - \alpha U_{j1}^{\beta}\right) S_{\text{creep},dj1}\right] \tag{22e}$$

4.4 Stage 2

For Stage 2 with $p_2 = 100$kPa, the final vertical effective stress $\sigma_{z2}^{'}$ is $\sigma_{z2}^{'} = \sigma_{z1}^{'} + p_2 = \sigma_{zi}^{'} + p_1 + p_2$ as in Fig. 8b at point 2 $(\sigma_{z2}^{'}, \varepsilon_{z2})$. The calculation of S_{fj} is dependent on the soil stress–strain state before and after loading increment as below:

$$S_{fj2} = \sum_{n=1}^{n=N} \begin{cases} \dfrac{C_r}{1+e_o} \log\left(\dfrac{\sigma_{z2}^{'} + \sigma_{\text{unit1}}^{'}}{\sigma_{z1}^{'} + \sigma_{\text{unit1}}^{'}}\right) h_n, & \text{if } \sigma_{z1}^{'} < \sigma_{z2}^{'} \le (\sigma_{zi}^{'} + \text{POP}) \\ \left[\dfrac{C_r}{1+e_o} \log\left(\dfrac{\sigma_{zi}^{'} + POP + \sigma_{\text{unit1}}^{'}}{\sigma_{z1}^{'} + \sigma_{\text{unit1}}^{'}}\right) + \dfrac{C_c}{1+e_o} \log\left(\dfrac{\sigma_{z2}^{'} + \sigma_{\text{unit2}}^{'}}{\sigma_{zi}^{'} + POP + \sigma_{\text{unit2}}^{'}}\right)\right] h_n, & \text{if } \sigma_{z1}^{'} < (\sigma_{zi}^{'} + \text{POP}) < \sigma_{z2}^{'} \\ \dfrac{C_c}{1+e_o} \log\left(\dfrac{\sigma_{z2}^{'} + \sigma_{unit2}^{'}}{\sigma_{z1}^{'} + \sigma_{unit2}^{'}}\right) h_n, & \text{if } (\sigma_{zi}^{'} + \text{POP}) \le \sigma_{z1}^{'} < \sigma_{z2}^{'} \end{cases} \tag{23a}$$

$$m_{vj2} = \frac{\varepsilon_{z2} - \varepsilon_{z1}}{p_2} = \frac{S_{fj2}}{H_j p_2} \tag{23b}$$

where $\varepsilon_{z2} = \varepsilon_{z1} + S_{fj2}/H_j$ is the final accumulated vertical strain without creep strain at Stage 2. Values of S_{f2} and m_{v2} for three layers $(H_j, j = 1, 2, 3)$ under Stage 2 are listed in Table 7. In this stage, average degree of consolidation for each layer U_{j1} under p_1 and U_{j2} under p_2 should be calculated independently using Walker and Indraratna [26]'s spectral method. For U_{j1}, the staged-consolidation time at Stage 2 should be from t_1 to $(t_1 + t_2)$. For U_{j2}, the staged-consolidation time at Stage 2 should be from 0 to t_2. Total S_{primary} should include the settlements produced by p_1 and p_2 with total time below:

$$S_{\text{primary}} = \sum_{j=1}^{3} S_{\text{primary},j} = \sum_{j=1}^{3} (U_{j1} S_{fj1} + U_{j2} S_{fj2}) \tag{24}$$

$S_{\text{creep}j2}$ only includes the creep settlement at the current loading stage under p_2 (*i.e.* $t_o < t < t_2$ for $S_{\text{creep},f}$ and $t_{\text{EOP,field}} < t < t_2$ for $S_{\text{creep},d}$). To calculate $S_{creepj2}$, the actual stress–strain state at Stage 2 and its corresponding equivalent time t_{e2} should be determined. First of all, the final creep strain $\varepsilon_{z,\text{creep1}}$ shown in Fig. 8b and accumulated total strain ε_{z1end} at the end of Stage 1 (point 1″) should be calculated by the following equations:

$$\varepsilon_{z,\text{creep1}} = \frac{S_{\text{creep}j,1}(t_1)}{H_j} \tag{25a}$$

$$\varepsilon_{z1end} = \varepsilon_{z1} + \varepsilon_{z,\text{creep1}} \tag{25b}$$

The new apparent pre-consolidation pressure σ'_{zp1} and the corresponding strain ε_{zp1} at the end of Stage 1 shown in Fig. 8b due to previous creep (or ageing) should be calculated by solving the following two equations:

$$\varepsilon_{zp1} = \varepsilon_{z1end} + \frac{C_r}{1+e_o}\log\frac{\sigma'_{zp1}+\sigma'_{\text{unit1}}}{\sigma'_{z1}+\sigma'_{\text{unit1}}} \tag{26a}$$

$$\varepsilon_{zp1} = \varepsilon_{zp} + \frac{C_c}{1+e_o}\log\frac{\sigma'_{zp1}+\sigma'_{\text{unit2}}}{\sigma'_{zp}+\sigma'_{\text{unit2}}} \tag{26b}$$

From Eqs. (26a, 26b), the apparent pre-consolidation pressure σ'_{zp1} can be solved as:

$$\sigma'_{zp1} = \frac{\left(\sigma'_{zp}+\sigma'_{\text{unit2}}\right)^{\frac{C_c}{C_c-C_r}}}{\left(\sigma'_{z1}+\sigma'_{\text{unit1}}\right)^{\frac{C_r}{C_c-C_r}}} \times 10^{\left(\varepsilon_{z1end}-\varepsilon_{zp}\right)\frac{1+e_o}{C_c-C_r}} - \sigma'_{\text{unit1}} \tag{26c}$$

where σ'_{unit1} is assumed to be equal to σ'_{unit2} here. If σ'_{zp1} is known, ε_{zp1} can be calculated using Eq. (26a) or (26b). With p_2 applied, if $(\sigma'_{z1}+p_2) = \sigma'_{z2} \geq \sigma'_{zp1}$ (*i.e.* the soil is in NC state at point 2_{NC}) as in Fig. 8b, the equivalent time $t_{e2} = 0$. Otherwise, $\sigma'_{z2} \leq \sigma'_{zp1}$, as the case of point 2_{OC} in OC state as shown in Fig. 8b or $(\sigma'_{z2}, \varepsilon_{z2})$ in OC state, t_{e2} at σ'_{z2} should be calculated as:or $(\sigma'_{z2}, \varepsilon_{z2})$ in OC state

$$t_{e2} = t_o \times 10^{(\varepsilon_{z2}-\varepsilon_{zp})\frac{V}{C_{\alpha e}}}\left(\frac{\sigma'_{z2}}{\sigma'_{zp}}\right)^{-\frac{C_c}{C_{\alpha e}}} - t_o \tag{27}$$

where $\varepsilon_{z2} = \varepsilon_{z1\text{end}} + \frac{C_r}{1+e_o}\log\frac{\sigma'_{z2}+\sigma'_{\text{unit1}}}{\sigma'_{z1}+\sigma'_{\text{unit1}}}$ is the vertical strain at point 2_{OC} in OC state, before creep at the beginning of Stage 2 loading. The value of t_{e2} is calculated for each sub-layer with thickness h_n for the point in either NC state or OC state. Therefore, $S_{\text{creep},fj2}$ and $S_{\text{creep},dj2}$ for each j-layer can be calculated using the following equations:

$$S_{\text{creep},fj2} = \sum_{n=1}^{n=N}\frac{C_{\alpha e}}{1+e_o}\log\frac{t_{e2}+t}{t_{e2}+t_o}h_n \text{ for } t_o \leq t \leq t_2 \tag{28a}$$

$$S_{\text{creep},dj2} = \sum_{n=1}^{n=N}\frac{C_{\alpha e}}{1+e_o}\log\frac{t_{e2}+t}{t_{e2}+t_{\text{EOP,field}}}h_n \quad \text{for } t_{\text{EOP,field}} \leq t \leq t_2 \tag{28b}$$

However, since $S_{\text{creep}j2}$ is calculated from the current stress–strain state under (p_1+p_2) loading, U_j in Eq. (22c) should be replaced by the accumulated average degree of consolidation $U_{\text{multi},j2}$ for multi-stages of loadings, which is calculated by:

$$U_{\text{multi},j2} = \frac{(U_{j2}p_1 + U_{j2}p_2)}{p_1+p_2} \tag{29}$$

Finally, the total consolidation settlements for j-layer and for all three layers in the period of Stage 2 are calculated by:

$$S_{\text{total}Bj2} = U_{\text{multi},j2}S_{fj2} + \left[\alpha U^{\beta}_{\text{multi},j2}S_{\text{creep},fj2} + \left(1-\alpha U^{\beta}_{\text{multi},j2}\right)S_{\text{creep},dj2}\right] \tag{30a}$$

$$S_{\text{total}B2} = \sum_{j=1}^{j=3}S_{\text{total}Bj2} = \sum_{j=1}^{j=3}U_{\text{multi},j2}S_{fj2} + \left[\alpha U^{\beta}_{\text{multi},j2}S_{\text{creep},fj2} + \left(1-\alpha U^{\beta}_{\text{multi},j2}\right)S_{\text{creep},dj2}\right] \tag{30b}$$

4.5 Stage 3

For Stage 3 of unloading $p_3 = -116$kPa, S_{fj3}, m_{vj3} and U_{j3} are calculated using the same procedures as Stages 1 and 2. It should be noted that, for this unloading stage, S_{fj3} is simply calculated by:

$$S_{fj3} = \sum_{n=1}^{n=N}\frac{C_r}{1+e_o}\log\left(\frac{\sigma'_{z3}+\sigma'_{\text{unit1}}}{\sigma'_{z2}+\sigma'_{\text{unit1}}}\right)h_n \tag{31}$$

where $\sigma'_{z2} = \sigma'_{zi}+p_1+p_2$, $\sigma'_{z3} = \sigma'_{zi}+p_1+p_2+p_3$, and $\sigma'_{z3} < \sigma'_{z2}$. As shown in Fig. 8b, point 3_{OC} must be in an OC state, but point 3_{OC} may be reached from the end of creep at point 2_{NC}. However, point 2 could be at point 2_{OC} in an OC state. If this case, Eq. (31) can still be used. Under unloading condition, as both S_{fj3} and p_3 are negative, m_{v3} is still positive, and therefore, the spectral method can be normally used to compute the degree of consolidation. The calculation of $S_{\text{primary},j}$ should contain the settlements produced in the previous stages during the current stage period in the following equation:

$$S_{\text{primary},j} = U_{j1}S_{fj1} + U_{j2}S_{fj2} + U_{j3}S_{fj3} \tag{32}$$

where U_{j1}, U_{j2} and U_{j3} are the average degree of consolidation under (i)p_1 from (t_1+t_2) to $(t_1+t_2+t_3)$, (ii) p_2 from t_2 to (t_2+t_3), (ii) p_3 from 0 to t_3, respectively. Calculation of $S_{\text{creep}j3}$ follows similar procedures as in Stage 2, not be elaborated here. $U_{\text{multi},j3}$ for calculating creep settlement should be calculated as:

$$U_{\text{multi},j3} = \frac{(U_{j1}p_1 + U_{j2}p_2 + U_{j3}p_3)}{p_1+p_2+p_3} \tag{33}$$

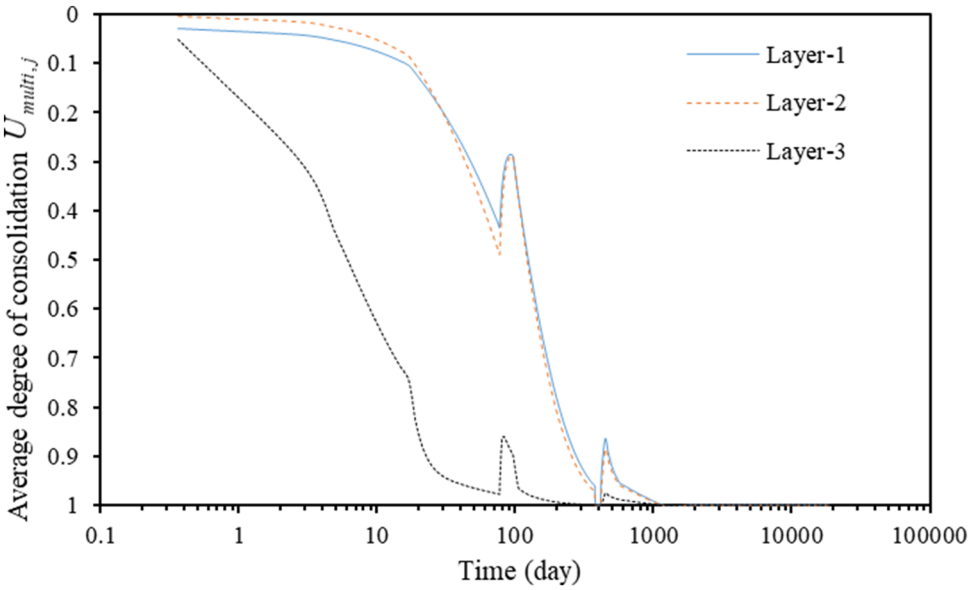

Fig. 9 Calculated curves of $U_{\text{multi},j}$ and total loading time in logarithmic scale for each j-layer under multi-staged four loadings

4.6 Stage 4

For Stage 4 with $p_4 = 74$kPa, similar procedures as those for Stages 1 and 2 are used for calculations of S_{fj4}, U_{j4} and $S_{\text{creep}j4}$. But $S_{\text{primary},j}$ and $U_{\text{multi},j4}$ should be calculated as:

$$S_{\text{primary},j} = U_{j1}S_{fj1} + U_{j2}S_{fj2} + U_{j3}S_{fj3} + U_{j4}S_{fj4} \tag{34}$$

$$U_{\text{multi},j4} = \frac{(U_j p_1 + U_{j2}p_2 + U_{j3}p_3 + U_{j4}p_4)}{p_1 + p_2 + p_3 + p_4} \tag{35}$$

where U_{j1},U_{j2}, U_{j3}, and U_{j4} is the average degree of consolidation under (i)p_1 from $(t_1 + t_2 + t_3)$ to $(t_1 + t_2 + t_3 + t_4)$, (ii) p_2 from $(t_2 + t_3)$ to $(t_2 + t_3 + t_4)$, (iii) p_3 from t_3 to $(t_3 + t_4)$, and (iv) p_4 from 0 to t_4.

The values of S_{fj} and m_{vj} for Stages 1 to 4 are listed in Tables 7. Using the spectral method and Eqs. (10b), (24), (26) and (28) the average degree of consolidation degree $U_{\text{multi},j}$ for each layer during four stages is calculated and plotted with time in Fig. 9.

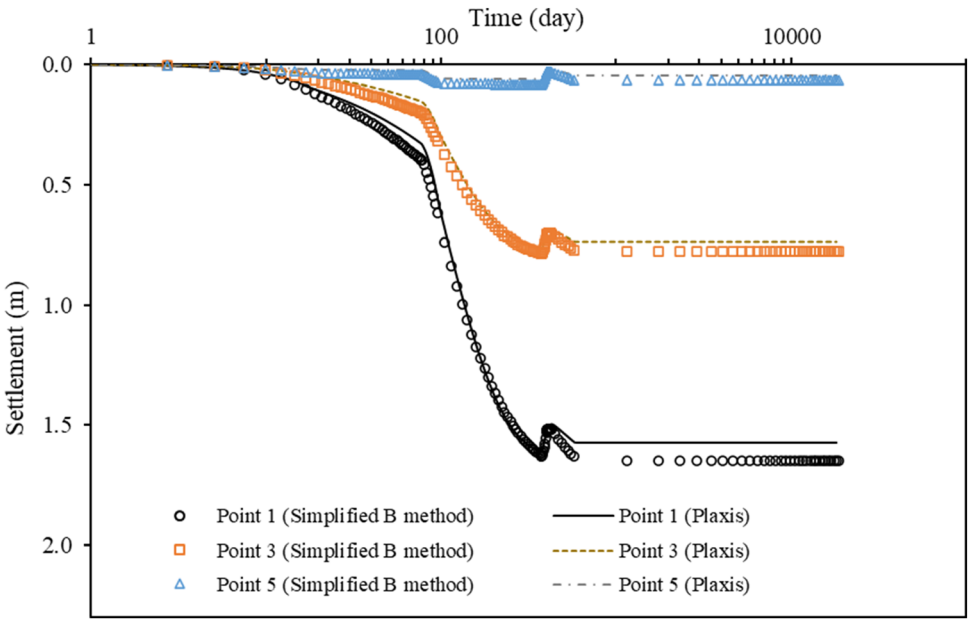

Fig. 10 Comparison of settlements with accumulated total loading time in logarithmic scale at three settlement monitoring points at z = 0 m, 3 m and 6 m from the simplified Hypothesis B method and fully coupled finite element modelling

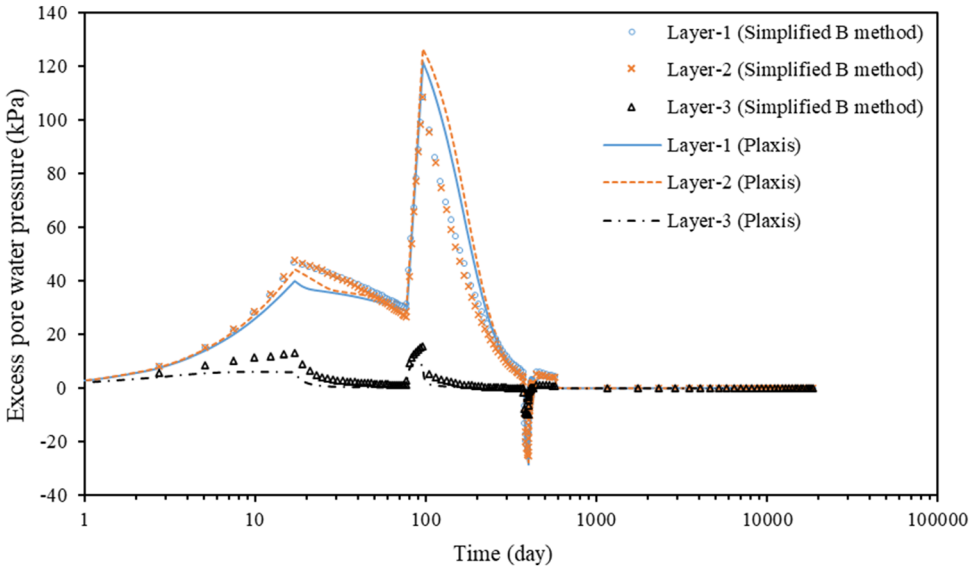

Fig. 11 Comparison of excess porewater pressure with log(total loading time) for three layers from the general simplified Hypothesis B method and fully coupled finite element modelling

4.7 Comparisons of results from the general simple method and fully coupled FE analysis

Figure 10 shows the computed settlements at three measurement points (0, 3 and 6 m) by both simplified Hypothesis B method and FE analysis. It can be found that the settlements at three different depths are close to those computed by FE analysis under four stages of loading, unloading and reloading. The settlements in 50 years in stage 4 are very small. This is because the soils are in over-consolidation state in stage 4 due to the surcharge in stage 2. The results demonstrated that surcharge loading before construction will significantly reduce long-term post-construction settlements.

$\overline{u}_j$ Figure 11 shows the average excess porewater pressure at the centre of each soil layer, compared with the computed excess porewater pressure at the above-mentioned measurement points in the FE model. It is found that excess porewater pressure computed by the spectral method adopted in the general simple method fit well with the one simulated by FE model. In conclusion, the proposed simplified Hypothesis B method is close to fully coupled FE analysis for the case with multiple layered soils under multi-staged loading conditions.

5 Consolidation settlements of test embankment on layered soils with vertical drains under staged loading from general simple method, fully coupled consolidation analyses and measurement

5.1 General descriptions of the test embankment

In this section, Test Embankment at Chek Lap Kok for Hong Kong International Airport (HKIA) project in 1980s is used as an example to demonstrate the validity of the new general simple method. Consolidation settlements of this HKIA Chek Lap Kok Test Embankment are calculated using the new general simplified Hypothesis B method and are compared with measured data and values from the simplified finite element (FE) method reported by Zhu et al. [49]. Details of the site conditions, properties of soils, parameters of vertical drains, construction process, parameters used in the FE model can be found in Koutsoftas et al. [18] and Zhu et al. [49]. The calculations of S_{fj},$\Delta\sigma_z^{'}$, $\Delta\varepsilon_z$, m_{vj} and c_{vj} for each layer under three stages are listed in Table 8.

Figure 6 shows soil profile and settlement monitoring points of Chek Lap Kok Test Embankment [13, 18]. Elevation in mPD (meter in Principal Datum), depth

Table 8 Calculated values of parameters of j-layers for HKIA Chek Lap Kok Test Embankment

	Stage	Layer H_j							
		1	2	3	4	5	6	7	8
S_{fj} (m)	1	0.4291	0.3035	0.0415	0.0160	0.0143	0.0035	0.0011	0.0009
S_{fj} (m)	2	0.4157	0.3796	0.0409	0.0214	0.0204	0.0052	0.0015	0.0013
$S_{fj}(m)$	3	0.2123	0.2101	0.0255	0.1128	0.1113	0.0290	0.0031	0.0028
$\Delta\sigma_z'$ (kPa)	1	52	52	52	52	52	52	52	52
$\Delta\sigma_z'$ (kPa)	2	100	100	100	100	100	100	100	100
$\Delta\sigma_z'$ (kPa)	3	105	105	105	105	105	105	105	105
$\Delta\varepsilon_z$	1	0.1426	0.0946	0.0072	0.0065	0.0054	0.0049	0.0003	0.0002
$\Delta\varepsilon_z$	2	0.1381	0.1182	0.0070	0.0087	0.0078	0.0072	0.0004	0.0003
$\Delta\varepsilon_z$	3	0.0705	0.0654	0.0044	0.0456	0.0423	0.0403	0.0008	0.0007
m_v (1/kPa)	1	2.741×10^{-3}	1.818×10^{-3}	1.375×10^{-4}	1.245×10^{-4}	1.043×10^{-4}	9.386×10^{-5}	5.182×10^{-6}	4.202×10^{-6}
m_v (1/kPa)	2	1.381×10^{-3}	1.182×10^{-3}	7.045×10^{-5}	8.683×10^{-5}	7.765×10^{-5}	7.242×10^{-5}	3.170×10^{-6}	3.178×10^{-6}
m_v (1/kPa)	3	6.716×10^{-4}	6.233×10^{-4}	4.187×10^{-5}	4.348×10^{-4}	4.031×10^{-4}	3.840×10^{-4}	7.165×10^{-6}	6.431×10^{-6}
c_v (m^2/yr)	1	1.27	1.91	68.78	3.17	3.78	4.20	3042.97	3752.62
c_v (m^2/yr)	2	2.51	2.93	134.30	4.54	5.08	5.44	4250.04	4962.32
c_v (m^2/yr)	3	5.17	5.57	225.95	0.91	0.98	1.03	2200.71	2451.95
c_r (m^2/yr)	1	2.30	3.47	137.56	7.85	9.37	10.42	6085.94	7505.24
c_r (m^2/yr)	2	4.57	5.33	268.60	11.26	12.59	13.50	8500.09	9924.63
c_r (m^2/yr)	3	9.39	10.12	451.91	2.25	2.43	2.55	4401.41	4903.91

coordinate, thickness values of four major layers, 8 settlement monitoring points by Sondex anchors, and 9 pore water pressure measurement points are all shown in Fig. 6. In this section, only 4 points at depths 0 m, 3 m, 6 m and 14.5 m are selected to calculate settlements for comparison with measured data.

Figure 7 shows soil profile and vertical drain with smear zone. It is noted that the vertical drain penetrated only 5.1 m into "lower marine clay". Therefore, "lower marine clay" is divided into two layers: "lower marine clay 1" with thickness of 5.1 m and "lower marine clay 2" with thickness of 0.72 m in order to calculate the average degree of consolidation of each layer better.

Values of parameters of soils and vertical drains for HKIA Chek Lap Kok Test Embankment are listed in Table 6. For more accurate calculation of settlements and the average degree of consolidation, as well as convenient calculation at settlement monitoring points, "upper marine clay" is divided into two main layers of $H_j = 3.01$ m and 3.21 m, "lower marine clay 1" is divided into $H_j = 2.47$ m and 2.63 m, "lower alluvium" is divided into two layers with $H_j = 4.165$ m each. There are a total of 8 layers (j = 1…8).

Figure 12 shows construction time ($t_{c1,}$ $t_{c2,}$ or t_{c3}), loading stage times ($t_{1,}$ $t_{2,}$ or t_3), and stage vertical pressures ($p_{1,}$ $p_{2,}$ or p_3) for each of three staged loadings. It should be noted that in situ monitoring of settlements by Sondex anchors was started 65 days after the construction began. The in situ settlement data from 65 to 909th day of total construction time were recorded and used for comparisons in this study.

5.2 Comparisons of results from the general simple method, fully coupled FE analyses, and measurement

In the general simplified Hypothesis B method, calculations of S_{fj}, m_v, U_j and $S_{\text{creep}j}$ for each j-layer under three loading stages are completed in a Microsoft Excel spreadsheet in the same way as that in Sect. 4. In this case, $\alpha = 0.8$ and $\beta = 0.3$ are used, which is also the same as in previous sections.

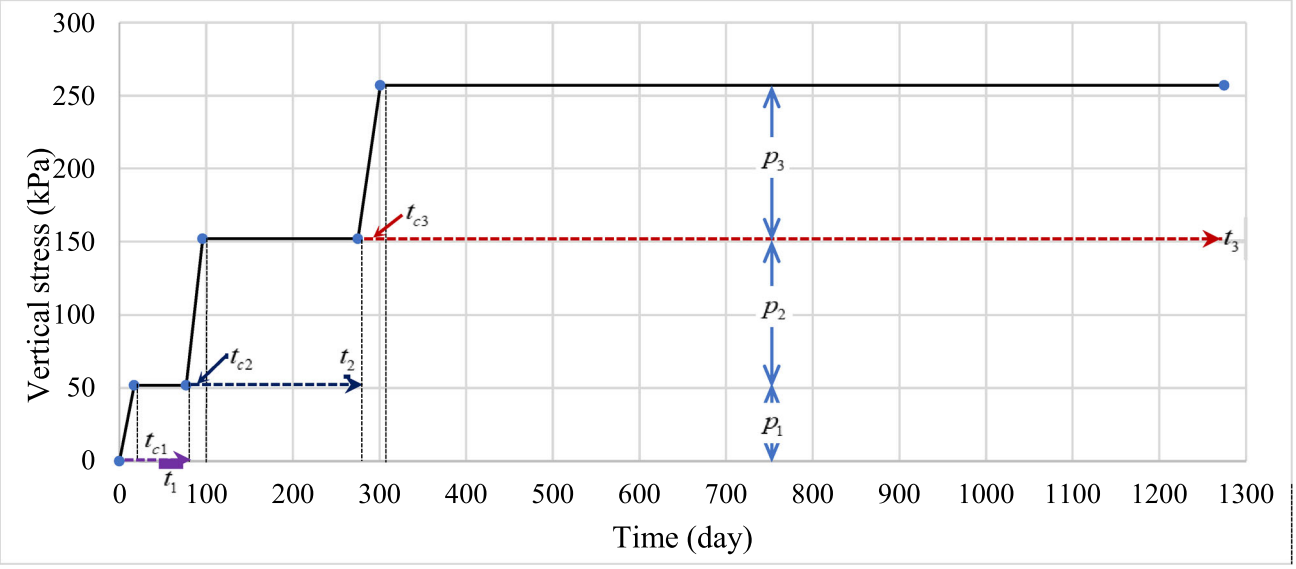

	Stage 1	Stage 1	Stage 1	Stage 2	Stage 2	Stage 3	Stage 3
Time (day)	0	17	77	96	275	301	1275
Stage pressure (kPa)	0	52	52	100	100	105	105
Total pressure (kPa)	0	52	52	152	152	257	257
t_c and stage ending time t_1, t_2, t_3 (day)		$t_{c1} = 17,$ $t_1 = 77$		$t_{c2} = 19,$ $t_2 = 198$		$t_{c3} = 26,$ $t_3 = 1000$	

Fig. 12 Construction time, stage time and vertical pressures of three staged loadings in HKIA Chek Lap Kok Test Embankment

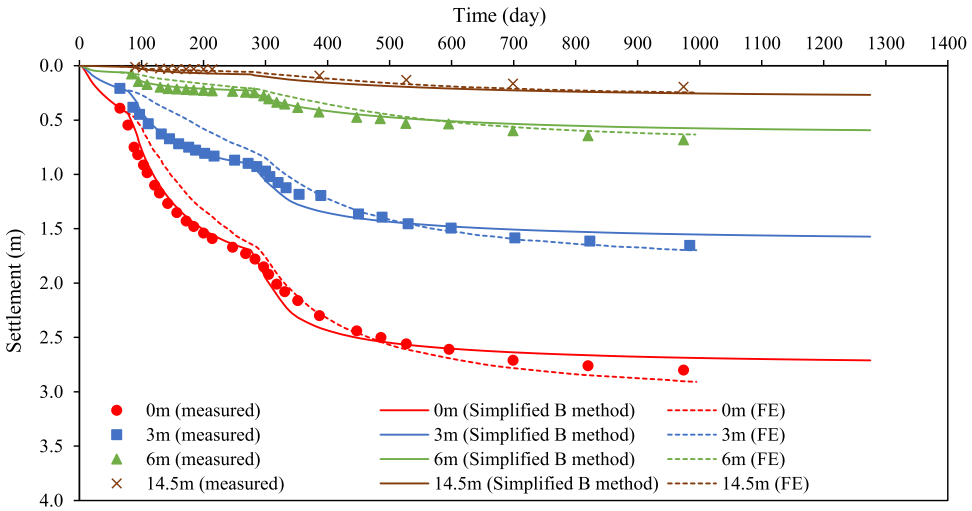

Fig. 13 Comparison of curves of settlements with total loading time at depths 0 m, 3 m, 6 m and 14.5 m from the general simplified Hypothesis B method, fully coupled finite element modelling and measurement

The total consolidation settlements S_{totalB} at depths of 0 m, 3 m, 6 m and 14.5 m are calculated using the general simplified Hypothesis B method for three stages of loading. Comparison of curves of settlements with accumulated time at depths of 0 m, 3 m, 6 m and 14.5 m from the general simplified Hypothesis B method, fully coupled finite element modelling and measurement is shown in Fig. 13. It is found that the values from the general simplified Hypothesis B method are in good agreement with measured data and values from fully coupled finite element modelling [49] using a 1-D elastic viscoplastic (1-D EVP) model [36, 37].

6 Summary and Conclusions

A new general simplified Hypothesis B method, also called general simple method, is proposed and verified for calculating consolidation settlements of layered clayey soils exhibiting creep without or with vertical drains under complicated staged loadings. This method is a new uncoupled method compared with fully coupled consolidation methods. Equations of this general simple method incorporating a new logarithmic stress function which avoids singularity problem are rigorously derived. Excess pore water pressure in "primary consolidation" is calculated by using a spectral method implemented in a Microsoft Excel spreadsheet. Two parameters, namely α and β, are introduced in this method. All other parameters in this method are convectional parameters, which can be easily determined from multi-staged oedometer tests. It is worthy to note that the two creep parameters $C_{\alpha e}$ and t_o are determined from a creep test under a vertical effective stress in a normal consolidation (NC) state. But, using the "equivalent time" (t_e) concept and theory of Yin and Graham [36, 37], the creep function using $C_{\alpha e}$ and t_o as well t_e can be used to calculate creep settlements in OC state and also in unloading/reloading states. Verification studies are carried out by comparing calculated values of settlements by this general simple method with values from fully coupled finite element analysis for Cases 1 and 2 as well as in situ measured data for Case 3. Based on these works, following conclusions can be made.

(a) From the case study of a single soil layer with OCR = 1 or 1.5 under instantaneous vertical loading, calculated settlements by using the new general simple method agree well with values from fully coupled finite element (FE) analyses by Plaxis and Consol. Selection of $\alpha = 0.8$ and $\beta = 0.3$ is found to have the best performance compared to other selections. It is also clearly revealed that Hypothesis A method underestimates the total settlements.

(b) From the case study for double layered soils under multi-staged loading–unloading–reloading, consolidation settlements in either short-term or long-term period are very close to values from an FE analysis. It can be concluded that the proposed general simplified Hypothesis B method has a stable performance and good accuracy for layered soils under complicated staged loading schemes.

(c) The general simple method is applied to calculate consolidation settlements in a real case in HKIA Chek Lap Kok Test Embankment with multi-layered soils and vertical drains under multi-staged loading. Calculated settlements by this new simple method are in good agreement with insitu measured data and also values from an FE analysis.

(d) Based on the above comparisons and validations, it is found that the new general simple method is accurate and easy to use for calculating consolidation settlements of single or layered soils with and without vertical drains under multi-staged loading, unloading and reloading using parameters from conventional oedometer tests.

Acknowledgements The work in this paper is supported by a Research Impact Fund (RIF) project (R5037-18), a Three-based Research Scheme Fund (TRS) project (T22-502/18-R), and three General Research Fund (GRF) projects (PolyU 152209/17E; PolyU 152179/18E; PolyU 152130/19E) from Research Grants Council (RGC) of Hong Kong Special Administrative Region Government of China. The authors also acknowledge the financial supports from Research Institute for Sustainable Urban Development of The Hong Kong Polytechnic University and three grants (BBAG, ZDBS, ZVNC) from the Hong Kong Polytechnic University.

References

1. Akai, K and Tanaka, Y (1999). Settlement behavior of an offshore airport KIA. In: Twelfth European Conference on Soil Mechanics and Geotechnical Engineering (Proceedings), Location: Amsterdam, Netherlands, AA Balkema, 1999-6-7 to 1999-6-10, pp 1041–1046
2. Barden L (1965) Consolidation of Clay with non-linear Viscosity. Geotechnique 15(4):345–362
3. Barden L (1969) Time-dependent deformation of normally consolidated clays and peats. J Soil Mech Found Div Am Soc Civ Engrs 95:1–31
4. Barron RA (1948) Consolidation of fine-grained soils by drain wells. Trans ASCE 113(2346):718–742
5. Berre T, Iversen K (1972) Oedometer tests with different specimen heights on a clay exhibiting large secondary compression. Geotechnique 22(1):53–70
6. Bjerrum L (1967) Engineering geology of Norwegian normally consolidated marine clays as related to the settlements of buildings. Geotechnique 17(2):83–118
7. British Standard 1377 (1990) Methods of test for soils for civil engineering purposes (Part 5). British Standsrds Institution, London

8. Chen ZJ, Feng WQ, Yin JH (2021) A new simplified method for calculating short-term and long-term consolidation settlements of multi-layered soils considering creep limit. Comput Geotech 138:104324
9. Feng WQ, Yin JH (2017) A new simplified hypothesis B method for calculating consolidation settlements of double soil layers exhibiting creep. Int J Numer Anal Method Geomech 2017(41):899–917
10. Garlanger JE (1972) The consolidation of soils exhibiting creep under constant effective stress. Geotechnique 22(1):71–78
11. Gibson RE, Lo KY (1961) A theory of consolidation for soils exhibiting secondary compression. Norwegian Geotechnical Institute, Oslo, pp 1–16
12. Graham J, Crooks JHA, Bell AL (1983) Time effects on the stress-strain behavior of natural soft clays. Geotechnique 33:165–180
13. Handfelt LD, Koutsoftas DC, Foott R (1987) Instrumentation for test fill in Hong Kong. J Geotech Eng ASCE 113(GT2):127–146
14. Hansbo S (1981) Consolidation of fine-grained soils by prefabricated drains. In: Proceedings of the Tenth International Conference on Soil Mechanics and Foundation Engineering, Stochholm, Sweden, 3, pp. 667–682
15. Hinchberger SD, Rowe RK (2005) Evaluation of the predictive ability of two elastic visco-plastic constitutive equations. Can Geotech J 42:1675–1694
16. Kelln C, Sharma JS, Hughes D, Graham J (2008) An improved elastic-viscoplastic soil model. Can Geot J 45(21):1356–1376
17. Knappett J (2019) Craig's soil mechanics, 9th edn. Taylor & Francis, Oxford
18. Koutsoftas DC, Foott R, Handfelt LD (1987) Geotechnical investigations offshore Hong Kong. J Geotech Eng ASCE 96(SM1):145–175
19. Leroueil S, Kabbaj M, Tavenas F, Bouchard R (1985) Stress-strain-time rate relation for the compressibility of sensitive natural clays. Geoetchnique 35(2):159–180
20. Ladd, CC, Foott, R, Ishihara, K, Schlosser, F and Poulos, HJ (1977). Stress-deformation and strength characteristics. In: Proc. 9th Int. Conf. Soil Mech. Fdn Engrg, Tokyo, 4210494. Estimating settlements of structures supported on cohesive soils. Special summer program
21. Mesri G, Godlewski PM (1977) Time- and stress-compressibility interrelationship. J Geotech Eng ASCE 103:417–430
22. Nash, DFT. and Ryde, SJ (2000) Modelling the effects of surcharge to reduce long term settlement of reclamations over soft clays. In: proceedings of Soft Soil Engineering Conference, Japan, 2000
23. Nash DFT, Ryde SJ (2001) Modelling consolidation accelerated by vertical drains in soils subject to creep. Geotechnique 51(3):257–273
24. Olson RE (1998) Settlement of embankments on soft clays. J Geotech Environ Eng 124(4):278–288
25. Plaxis (2015) See: https://www.plaxis.com/news/software-update/update-pack-plaxis-2d-2015-02/
26. Walker R, Indraratna B (2009) Consolidation analysis of a stratified soil with vertical and horizontal drainage using the spectral method. Géotechnique 59:439–449. https://doi.org/10.1680/geot.2007.00019
27. Walker R, Indraratna B, Sivakugan N (2009) Vertical and radial consolidation analysis of multilayered soil using the spectral method. J Geotech Geoenviron Eng 135:657–663. https://doi.org/10.1061/(asce)gt.1943-5606.0000075
28. Walker R, Indraratna B (2006) Vertical drain consolidation with parabolic distribution of permeability in smear zone. J Geotech Geoenviron Eng 132:937–941. https://doi.org/10.1061/(asce)1090-0241(2006)132:7(937)
29. Terzaghi K (1943) Theoretical soil mechanics. Wiley, New York
30. Vermeer, PA and Neher, HP (1999) A soft soil model that accounts for creep. In: proceedings of "Beyond 2000 in Computational Geotechnics10 Years of Plaxis International, Balkema, pp 249–261
31. Yin JH (1990) Constitutive modelling of time-dependent stress-strain behaviour of soils. Ph.D. thesis, Univ. of Manitoba, Winnipeg, Canada, March, 1990, p 314
32. Yin JH (1999) Non-linear creep of soils in oedometer tests. Géotechnique 1999(49):699–707. https://doi.org/10.1680/geot.1999.49.5.699
33. Yin JH (2011) From constitutive modeling to development of laboratory testing and optical fiber sensor monitoring technologies. Chin J Geotech Eng 33(1):1–15
34. Yin JH (2015) Fundamental issues on constitutive modelling of the time-dependent stress-strain behaviour of geomaterials. Int J Geomech 15(5):A4015002
35. Yin JH, Feng WQ (2017) A new simplified method and its verification for calculation of consolidation settlement of a clayey soil with creep. Can Geotech J 54(3):333–347
36. Yin JH, Graham J (1989) Visco-elastic-plastic modeling of one-dimensional time-dependent behaviour of clays. Can Geotech J 26:199–209
37. Yin JH, Graham J (1994) Equivalent times and one-dimensional elastic visco-plastic modeling of time-dependent stress-strain behavior of clays. Can Geotech J 31:42–52
38. Yin JH, Graham J (1996) Elastic visco-plastic modelling of one-dimensional consolidation. Géotechnique 46(3):515–527
39. Yin JH, Graham J (1999) Elastic visco-plastic modelling of the time-dependent stress-strain behavior of soils. Can Geotech J 36(4):736–745
40. Yin JH, Zhu G (2020) Consolidation analyses of soils. CRC Press, Florida
41. Zhu GF, Yin JH (1998) Consolidation of soil under depth-dependent ramp load. Can Geotech J 35(2):344–350
42. Zhu GF, Yin JH (1999) Finite element analysis of consolidation of layered clay soils using an elastic visco-plastic model. Int J Numer Anal Methods Geomech 23:355–374
43. Zhu GF, Yin JH (1999) Consolidation of double soil layers under depth-dependent ramp load. Géotechnique 49(3):415–421
44. Zhu GF, Yin JH (2000) Elastic visco-plastic finite element consolidation modeling of Berthierville test embankment. Int J Numer Anal Methods Geomech 24:491–508
45. Zhu GF, Yin JH (2001) Consolidation of soil with vertical and horizontal drainage under ramp load. Géotechnique 51(2):361–367
46. Zhu GF, Yin JH (2001) Design charts for vertical drains considering construction time. Can Geotech J 38(5):1142–1148
47. Zhu GF, Yin JH (2004) Consolidation analysis of soil with vertical and horizontal drainage under ramp loading considering smear effects. Geotext Geomembr 22(1 & 2):63–74
48. Zhu GF, Yin JH (2012) Analysis and mathematical solutions for consolidation of a soil layer with depth-dependent parameters under confined compression. Int J Geomech 12(4):451–461
49. Zhu GF, Yin JH, Graham J (2001) Consolidation modelling of soils under the Test Embankment at Chek Lap Kok International Airport in Hong Kong using a simplified finite element method. Can Geotech J 38(2):349–363

Yin, J.-H. & Graham, J. (1996). *Géotechnique* 46, No. 3, 515–527

Elastic visco-plastic modelling of one-dimensional consolidation

J.-H. YIN* and J. GRAHAM†

This paper incorporates an elastic visco-plastic (EVP) constitutive model into the consolidation equation to calculate settlements and excess pore water pressures in clays under multi-stage constant vertical loads in one-dimensional vertical straining. A finite difference method is used to solve the resulting non-linear differential consolidation equation. Results from the model are compared with test data and results from other models. The EVP model is also used to simulate consolidation in different thicknesses of clay to investigate the influence of the thickness on total settlements, dissipation of pore water pressures, strains and stresses. Consolidation analysis using the model can describe phenomena caused by the viscous nature of clays: excess pore water pressures can become larger than their initial values immediately after loading, effective stresses in the clay may become smaller than their initial values, and the relationship between strains and effective stresses at the end of primary consolidation is not unique, but depends on the thickness of the clay layer.

KEYWORDS: clays; consolidation; constitutive relations; settlement; time dependence.

Un modèle de comportement élastique-viscoplastique (EPV) est injecté dans l'équation de consolidation afin de calculer les tassements et les excès de pression interstitielle dans des argiles soumises à des incréments de chargements verticaux, constants, associés à une déformation verticale unidimensionnelle. La méthode des différences finies est utilisée pour résoudre l'équation différentielle, non linéaire. Les résultats, obtenus à l'aide de ce modèle, sont comparés à des résultats expérimentaux et à des résultats issus d'autres modèles. Le modèle EPV est aussi utilisé pour simuler la consolidation de différentes épaisseurs d'argiles afin de déterminer l'influence de l'épaisseur sur les tassements totaux, la dissipation des excès de pression interstitielle, les contraintes et les déformations. En utilisant ce modèle, on peut décrire les phénomènes dus à la viscosité des argiles: les pressions interstitielles peuvent revenir à leurs valeurs initiales immédiatement après chargement, les contraintes effectives dans les argiles peuvent devenir inférieures à leurs valeurs initiales et la relation, reliant contraintes effectives et déformations à la fin de la consolidation primaire, n'est pas unique mais dépend aussi de l'épaisseur de la couche d'argile.

INTRODUCTION

One-dimensional (1-D) loading of clay soils produces pore water pressures in excess of the original equilibrium water pressures. With increasing time, water flows away from the highly stressed zone, the excess pore water pressures decay towards equilibrium values, and the clay compresses.

It is commonly assumed that

(*a*) the soil is fully saturated
(*b*) the solid particles and water are incompressible
(*c*) compression and flow are one-dimensional (vertical)
(*d*) strains are small
(*e*) Darcy's law is valid at all hydraulic gradients
(*f*) the hydraulic conductivity remains constant throughout the process.

Of these assumptions, (*e*) may be questioned in smectitic clays (Dixon, Sri Ranjan & Graham, 1992), and (*f*) may need to be modified in soft, compressible clays. The assumptions and the condition of continuity require that

$$\frac{k}{\gamma_w}\frac{\partial^2 u}{\partial z^2} = -\frac{\partial \varepsilon_z}{\partial t} \qquad (1)$$

where k is the coefficient of hydraulic conductivity, γ_w is the unit weight of water, u is the pore water pressure, z is the vertical co-ordinate axis, ε_z is the vertical strain, and t is time. The amount of the resulting compression depends on how the clay converts stress changes to strains. An analyst has

Manuscript received 5 January 1993; revised manuscript accepted 9 August 1995.
Discussion on this paper closes 2 December 1996; for further details see p. ii.
* Hong Kong Polytechnic University, Kowloon, Hong Kong.
† University of Manitoba, Winnipeg.

the option of modelling this in many ways through the introduction of a suitable constitutive model.

Terzaghi (1943) (from Terzaghi & Fröhlich, 1936) assumed a unique linear relationship between void ratio e and vertical effective stress σ'_z that is independent of loading history and process. The coefficient of volume compressibility $m_v = \partial\varepsilon_z/\partial\sigma'_z$ which describes the e–σ'_z relationship, and the consolidation coefficient $c_v = k/m_v\gamma_w$ which defines the rate of consolidation, were assumed to remain constant. Both assumptions can involve significant approximations to real soil behaviour; in particular, that straining will stop when excess pore water pressures have reduced to zero.

To overcome these limitations, two different approaches (here called hypothesis A and hypothesis B) are commonly employed. In hypothesis A (Ladd, 1973; Ladd, Foott, Ishihara, Schlosser & Poulos, 1977; Mesri & Godlewski, 1977; Mesri & Choi, 1985) primary consolidation strains associated with transferring pore water pressures into effective stresses are separated from secondary consolidation strains arising from viscous deformations. Terzaghi's consolidation theory is used to calculate the settlements at the end of primary (EOP) consolidation, and a separate coefficient of secondary consolidation $C_{\alpha\varepsilon}$ (or $C_{\alpha t}$) is then used to calculate the arbitrarily separated viscous deformations.

One implication of hypothesis A is that the EOP relationship between void ratio e and effective stress σ'_z is independent of the thickness of the soil layer. This conflicts with laboratory data reported by Berre & Iversen (1972) and with field data reported by Kabbaj, Tavenas & Leroueil (1988) which suggest that hypothesis A is not generally valid.

Hypothesis B (Suklje, 1957; Barden, 1965, 1969; Bjerrum, 1967) assumes that creep occurs during the whole consolidation process. This is more consistent with the approach used in rheology and visco-plastic theories in continuum mechanics. The key to the approach lies in producing a reliable constitutive relationship for the time-dependent stress–strain behaviour of clays. Tan (1957), Gibson & Lo (1961), and Lo (1961) developed linear rheological models using combinations of linear elastic springs and linear dashpots to describe time-dependent stress–strain behaviour. Barden (1965, 1969) and Berry & Poskitt (1972) proposed non-linear rheological models with linear elastic springs and non-linear dashpots for the time-dependent behaviour of clays. Both models have been used in calculations of 1-D consolidation in which creep (or viscous) strains play a significant role.

Bjerrum (1967) presented a conceptual model that took a different approach but also conforms with hypothesis B. He separated strains into 'instant' and 'delayed' compressions, and used 'time lines' to model the reduced creep rates that come with increasing durations of loading. His model permitted a better understanding of the apparent preconsolidation pressures and overconsolidation ratios (OCRs) that result from ageing. Garlanger (1972) developed this model into quantitative mathematical equations, and applied them to calculate consolidation deformations. Later, Magnan (1984), Leroueil, Kabbaj, Tavenas & Bouchard (1985a) and Kabbaj, Oka, Leroueil & Tavenas (1985) described a related stress–strain–strain rate relationship and used it to model consolidation during multi-stage loading. Similar work has been reported by Leroueil, Magnan & Tavenas (1985b), Magnan & Lepidas (1987) and Imai (1989).

ELASTIC VISCO-PLASTIC MODELLING USING EQUIVALENT TIME

The authors have developed this earlier work into a general elastic visco-plastic (EVP) constitutive model for 1-D straining (Yin & Graham 1989a, 1989b, 1994) which allows treatment of relaxation and strain rate effects as well the more customary load increments with creep. Although the EVP model appears at first sight to contain ideas similar in some ways to those used by Christie & Tonks (1985) and Magnan & Lepidas (1989), it was developed independently and its mathematical structure is different. The model develops the idea of 'equivalent time' which allows modelling of creep strains in both the overconsolidated and normally consolidated ranges using a constant creep parameter ψ, rather than the more common parameter $C_{\alpha\varepsilon}$ (or $C_{\alpha t}$) which varies with both pressure and OCR.

The authors have recently shown how the model is calibrated (Yin & Graham, 1994) and how it can be used to predict some unanticipated pore water pressure responses in soft clays (Yin, Graham, Clark & Gao, 1994). The latter paper gave only an outline of how the EVP model can be incorporated into the consolidation equation. The present paper discusses implementation of the EVP model in 1-D consolidation analysis, verification, and simulation of consolidation in clays with different thicknesses.

Since the EVP model has recently been described in detail, only a broad outline is presented here. In Fig. 1, strains along the instant time line are recoverable, and hence elastic (Christie & Tonks, 1985). Other strains are non-recoverable, with stress-dependent and time-dependent plastic components. Equivalent time t_e is the duration of straining at constant effective pressure σ' from a reference time line ($t_e = 0$) to the

current (σ'_z, ε_z, t_e) state, where ε_z is total vertical strain. The reference time line can be chosen at the discretion of the analyst, usually from a loading increment in the normally consolidated range of behaviour (Yin & Graham, 1994). Time lines are then defined as lines in (σ'_z, ε_z) space that have equal values of equivalent time t_e, but not necessarily equal real time durations t of loading. They represent equal durations t of loading when specimens start from normally consolidated states. When specimens are initially overconsolidated, the loading durations for a given strain vary with OCR and with the load increment. Time lines are also lines of constant creep strain rates $\dot{\varepsilon}_z$ when a logarithmic function is used to fit observations of creep behaviour.

The use of equivalent time allows the model to be structured so that (σ'_z, ε_z, t_e) states (or (σ'_z, ε_z, $\dot{\varepsilon}_z$) states) are independent of stress path. (In creep, total strain rate is equal to creep strain rate.) This means that in Fig. 1, strain rates at point 1 are the same whether the path followed in the test has been (*a*) elastic straining from 3 to 1″ followed by creep straining from 1″ to 1, or (*b*) loading with elastic straining to 2″, creep straining from 2″ to 2, and then unloading from 2 to 1.

Experience suggests that some overconsolidated natural clays exhibit time-independent behaviour and do not creep. The limit time line in Fig. 1 is therefore defined as the time line that has an equivalent time $t_e = \infty$, with a creep rate equal to zero. The behaviour above the limit time line is time-dependent and elastic visco-plastic. Below the limit time, it is time-independent. The logarithmic creep function used in the remainder of this paper (equation (2a)) implies creep continuing until $t_e = \infty$. However, it often offers a good approximate fitting to the creep behaviour of clays for time periods of practical interest. Logarithmic functions have also been used here to model instantaneous compressions (equation (2b)) and stress-dependent plastic compressions (equation (2c)), although this is not a formal requirement of the model (Yin & Graham, 1989b)

$$\varepsilon_z^{vp} = \psi/V \times \ln[(t_0 + t_e)/t_0] \quad \text{for} - t_0 < t_e < \infty \tag{2a}$$

$$\varepsilon_z^{e} = \varepsilon_{z0}^{e} + \kappa/V \times \ln(\sigma'/\sigma'_u) \tag{2b}$$

$$\varepsilon_z^{ep} = \varepsilon_{z0}^{ep} + \lambda/V \times \ln(\sigma'_z/\sigma'_{z0}) \tag{2c}$$

where σ'_u is a unit effective stress.

General equations

If the equivalent time t_e is known, the strain at any state point (σ'_z, ε_z) is

$$\varepsilon_z = \varepsilon_z^{ep} + \varepsilon_z^{vp} = \varepsilon_{z0}^{ep} + \lambda/V \ln(\sigma'_z/\sigma'_{z0}) + \psi/V \ln[(t_0 + t_e)/t_0] \tag{3}$$

This is a general equation which can be solved for any 1-D loading condition once the equivalent time t_e is known. Detailed information on the evaluation of t_e is given by Yin & Graham (1994).

If a general condition (σ'_z, ε_z) is not on the reference time line, then equation (3) allows the equivalent time to be calculated uniquely

$$t_e = -t_0 + t_0 \exp[(\varepsilon_z - \varepsilon_{z0}^{ep})V/\psi](\sigma'_z/\sigma'_{z0})^{-\lambda/\psi} \tag{4}$$

Continuous loading or unloading can be considered as a series of infinitesimal incremental loads $d\sigma'_z$ for real time dt, for example from point i to point $(i+1)$ in Fig. 1. The incremental strain $d\varepsilon_z$ resulting from $d\sigma'_z$ is the sum of the incremental elastic strain $d\varepsilon_z^e$ and the incremental creep strain $d\varepsilon_z^{vp}$

$$d\varepsilon_z = d\varepsilon_z^e + d\varepsilon_z^{vp} \tag{5}$$

In equation (5), $d\varepsilon_z^e$ is calculated by differentiating equation (2b), and $d\varepsilon_z^{vp}$ is equal to $\dot{\varepsilon}_z^{vp} \times dt$. Equation (5) becomes

$$d\varepsilon_z = \kappa/V \frac{1}{\sigma'_z} d\sigma'_z + \dot{\varepsilon}_z^{vp}\, dt \tag{6}$$

The creep strain rate $\dot{\varepsilon}_z^{vp}$ in equation (6) can be calculated by differentiating equation (2a) with respect to equivalent time t_e

$$\dot{\varepsilon}_z^{vp} = d\varepsilon_z^{vp}/dt_e = \psi/V \frac{1}{t_0 + t_e} \tag{7}$$

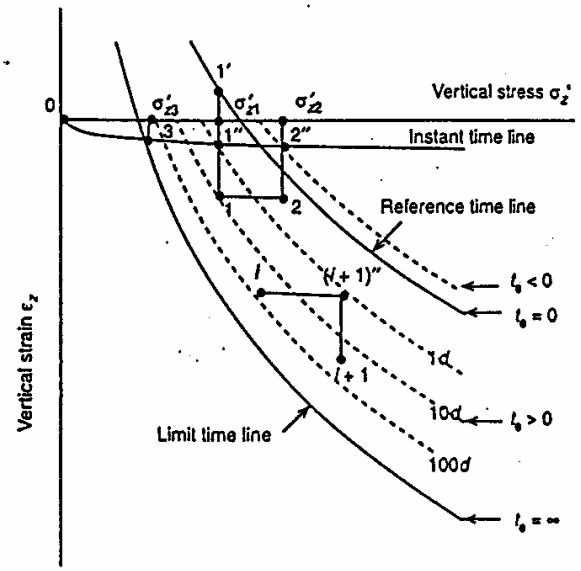

Fig. 1. Illustration of instant time line, time lines, equivalent times, reference time line and limit time line (Yin & Graham, 1989b)

From equation (4), equation (7) becomes

$$\dot{\varepsilon}_z^{vp} = \frac{\psi/V}{t_0} \exp\left[-\left(\varepsilon_z - \varepsilon_{z0}^{cp}\right)V/\psi\right](\sigma'_z/\sigma'_{z0})^{\lambda/\psi} \tag{8}$$

Equations (7) and (8) show that the creep strain rate at any condition σ'_z, ε_z is uniquely related to equivalent time.

Subsitution of equation (8) in equation (6) gives a σ'_z, ε_z, $\dot{\sigma}'_z$, $\dot{\varepsilon}_z$-model for any 1-D loading conditions

$$\frac{\partial \varepsilon_z}{\partial t} = \frac{\kappa/V}{\sigma'_z}\left(\frac{\partial \sigma'_z}{\partial t}\right) + \frac{\psi/V}{t_0} \times \exp\left(-(\varepsilon_z - \varepsilon_{z0}^{cp})\frac{V}{\psi}\right)\left(\frac{\sigma'_z}{\sigma'_{z0}}\right)^{\lambda/\psi} \tag{9}$$

where κ/V, λ/V, σ'_{z0}, ψ/V, t_0 and ε_{z0}^{cp} are six fitting parameters used in the model (Yin & Graham, 1994). The additional generality associated with the $\dot{\sigma}'_z$ term (compared with the σ'_z, ε_z, $\dot{\varepsilon}_z$-model used for example by Kabbaj *et al.* (1988)) allows the same general equation to be used to model relaxation and constant stress rate tests.

The number of parameters in this EVP model is the same as in conventional approaches using hypothesis A. The variable V represents the specific volume of the clay. The parameter κ/V is similar to C_r, which defines unloading–reloading behaviour. The parameter λ/V is similar to C_c, the compression index, which defines elastic–plastic behaviour; σ'_{z0} has a somewhat similar role to the preconsolidation pressure p'_c, and ε_{z0}^{cp} is related to initial void ratio e_0. The creep parameter ψ/V is similar to the coefficient of secondary consolidation $C_{\alpha\varepsilon}$ (or $C_{\alpha\varepsilon}$) but is now independent of OCR, and t_0 is similar to t_{EOP}, the time at the EOP consolidation. However, the detailed definitions of these parameters used in the EVP model are not the same as those in the conventional approach.

Yin & Graham (1994) discussed these modelling parameters in more detail, and showed how they (plus the coefficient of consolidation c_v and hydraulic conductivity k) could be determined from compression data of Berre & Iversen (1972) for natural post-glacial marine clay from Drammen, Norway. Values of the modelling parameters are given in Table 1.

In Table 1, c_v was determined using Casagrande's log time method. The value of k was estimated using the relation $k = c_v m_v \gamma_w$, with m_v being calculated from $m_v = \Delta\varepsilon_z/\Delta\sigma'_z$ at the end of primary consolidation in increments 4 and 5 of test 7. The values agree well with those given by Berre & Iversen (1972).

CONSOLIDATION EQUATION USING THE EVP CONSTITUTIVE MODEL

This section shows how the new EVP model can be incorporated into the consolidation equation to allow the computation of time-dependent straining and pore water dissipation in 1-D compression. In equation (1), $\partial^2 u/\partial z^2 = \partial^2 u_e/\partial z^2$, where $u_e(z, t)$ is the excess pore water pressure above an initial equilibrium value u_0, and $u(z, t) = u_0 + u_e(z, t)$. The process of consolidation causes u_e to decrease to zero, at which stage u is again equal to u_0. During consolidation, the effective stress σ'_z in equation (1) can be written as $\sigma'_z = \sigma_z - u$, and so equation (9) becomes

$$\frac{\partial \varepsilon_z}{\partial t} = \frac{\kappa/V}{\sigma_z - u}\left(\frac{\partial \sigma_z}{\partial t} - \frac{\partial u}{\partial t}\right) + \frac{\psi/V}{t_0} \times \exp\left(-\varepsilon_z \frac{V}{\psi}\right)\left(\frac{\sigma_z - u}{\sigma'_{z0}}\right)^{\lambda/\psi} \tag{10}$$

Equations (1) and (10) are a general differential system for solving 1-D consolidation problems under any load conditions and loading history.

Consider a simple case of external loading in which the total stress $\sigma_z(z)$ may vary with depth, but not with time. Using the condition $\partial\sigma_z/\partial t = 0$, equation (10) becomes

$$\frac{\partial \varepsilon_z}{\partial t} = \frac{-\kappa/V}{\sigma_z - u}\frac{\partial u}{\partial t} + \frac{\psi/V}{t_0} \times \exp\left(-\varepsilon_z \frac{V}{\psi}\right)\left(\frac{\sigma_z - u}{\sigma'_{z0}}\right)^{\lambda/\psi} \tag{11}$$

If equation (11) is introduced into equation (1)

$$\frac{k}{\gamma_w}\frac{\partial^2 u}{\partial z^2} = \frac{\kappa/V}{\sigma_z - u}\frac{\partial u}{\partial t} - \frac{\psi/V}{t_0} \times \exp\left(-\varepsilon_z \frac{V}{\psi}\right)\left(\frac{\sigma_z - u}{\sigma'_{z0}}\right)^{\lambda/\psi} \tag{12}$$

Table 1. Soil parameters in the modelling of 1-D consolidation (based on data from Berre & Iversen (1972), test 7, load increments 4 and 5)

κ/V	λ/V	σ'_{z0}: kPa	ψ/V	t_0: min	k: m/min	ε_{z0}^{cp}	c_v: m²/min	m_v: m²/kN
0·004	0·158	79·2	0·007	40	$1·0 \times 10^{-7}$	0	$1·51 \times 10^{-4}$	$6·75 \times 10^{-5}$

The strain ε_z in equation (12) is solved by combining equations (11) and (12).

The parameters $m_v = \partial\varepsilon_z/\partial\sigma'_z = (\kappa/V)/(\sigma_z - u)$ and $c_v = k/(m_v\gamma_w)$ can now be introduced. In Terzaghi's theory these parameters are constant, but in the new model they depend on time t and depth z. It will also be possible in future work to use more realistic, pressure-dependent, or voids ratio-dependent, hydraulic conductivities. Equations (11) and (12) then become

$$c_v\frac{\partial^2 u}{\partial z^2} = \frac{\partial u}{\partial t} - \frac{1}{m_v}g(u, \varepsilon_z) \tag{13a}$$

$$\frac{\partial \varepsilon_z}{\partial t} = -m_v\frac{\partial u}{\partial t} + g(u, \varepsilon_z) \tag{13b}$$

where

$$g(u, \varepsilon_z) = \frac{\psi/V}{t_0}\exp\left(-\varepsilon_z\frac{V}{\psi}\right)\left(\frac{\sigma_z - u}{\sigma'_{z0}}\right)^{\lambda/\psi} \tag{13c}$$

FINITE DIFFERENCE SOLUTIONS OF 1-D CONSOLIDATION

Equations (13) can now be used to solve consolidation problems in which the total stress $\sigma_z(z)$ remains constant with respect to time. They form a highly non-linear system of partial differential equations which has been solved using the Crank–Nicholson finite difference procedure. With the terminology shown in Fig. 2, equation (13a) becomes

$$(c_v)_{i,j}\frac{1}{2(\Delta z)^2}[(u_{i+1,j+1} - 2u_{i,j+1} + u_{i-1,j+1}) + (u_{i+1,j} - 2u_{i,j} + u_{i-1,j})] = \frac{1}{\Delta t}(u_{i,j+1} - u_{i,j}) - \left(\frac{1}{m_v}g(u, \varepsilon_z)\right)_{i,j} \tag{14}$$

where the subscripts i (0, 1 ..., n) represent variation in depth, described by the z co-ordinate, and the subscripts j (0, 1, ..., m) represent variation in the time t co-ordinate. The depth increment $\Delta z = z_{i+1} - z_i$ has been kept constant, but the time increment $\Delta t = t_{j+1} - t_j$ has been allowed to increase as consolidation proceeds. c_v, m_v and $g(u, \varepsilon_z)$ in equations (13) may vary with depth and time. As a simple approximation, their values at (i, j) are used in equation (14).

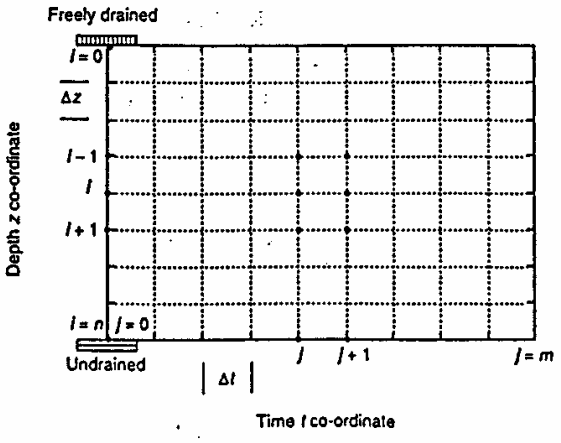

Fig. 2. Finite difference grid and boundaries

Defining $r = [c_v\Delta t/(\Delta z)^2]_{i,j}$ allows equation (14) to be rewritten

$$-0{\cdot}5r \times u_{i-1,j+1} + (1 + r)u_{i,j+1} - 0{\cdot}5r \times u_{i+1,j+1} = 0{\cdot}5r \times u_{i-1,j} + (1 - r)u_{i,j} + 0{\cdot}5r \times u_{i+1,j} + \Delta t\left(\frac{1}{m_v}g(u, \varepsilon_z)\right)_{ij} \tag{15}$$

where $(i = 1, 2, 3 \ldots n - 1;\ j = 0, 1, 2, \ldots m - 1)$.

Similarly, equation (13b) becomes:

$$(\varepsilon_z)_{i,j+1} = (\varepsilon_z)_{i,j} - (m_v)_{i,j}(u_{i,j+1} - u_{i,j}) + \Delta t[g(u, \varepsilon_z)]_{i,j} \tag{16}$$

Figure 2 shows the boundary conditions used in the remainder of the paper. The initial thickness of the soil layer before consolidation is H_0. The top of the soil layer ($z = 0$) is freely draining, i.e. the pore water pressure u is constant, and $u_e = 0$. (In the special confined triaxial consolidation (modified oedometer) tests of Berre & Iversen (1972), the pore water pressure at the freely draining boundary can be considered zero, even though a back pressure was applied. The back pressure increased both the total principal stresses and the pore water pressures, but did not change the effective stresses in the specimens.) At the bottom of the layer ($z = H_0$), a zero drainage boundary is represented by $\partial u/\partial z = 0$.

In finite difference form, the two boundary conditions are written

(*a*) $u_{0,j} = 0$ (where $j = 0, 1, 2, \ldots m$)
(*b*) $u_{n,j} - u_{n-1,j} = 0$ (where $j = 0, 1, 2, \ldots m$)

It is shown above that the compression behaviour of viscous clays is uniquely related to their $(\sigma'_z, \varepsilon_z, t_e)$ state, and hence to their past loading history. Because deformations during consolidation depend not only on the initial pore water pressures but also on the initial state $(\sigma'_z, \varepsilon_z)_{i,0}$, three sets of initial values, at time $t = +0$, are required before computation begins

(*a*) $(\sigma_z)_{i,0}$ $(i = 0, 1, 2 \ldots n)$
(*b*) $(\varepsilon_z)_{i,0}$ $(i = 0, 1, 2 \ldots n)$
(*c*) $u_{i,0}$ $(i = 0, 1, 2 \ldots n)$.

Conditions (*a*) and (*c*) show that the initial effective stresses can be written

$$(\sigma'_z)_{i,0} = (\sigma_z)_{i,0} - u_{i,0} \quad (i = 0, 1, 2 \ldots n)$$

Using these boundary conditions and initial conditions, equations (13c), (15) and (16) form a linear tridiagonal equation system for the unknowns $u_{i,j}$, $(\varepsilon_z)_{i,j}$ $(i = 1, 2, 3, \ldots n-1, j = 1, 2, 3 \ldots m)$. The time dependent settlement S_t at the top of the soil layer $(z = 0)$ is given by the sum

$$S_t = \int_{z=0}^{z=H_0} \varepsilon_z(t, z)\, dz \tag{17}$$

where the strain ε_z is a function of time and depth. An approximate numerical solution of equation (17) can be written

$$S_j = \left(0{\cdot}5(\varepsilon_z)_{0,j} + \sum_{i=1}^{i=n-1} (\varepsilon_z)_{i,j} + 0{\cdot}5(\varepsilon_z)_{n,j}\right)\Delta z \tag{18}$$

Numerical solutions of equations (15), (16) and (18) can readily be programmed for solution by microcomputer.

STRAINS AND PORE WATER PRESSURES IN SPECIMENS OF DIFFERENT THICKNESS

Berre & Iversen (1972) presented strain and pore water pressure data from modified oedometer tests on specimens with four different initial thicknesses: 18·8 mm (test 7), 75·7 mm (test 6), 150·1 mm (test H6) and 450·1 mm (test H4). Specimen H4 was instrumented in three separate segments, with free drainage at the top of the topmost segment and no drainage at the bottom of the third and lowest segment. Pore water pressures were measured at the bottom of each segment. Average strains (or settlements) were measured in each segment (Berre & Iversen, 1972).

The material was a carefully sampled, lightly overconsolidated, marine post-glacial clay from 5·2 m to 6·7 m depth. Its clay fraction ($< 2\,\mu$m) was 45%, natural water content 57%–60%, liquid limit 54%–60%, plastic limit 28%–34%, OCR ~1·35, and sensitivity 10–12. The tests involved multi-stage loading with various time durations. They allowed examination of any creep straining that might occur during primary consolidation.

Selected test data are summarized in Table 2, and results are shown in Figs 3–6. Increment 4 in

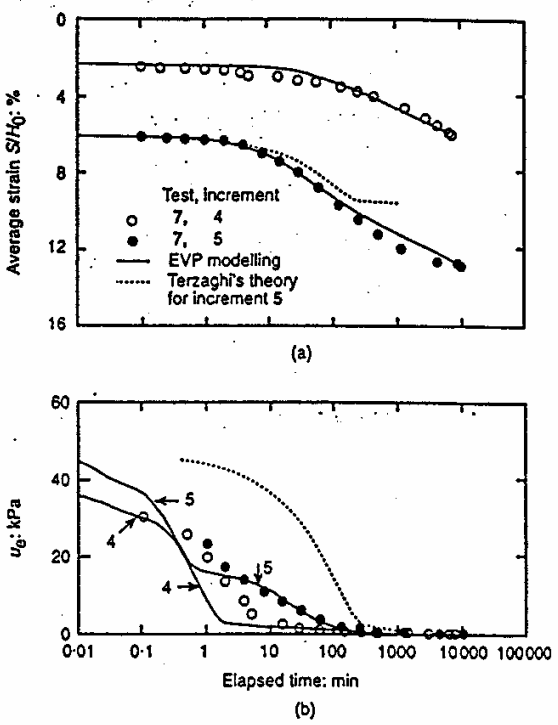

Fig. 3. Comparison of measured and calculated results using the EVP model and Terzaghi's theory: (a) S/H_0–time; (b) u_e–time; test 7 (Berre & Iversen, 1972)

Table 2. Thickness, initial stress, strain, pore water pressure, and duration times from oedometer tests on Drammen clay (after Berre & Iversen, 1972)

Test	Increment	H_0: m	$(\varepsilon_z)_{i,0}$: %	σ_{z0}: kPa	$(\sigma_z)_{i,0}$: kPa	$u_{i,0} = \Delta\sigma_z$: kPa	t: min
7	4	0·0188	2·25	55·3	92·5	37·2	7055
	5	0·0188	6·08	92·5	140·2	47·7	10000
6	4	0·0757	1·25	55·9	93·3	37·4	8060
	5	0·0757	5·51	90·3	140·5	47·7	5694
H6	4	0·150	1·20	55·2	92·5	37·3	11230
	5	0·150	4·53	92·5	140·2	47·7	10000
H4	4						
	Top	0·450	1·15	53·4	89·2	35·8	30440
	Middle	0·450	1·25	53·4	89·2	35·8	30440
	Lower	0·450	1·50	53·4	89·2	35·8	30440
H4	5						
	Top	0·450	4·25	89·2	134·7	45·5	61450
	Middle	0·450	5·21	89·2	134·7	45·5	61450
	Lower	0·450	6·30	89·2	134·7	45·5	61450

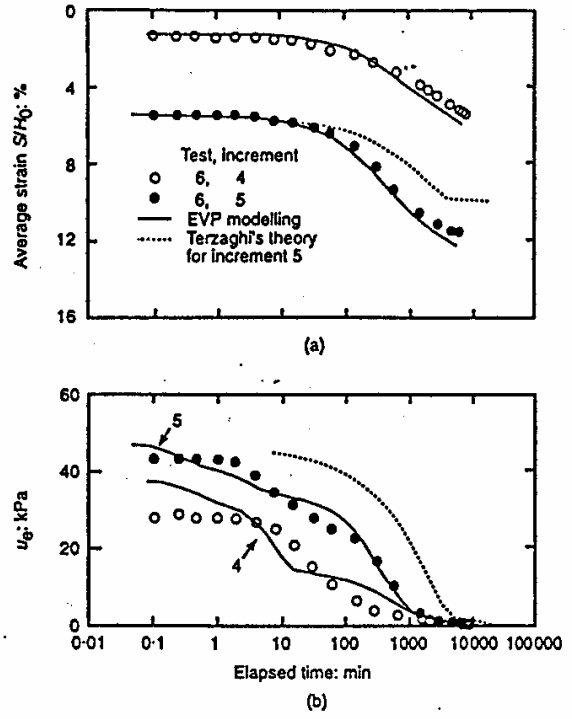

Fig. 4. Comparison of measured and calculated results using the EVP model and Terzaghi's theory: (a) S/H_0–time; (b) u_e–time; test 6 (Berre & Iversen, 1972)

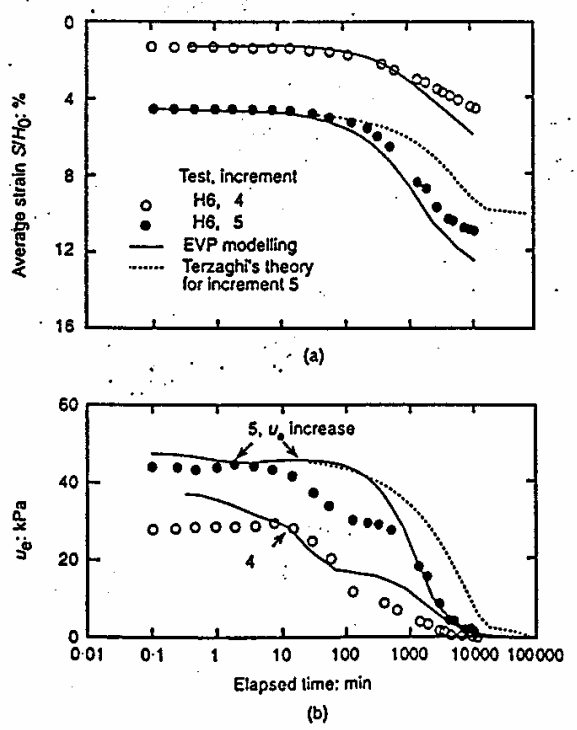

Fig. 5. Comparison of measured and calculated results using the EVP model and Terzaghi's theory: (a) S/H_0–time; (b) u_e–time; test H6 (Berre & Iversen, 1972)

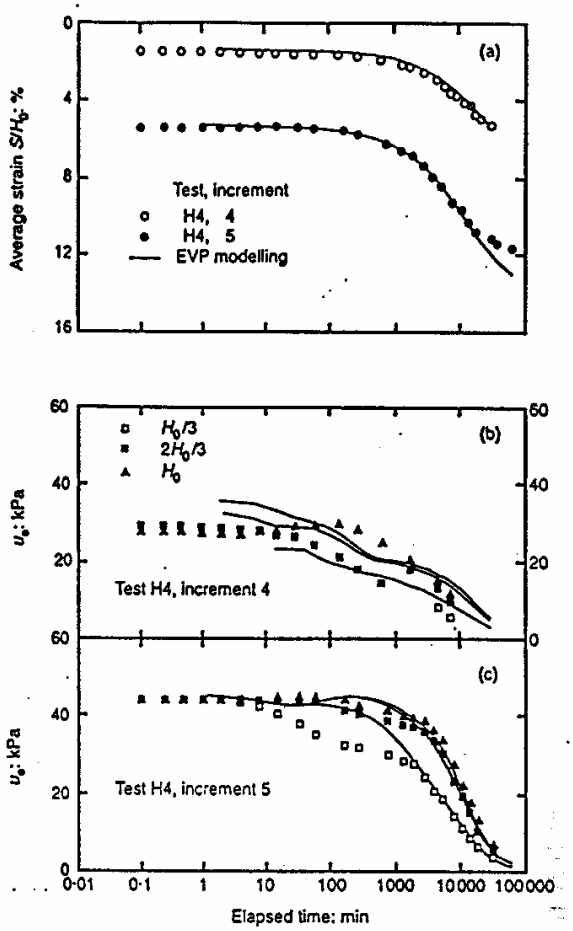

Fig. 6. Comparison of measured and calculated results using the EVP model: (a) S/H_0–time; (b) u_e–time for increment 4; (c) u_e–time for increment 5; test H4 (Berre & Iversen, 1972)

Table 2 straddles the in situ stress, and since the clay is only lightly overconsolidated, this produces a normally consolidated specimen. Increment 5 is in the normally consolidated range (Berre & Iversen, 1972) (Fig. 6) and should therefore be accompanied by significant creep straining in this relatively sensitive clay. In Table 2, H_0 is the initial thickness of the specimens. The initial strains $(\varepsilon_z)_{i,0}$ at the start of a new load increment are the strains that have been accumulated up to the end of loading under the previous total stress σ_{z0}, i.e. the 'original' stress with $u_e = 0$ before the new loading was applied. (The results have been reported using axis translation so that $u = 0$ at equilibrium, when $u_e = 0$, and $\sigma_{z0} = \sigma'_{z0}$. The initial total stress $(\sigma_z)_{i,0}$ is the new value of σ_z immediately after loading, i.e. at $t = +0$. The initial pore water pressure $u_{i,0}$ at $t = +0$ is equal to the total stress increment $\Delta\sigma_z$. The times t were the durations of the increments in Berre & Iversen's tests.

The consolidation equations (equations 13) have been solved for the conditions in Berre & Iversen's tests 6, H6 and H4 using the finite difference procedure outlined above with the parameters in Table 1 derived from test 7. Modelling results are compared with measured values to examine the validity of the new EVP model. For comparison, see calculations from Terzaghi's theory using the approach outlined in Appendix 2 are also given. When considering specimens with different thicknesses, values of measured and calculated average strains S/H_0 rather than total settlements S are compared. For a load increment $\Delta\sigma_z$, the increment in the time-dependent average strain $\Delta(S/H_0)$ during primary consolidation is

$$\Delta(S/H_0) = (\Delta S_{100}/H_0) \times U, \quad \text{for } 0 < t \leq t_{EOP} \tag{19}$$

where U is the average degree of consolidation obtained from traditional solutions of Terzaghi's theory.

Comparison of model predictions and laboratory data

The results of EVP modelling for each of the tests in Table 2 are now examined. Results from the EVP model are obtained by solving the appropriate boundary value problem using equations (13).

Test 7. Fig. 3 shows comparison of measured results, EVP modelling, and Terzaghi's theory for Berre & Iversen's test 7. Results are shown for average strain S/H_0 against time (Fig. 3(a)) and excess pore water pressure u_e against time (Fig. 3(b)). Terzaghi's theory underestimates the average strain (or settlement) for increment 5, and its S-shaped pattern of pore water pressure response differs from both the measured response and the more complex response predicted by the EVP model. Since test 7 was used to determine the modelling parameters in the EVP constitutive equation (equation (9)), the good agreement shown in Fig. 3 for average strains is to be expected.

Test 6. Figs 4(a) and 4(b) show comparisons of measured data and modelling predictions for test 6. Again, the EVP model agreed well with the test data, while Terzaghi's theory underestimates the average strain in the specimen, and its u_e–t relationship differs from both the measured values and the EVP modelling. The measured initial excess pore water pressures for increment 4 were lower than the value of $u_{i,0} = 37{\cdot}4$ kPa that would be expected from the change in stress $\Delta\sigma_z = 37{\cdot}4$ kPa in a saturated clay.

Test H6. Figs 5(a) and 5(b) show good agreement between measured and predicted average strains up to about 1000 min of increment duration, but thereafter the calculated values are larger. The predicted values of $u_{i,0} = \Delta\sigma_z$ were 37·3 kPa and 47·7 kPa for increments 4 and 5 respectively; these are again larger than the measured values.

Test H4. The predicted average strains agree well with the measured data for increment 4, and also for about the first 20 000 min for increment 5 (Fig. 6). Again the measured pore water pressures are lower than expected. The EVP modelling agrees well with the test data for increment 5, except that the model overestimated the u_e at $z = \frac{1}{3}H_0$ in the middle stage of the testing. The measured data show some increases in u_e at $z = H_0$, the undrained boundary, in increment 4; and at $z = \frac{2}{3}H_0$ and H_0 in increment 5 (i.e. at the bottoms of the middle and lowest segments of the specimen). Fig. 6(c) shows that the EVP model can simulate this phenomenon of local pore water pressure increase during the consolidation process.

Berre & Iversen (1972) compared measured data and results calculated for test 7, increment 5, using the linear rheological model suggested by Gibson & Lo (1961) and the non-linear rheological model of Barden (1965). Figs 7(a) and 7(b) show that the new EVP model produces reasonable modelling, while Gibson & Lo's model underestimates the average strains in the middle stage of the testing and overestimates the pore water pressures except at the end of the increment.

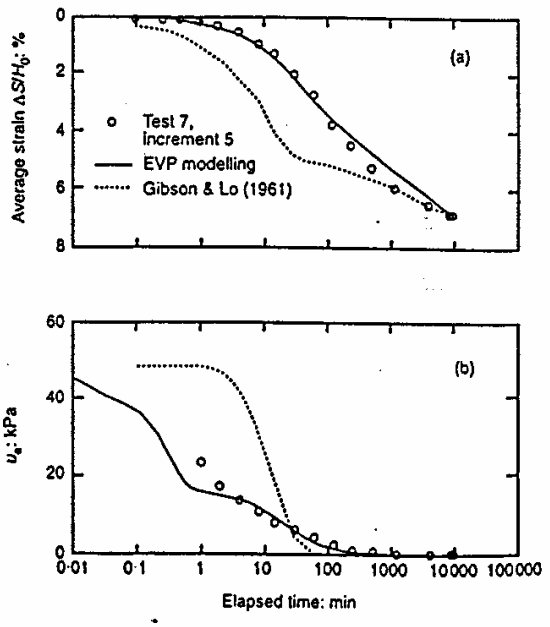

Fig. 7. Comparison of measured and calculated results using the EVP model and Gibson & Lo's (1961) model: (a) S/H_0–time; (b) u_e–time; test 7, increment 5 (Berre & Iversen, 1972)

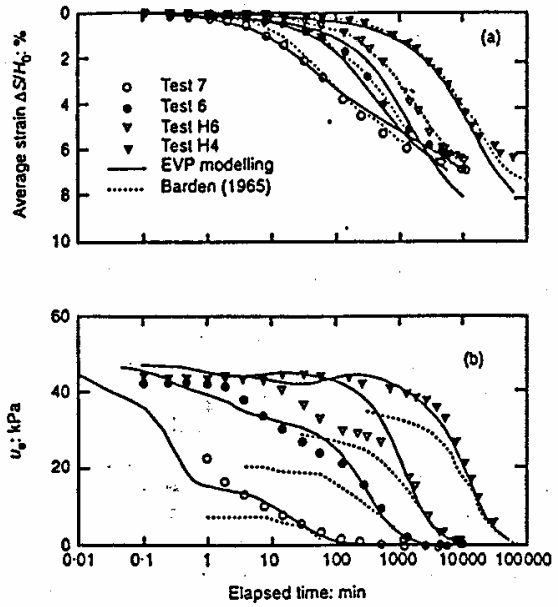

Fig. 8. Comparison of measured and calculated results using the EVP model and Barden's (1965) model: (a) S/H_0–time; (b) u_e–time; tests 7, 6, H6 and H4 at increment 5 (Berre & Iversen, 1972)

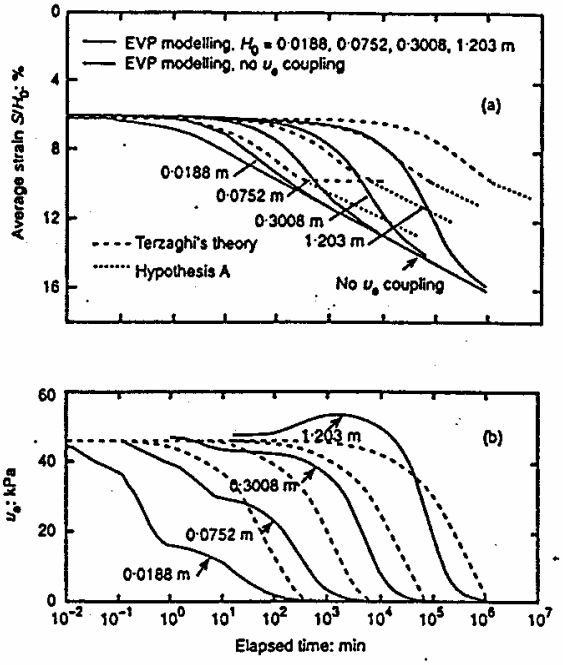

Fig. 9. Comparison of results calculated using the EVP model and Terzaghi's theory with hypothesis A for clay layers $H_0 = 0{\cdot}0188$ m, 0·0752 m, 0·3008 m and 1·203 m: (a) S/H_0–time; (b) u_e–time

Figures 8(a) and 8(b) show similar comparisons with Barden's model, which predicts the average strain increments for Increment 5 in all four tests quite well (Berre & Iversen, 1972). However, Barden's predicted pore water pressures are much lower than the measured values. In general, predictions from the EVP model are in good agreement with the test data for all four tests. Remaining discrepancies may be associated with the assumption of constant hydraulic conductivity k in (equations (13a) and (13b)) which is known to vary non-linearly with effective stress. Another reason for the discrepancies may be the assumption of constant values of the logarithmic fitting functions κ, λ and ψ. Yin & Graham (1989a) showed how power law functions could produce better modelling in highly structured clay.

SIMULATION OF CONSOLIDATION IN CLAYS WITH DIFFERENT THICKNESSES

Figure 9 shows average strains S/H_0 and excess pore water pressures u_e for four different clay layers that were assumed to be freely drained at the top and completely undrained at the bottom. The dashed lines in Fig. 9(a) show non-viscous settlements predicted by Terzaghi's equation; the dotted lines add the viscous component. The figure includes non-coupled EVP modelling using equation (22b) from Yin & Graham (1994), and the new coupled EVP model given by equations (13). The parameters for the EVP modelling are again those in Table 1, with initial conditions $(\varepsilon_z)_{i,0} = 6{\cdot}08\%$, $\sigma'_{z0} = 92{\cdot}5$ kPa (the previous effective stress level), $u_{i,0} = 47{\cdot}7$ kPa. The total stress $(\sigma_z)_{i,0}$ under the new loading is 140·2 kPa. Four different thicknesses are used: $H_0 = 0{\cdot}0188$, 0·0752, 0·3008 and 1·203 m. The conditions for $H_0 = 0{\cdot}0188$ m are the same as for test 7, increment 5 in Table 2. The remaining conditions are for clay layers of different thicknesses which start from the same void ratio and experience the same stress increase.

In general, the EVP model calculates larger settlements than Terzaghi's theory. After the excess pore water pressures have dissipated, the average strains calculated using the new EVP model for the four different thicknesses approach the line calculated using the model described by Yin & Graham (1994). It will be remembered that the earlier model did not take account of delays in settlements caused by pore water pressure coupling.

Figure 9(b) shows the variation of excess pore water pressure u_e with time at the undrained (impervious) bottoms of the consolidating layers. As expected, the u_e–time curves calculated by the EVP model are different from the S-shaped curves calculated using Terzaghi's theory. In the general area of the arrows in Fig. 9(b), the dissipation rates of excess pore water pressures $(-\partial u_e/\partial t)$ decrease at various stages in the consolidation process depending on the thickness of the consolidation layer. Later they increase again, before finally

approaching zero when consolidation is complete. The pattern of such changes in $(-\partial u_e/\partial t)$ depends on the thickness of the consolidation layer, and on the hydraulic conductivity k, the viscous stress–strain behaviour of the clay, and the initial stress–strain states and loading conditions.

When the thickness increases beyond a certain value (for example the layer with $H_0 = 1{\cdot}203$ m in Fig. 9(b)), the rate $(-\partial u/\partial t)$ can become negative during part of the consolidation process. That is, the dissipation rates can become negative, and the apparently anomalous result follows that excess pore water pressures can actually increase locally for some time (see for example Lambe & Whitman, 1969; Chang, 1981; Crooks, Becker, Jefferies & McKenzie, 1984; Kabbaj *et al.*, 1988). Associated with these decreases and subsequent increases in $(-\partial u/\partial t)$ are corresponding decreases and increases in the rate of change of effective stresses. Figs 10(a) and 10(b) show isochrones of excess pore water pressures u_e and strains ε_z respectively for the clay layer with initial thickness $H_0 = 1{\cdot}203$ m. Fig. 10(a) shows again that in the early stages of consolidation, pore water pressures at the bottom of the layer can be larger than the applied stress increase of 47·7 kPa. This is dealt with more fully in Yin *et al.* (1994).

The reason for the increasing pore water pressures is that vertical strains in the lower 70% of the clay are almost constant during the early stages of consolidation (Fig. 10(b), line 1). This means that the clay is in a state of 'relaxation' which is similar to 'creep', but now with constant strain and decreasing effective stress. Continuing viscous compressions must be balanced by elastic expansions, and therefore by decreasing effective stresses and increasing pore water pressures. An understanding of this mechanism can only be derived from a $(\sigma'_z, \varepsilon_z, \dot{\sigma}'_z, \dot{\varepsilon}_z)$ model such as equation (9). Naturally the effect is most clearly observed when the loading is sufficient to exceed the previous preconsolidation pressure, as in the Halifax clay tests of Yin *et al.* (1994). In the overconsolidated range, creep rates will be much smaller (Fig. 1) and the effect is unlikely to develop.

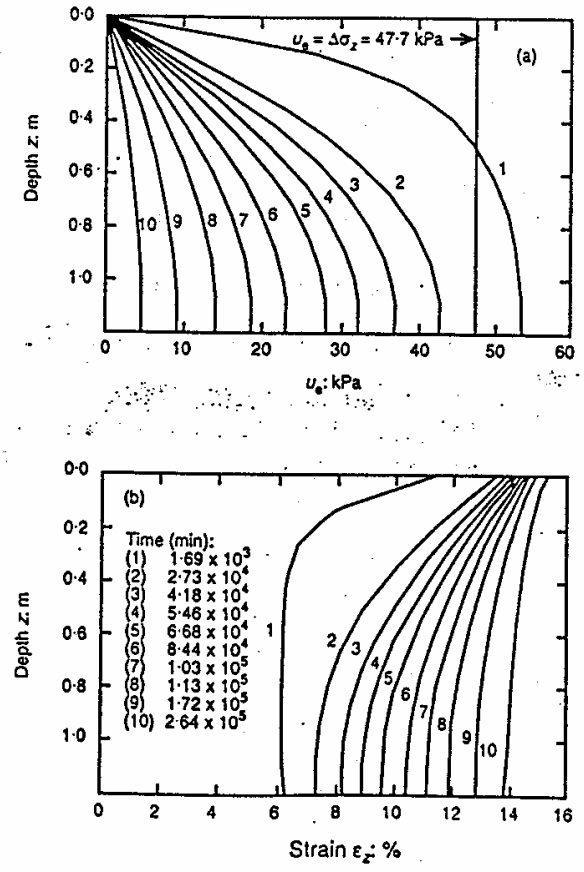

Fig. 10. (a) Excess pore water pressure isochrones, (b) strain isochrones in the clay layer $H_0 = 1{\cdot}203$ m, simulated using the EVP model

RELATIONSHIP BETWEEN AVERAGE STRAIN S/H_0 AT EOP AND THICKNESS OF CLAY LAYER

Two hypotheses (A and B) relating the EOP voids ratio and effective stress to the thickness of the consolidating layer are outlined above. Mesri & Choi (1985) concluded that the EOP e–$\log\sigma'_z$ is unique and independent of the thickness. This supports hypothesis A. However, Kabbaj *et al.* (1988) found that the EOP e–$\log\sigma'_z$ relationship from thin laboratory specimens underestimated *in situ* settlements at three normally consolidated test embankment sites. They concluded that hypothesis A is not valid.

Yin & Graham (1990) used the EVP model to show that the EOP e–$\log\sigma'_z$ relationship is not unique, but a function of t_{EOP} (or t_p), the time required to complete primary consolidation. This paper has extended that work by formally incorporating the EVP model into the consolidation equation and investigating how the EOP e–$\log\sigma'_z$ relationship (or the equivalent S/H_0–σ'_z relationship) varies with the thickness of consolidating layers.

Results are shown in Fig. 11 for the stage when the maximum excess pore water pressure u_e has been reduced to 0·5 kPa, which can be considered negligibly small. The average strains S/H_0 clearly depend quite strongly on the layer thickness H_0. Fig. 11 shows that the average strains increase with increasing layer thickness. However, the gradient $d(S/H_0)/dH_0$ decreases with increasing layer thickness, and the relationship between S/H_0 and $\log H_0$ is almost linear (Fig. 11(b)). Fig. 11(b) supports the earlier conclusion that arbitrary separation of consolidation strains into primary and secondary components lacks a physical or mathematical basis.

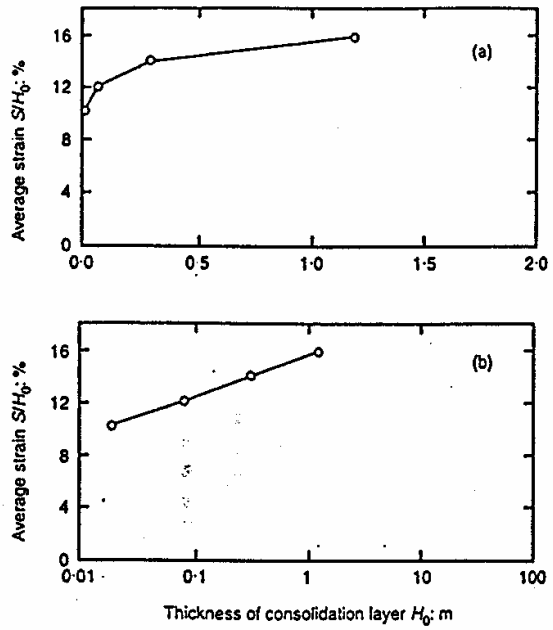

Fig. 11. Relationship of average strains S/H_0 with thickness of the consolidation layer H_0 at EOP consolidation ($u_e = 0{\cdot}5$ kPa, simulated using the EVP model): (a) S/H_0–H_0, (b) S/H_0–log H_0; the initial strain before the application of $\Delta\sigma'_z = 47{\cdot}7$ kPa is $\varepsilon_z = 6{\cdot}08\%$.

CONCLUSIONS

A new EVP model has been incorporated into the consolidation equation, and solutions have been obtained using finite differences. Results calculated using the model agree well with the test data reported by Berre & Iversen (1972). Complex pore water pressure data are modelled quite well, although average settlements are at times overestimated.

The model allows an understanding of the observation that excess pore water pressure dissipation rates ($-\partial u_e/\partial t$) in thin layers of viscous clays may decrease part of the way through the consolidation process, and then increase again, before finally reducing to zero when consolidation is complete. Simulation of the consolidation of four different thicknesses of clay shows that the average strains at the EOP consolidation increase with increasing thickness of layers.

ACKNOWLEDGEMENTS

The authors are grateful for support and encouragement from the Natural Science and Engineering Research Council of Canada (NSERC) and the Centre for Cold Oceans Resources Engineering (C-CORE), Memorial University of Newfoundland, St. John's, Newfoundland.

NOTATION

c_v	coefficient of consolidation $k/m_v\gamma_w$
C_{ue}, $C_{\varepsilon e}$	logarithmic creep functions with respect to voids ratio, strain
$g(u, \varepsilon_z)$	creep function in EVP consolidation equation
H_0	initial thickness of soil layer
k	coefficient of hydraulic conductivity
m_v	coefficient of volumetric compressibility $\partial\varepsilon_z/\partial\sigma'_z$
r	$c_v\Delta t/(\Delta z)^2$
S	settlement
t, t_e	time, equivalent time
t_0	curve-fitting parameter related to choice of reference time line
u, u_e	pore water pressure, excess pore water pressure
V	specific volume, volume occupied by unit volume of solids
γ_w	unit weight of water
ε	strain
ε^e_{z0}, ε^{ep}_{z0}	'fixing' strains for instantaneous line and reference time line
κ, λ	logarithmic material constants for instantaneous strains and stress-dependent plastic strains
σ, σ'	stress, effective stress
ψ	logarithmic material constant for creep

Superscripts

e, tp, ep	instantaneous (elastic), time-dependent plastic, stress-dependent plastic

Subscripts

0	'original' from previous loading
EOP	end of primary consolidation
i, j	counters for position z and time t
z	vertical

APPENDIX I. CALCULATIONS BASED ON TERZAGHI'S THEORY

For the calculations involving Terzaghi's theory (hypothesis A), the settlement S_{100} (and hence the average strain S_{100}/H_0) at the EOP consolidation must be calculated before the time-dependent average strain S/H_0 can be evaluated. The average strain can be calculated from

$$\Delta S_{100}/H_0 = C_r/V \times \log(\sigma'_{zc}/\sigma'_{z0}) + C_c/V \times \log((\sigma'_z)_i/(\sigma'_{zc}) \quad (20)$$

where C_r and C_c are respectively the compression indexes fitted to data in unloading–reloading cycles, and first-time loading at EOP. The value of σ'_{zc} is the intercept point of an unloading–reloading line and the first loading line at EOP, and is interpreted as the preconsolidation pressure in normal soil mechanics. For test 7 presented by Berre & Iversen (1972), it has been estimated that $C_r/V = 0{\cdot}0092$, $C_c/V = 0{\cdot}380$, and the first loading line was $\varepsilon_z = C_c/V \log(\sigma'_z/77{\cdot}6)$ at EOP. Using these parameters and equation (14), the average strain increments $\Delta S_{100}/H_0$ at EOP for load increment 5 of tests 7, 6 and H6 were found to be 2·68%, 4·63% and 5·61%, respectively.

The average strain during secondary consolidation is

$$\Delta(S/H_0) = C_{\alpha\varepsilon}/V \log(t/t_{EOP}) \text{ for } t_{EOP} \leqslant t < \infty \quad (21)$$

where $C_{\alpha\varepsilon}$ is the coefficient of secondary consolidation, estimated from test 7 to be 0·0161. The total time-dependent average strain is then

$$S/H_0 = (S/H_0)_0 \Delta S_{100}/H_0 + \Delta(S/H_0) \quad (22)$$

where $(S/H_0)_{i-1}$ is the accumulated average strain up to the end of the last loading σ'_{i0}. The excess pore water pressures u_e at the undrained boundary can also be obtained from Terzaghi's theory. As mentioned above, these values can then be compared with corresponding measured values, and values from the EVP model from (equations (7) and (8)).

REFERENCES

Barden, L. (1965). Consolidation of clay with non-linear viscosity. *Géotechnique* 15, No. 4, 345–362.

Barden, L. (1969). Time-dependent deformation of normally consolidated clays and peats. *J. Soil Mech. Fdn Div. Am. Soc. Civ. Engrs* 95, SM1, 1–31.

Berre, T. & Iversen, K. (1972). Oedometer tests with different specimen heights on a clay exhibiting large secondary compression. *Géotechnique* 22, No. 1, 53–70.

Berry, P. L. & Poskitt, T. J. (1972). The consolidation of peat. *Géotechnique* 22, No. 1, 27–52.

Bjerrum, L. (1967). Seventh Rankine Lecture. Engineering geology of Norwegian normally-consolidated marine clays as related to settlement of buildings. *Géotechnique* 17, No. 2, 81–118.

Chang, Y. C. E. (1981). *Long term consolidation beneath the test fill at Väsby, Sweden.* Report 13, Swedish Geotechnical Institute, Linköping.

Christie, I. F. & Tonks, D. M. 1985. Developments in the time lines theory of consolidation. *Proc. 11th Int. Conf. Soil Mech. Fdn Engng, San Francisco* 2, 423–426.

Crooks, J. H. A., Becker, D. E., Jefferies, M. G. & McKenzie, K. (1984). Yield behaviour and consolidation: I, pore pressure responses. *Proceedings of symposium on sedimentation consolidation models: predictions and validations*, pp. 356–381. New York: American Society of Civil Engineers.

Dixon, D. A., Sri Ranjan, R. & Graham, J., 1992. Applicability of Darcy's law in laboratory measurement of water flow through low permeability clays. *Proc. 45th Can. Geotech. Conf., Toronto*, 95-1–95-6.

Garlanger, J. E. (1972). The consolidation of soils exhibiting creep under constant effective stress. *Géotechnique* 22, No. 1, 71–78.

Gibson, R. E. & Lo, K.-Y. (1961). *A theory of consolidation for soils exhibiting secondary compression.* Publication 41, pp. 1–16. Oslo: Norwegian Geotechnical Institute.

Imai, G. 1989. A unified theory of one-dimensional consolidation with creep. *Proc. 12th Int. Conf. Soil Mech., Fdn Engng, Rio de Janeiro* 1, 57–60.

Kabbaj, M., Oka, F., Leroueil, S. & Tavenas, F. (1985). Consolidation of natural clays and laboratory testing. In *Consolidation of soils: testing and evaluation*, STP892, pp. 378–401. Philadelphia: American Society for Testing and Materials.

Kabbaj, M., Tavenas, F. & Leroueil, S. (1988). In situ and laboratory stress–strain relationship. *Géotechnique* 38, No. 1, 83–100.

Ladd, C. C. (1973). *Estimating settlements of structures supported on cohesive soils.* Special summer program 1.34s, Massachusetts Institute of Technology, Cambridge.

Ladd, C. C., Foott, R., Ishihara, K., Schlosser, F. & Poulos, H. J. (1977). Stress–deformation and strength characteristics. *Proc. 9th Int. Conf. Soil Mech., Fdn Engrg. Tokyo*, 421–494.

Lambe, T. W. & Whitman, R. V. 1969. *Soil mechanics.* New York: Wiley.

Leroueil, S., Kabbaj, M., Tavenas, F. & Bouchard, R. (1985a). Stress–strain–strain rate relationship for the compressibility of sensitive natural clays. *Géotechnique* 35, No. 2, 159–180.

Leroueil, S., Magnan, J. P. & Tavenas, F. (1985b). *Remblais sur argiles molles.* Paris: Lavoisier.

Lo, K. Y. (1961). Secondary compression of clays. *J. Soil Mech. Fdn Div. Am. Soc. Civ. Engrs* 87, SM4, 61–87.

Magnan, J. P. (1984). *Modélisation numériques du comportement des argiles molles naturelles.* DSc thesis, Université Pierre et Marie Curie, Paris.

Magnan, J. P. & Lepidas, I. (1987). Influence of creep, anisotropy and overconsolidation on the results of finite element analyses of embankments on soft clays. *Proceedings of international symposium on geotechnical engineering on soft soils*, Mexico City, vol. 1, pp. 265–272.

Magnan, J. P. & Lepidas, I. (1989) Calcul des tassements primaire et secondare sur la base des essais oedométriques. *Proc. 12th Int. Conf. Soil Mech., Fdn Engrg, Rio de Janeiro* 3, 1747–1748.

Mesri, G. & Choi, Y. K. (1985). The uniqueness of end of primary (EOP) void ratio effective stress relationship. *Proc. 11th Int. Conf. Soil Mech., San Francisco* 2, 587–590.

Mesri, G. & Godlewski, P. M. (1977). Time and stress–compressibility interrelationship. *J. Geotech. Engng Div. Am. Soc. Civ. Engrs* 105, No. 1, 106–113.

Suklje, L. (1957). The analysis of the consolidation process by the isotache method. *Proc. 4th Inst. Conf. Soil Mech., London* 1, 200–206.

Tan, T. K. (1957). *Secondary time effects and consolidation of clays.* Publication of Institute of Civil Engineering and Architecture, Academia Sinica, P.R. China.

Terzaghi, K. (1943). *Theoretical soil mechanics.* New York: Wiley.

Terzaghi, K. & Fröhlich, (1936). *Theorie der Seizing von Tonschichten.* Leipzig: Deuticke, 168.

Yin, J.-H. & Graham, J. (1989a). Viscous-elastic–plastic modelling of one-dimensional time-dependent behaviour of clays. *Can. Geotech. J.* 26, 199–209.

Yin, J.-H. & Graham, J. (1989b). General elastic viscous plastic constitutive relationships for 1-D straining in clays. *Proc. 3rd. Intl. Symp. Numer. Models Geomech.*, Elsevier Applied Science, 108–117.

Yin, J.-H. & Graham, J. (1990). Reply to the discussion on 'Viscous-elastic–plastic modelling of one-dimensional time-dependent behaviour of clays' by J.-H. Yin and J. Graham. *Can. Geotech. J.* 27, 262–265.

one-dimensional elastic visco-plastic modelling of time-dependent stress–strain behaviour of clays. *Can. Geotech. J.* **31**, 42–52.

Yin, J.-H., Graham, J., Clark, J. I. & Gao, L. (1994). Modelling unanticipated pore water pressures in soft clays. *Can. Geotech. J.* **31**, 773–778.